2010

Regulation of Anaphase Promoting Complex Coactivators

Jonathan Robbins

REGULATION OF ANAPHASE PROMOTING COMPLEX COACTIVATORS

A Thesis Presented to the Faculty of

The Rockefeller University

in Partial Fulfillment of the Requirements for

the degree of Doctor of Philosophy

by

Jonathan Robbins

June 2010

REGULATION OF ANAPHASE PROMOTING COMPLEX COACTIVATORS

Jonathan Robbins, Ph.D.

The Rockefeller University 2010

Ubiquitin-mediated proteolytic degradation is fundamental to eukaryotic cell cycle progression. From late mitosis through early G1, the Anaphase Promoting Complex (APC) is essential for cell-cycle relevant proteolytic degradation, and its activity is targeted to appropriate substrates by the evolutionarily conserved coactivators Cdc20 and Cdh1. After an initial wave of APC-Cdc20 activity, APC-Cdh1 degrades multiple mitotic proteins from mitotic exit through G1; inhibitory phosphorylation of Cdh1 by CDK and Polo kinase may allow accumulation of Cdh1 targets in the subsequent cell cycle. I demonstrate lethality of exact endogenous gene replacement of *CDH1* with the CDK-unphosphorylatable *CDH1-m11* allele; neither polo kinase sites nor polo interaction motifs are required for Cdh1 regulation. *CDH1-m11* cells arrest in the first cycle with replicated DNA;~30% of these cells have bipolar spindles. Construction of bipolar spindles in these cells is strikingly sensitive to gene dosage of the stoichiometric Cdh1 inhibitor *ACM1*. *CDH1-m11* cells with bipolar spindles fail to progress to anaphase, suggesting that Cdh1 inhibits multiple spindle-regulatory pathways. Expression of undegradable mitotic cyclin causes spindle pole body separation (a key step in bipolar spindle assembly) in *CDH1-m11* cells; thus mitotic cyclins are a significant target for Cdh1 with respect to bipolar spindle assembly, and reciprocally, cyclin-Cdk activity is the most significant mechanism for Cdh1 inactivation.

Cdc20 has been proposed to be a Cdh1 target, but regulation of Cdc20 proteolysis has been controversial. My experiments demonstrate that degradation of Cdc20 can be dependent on Cdh1 and Cdc20 destruction boxes, but Cdh1- and db-independent modes of Cdc20 proteolysis are also effective in limiting Cdc20 levels.

To better understand the mechanisms by which multisite CDK phosphorylation inhibits Cdh1, I employed a novel recombination approach to create a series of partially unphosphorylatable *CDH1* alleles ablating contiguous sites beginning at either the N or C terminus. Strains lacking N-terminal phosphorylation sites were strictly dependent upon *ACM1* and S-phase cyclins for viability, and a fraction of cells displayed evidence of hyperactive APC-Cdh1, in contrast to a non-overlapping larger set of C-terminal site ablations.

Dedicated to my family,

without whom none of this

would have been possible

ACKNOWLEDGEMENTS

I owe very much to very many people:

Firstly, I would like to thank my family for everything. You have always been there for me, afforded me every possible opportunity, and made it so that my biggest worries have been about the workings of the yeast cell cycle.

I would like to thank all the members of the Cross lab, past and present, for making the lab a wonderful place to be: My advisor Fred Cross for his guidance, patience, and insight, for allowing me to follow my curiosity in lab while preventing me from doing anything truly ill-conceived, and most importantly, for teaching me by example and by instruction how to do science purely and properly. Stefano Di Talia for his advice, for fascinating discussions about math, the cell cycle, and development, for both teaching and helping me time and time again. Ben Drapkin, whose expertise and infinite knowledge of experimental details was an invaluable asset, and who both developed and taught me many of the protocols on which I routinely relied. Lea Schroeder and Veronica Di Talia, for showing me the ropes and keeping me sane. Andrea Procko and Catherine Oikonomou for their cheerful encouragement. Frej Tulin, Nick Buchler, Kresti Pecani, Lucy Bai, Ying and Jan (Lu and Skotheim) for many wonderful scientific conversations. Daphnie Grant, Bic-Hang Leung, Beth Anne Hatton and Marianne Labriola for their tireless efforts to keep the lab functioning.

I would like to thank Marta Delgado, Cris Rosario, Emily Harms, Kristen Kullen, and Michelle Sherman at the Rockefeller Dean's Office, and Ruthie Gotian, Renee Horton, Elaine Velez, and Irma Torres at the MD/PhD Program for always going out of

their way to be as helpful as possible, and making the programs such pleasures to be in. Olaf Andersen, for all of his valuable advice and guidance over the years (and undoubtedly for years to come).

Mitch Lazar and Bruce Hug, my undergraduate mentors who introduced me to the beauty of science and whose example inspired me along this path.

I would like to thank the members of my faculty advisory committee—Hiro Funabiki, Dave Allis, Rob Fisher, and my external examiner Fred Chang—for their attentiveness and helpful advice.

Many outside investigators have kindly provided strains and plasmids used in this study, including: Angelika Amon, Henrik Dohlman, Elaine Elion, Francisco Estruch, Mark Hall, Myles Hoyt, Kim Nasymth, David Pellman, Lucy Pemberton, Elmar Schiebel, Michael Schwab, and Peter Sorger.

TABLE OF CONTENTS

LIST OF FIGURES

LIST OF TABLES

CHAPTER ONE

Introduction

Oscillations in CDK activity drive the cell cycle

The oscillation of cyclin dependent kinase (CDK) activity lies at the heart of the cell cycle, serving to coordinate the events of the cell cycle in a temporally appropriate manner. CDK activity is dependent upon CDK binding to a partner cyclin (Draetta et al., 1989); canonical cyclins are synthesized and destroyed in each cell cycle (Evans et al., 1983). This oscillation in CDK activity serves to coordinate budding, DNA replication, spindle pole body (SPB) duplication and separation, mitotic spindle assembly, mitotic entry, DNA segregation, mitotic spindle disassembly, mitotic exit, and cytokinesis such that each occurs once and only once during a cell cycle (Stern and Nurse, 1996). Specifically, the cell cycle begins at a low CDK state, during which DNA replication origins can be efficiently loaded. The transcriptional induction of G1 cyclins then allows for polarized growth, budding and progression through G1 (Cross and Tinkelenberg, 1991; Dirick and Nasmyth, 1991; Richardson et al., 1989; Skotheim et al., 2008). The G1 cyclins, which are unstable proteins whose levels fall rapidly after transcriptional shutoff (Schneider et al., 1998), activate expression and activity of the B-type cyclins Clb5 and Clb6 which are required for replication origin firing and efficient DNA replication (Epstein and Cross, 1992; Schwob and Nasmyth, 1993). These are temporally followed by the remaining B-type cyclins which promote mitotic entry, the shutoff of G1 cyclin transcription, and the switch to isotropic growth (Amon et al., 1993). To exit from mitosis, the CDK activity of the mitotic B-type cyclins must be reduced; this occurs

largely by cyclin destruction. The cell cycle thus progresses by alternating between a CDK-driven phase and a destruction driven phase (Figure 1.1). The resultant low CDK state must be maintained to allow for proper loading of replication origins and the subsequent transcriptional induction of G1 cyclins so as to start the cell cycle anew (Wäsch and Cross, 2002).

The anaphase-promoting complex (APC) is a ubiquitin ligase responsible for the destruction of cyclins

The APC is in large part responsible for cyclin degradation at the end of mitosis: the cell cycle ends in highly efficient and specific protein destruction orchestrated by the APC, which mediates the sequential degradation of cyclins and other relevant cell cycle proteins and machinery (King et al., 1995; Sudakin et al., 1995).

The APC is a large ubiquitin E3 ligase comprised of at least 13 proteins, and functions in coordination with two homologous mitotic coactivators, Cdc20p and Cdh1 (Schwab et al., 1997; Thornton et al., 2006; Visintin et al., 1997; Yoon et al., 2002; Zachariae et al., 1998b). The APC and both coactivators are conserved throughout eukaryotic evolution. The core APC catalyzes the transfer of ubiquitin from ubiquitin conjugating enzymes (E2s) to substrates, thus marking them for proteasomal destruction (Figure 1.2) (Gmachl et al., 2000; Leverson et al., 2000). The APC utilizes two E2s sequentially to ubiquitinate substrates: Ubc4 attaches a single ubiquitin which is then efficiently converted to a ubiquitin chain via Ubc1 (Rodrigo-Brenni and Morgan, 2007).

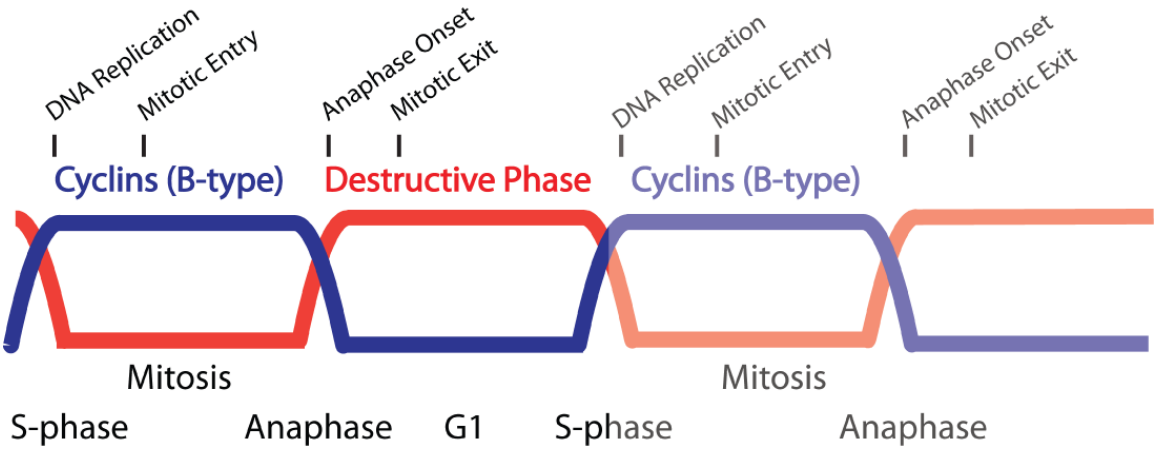

Figure 1.1 Cell cycle progression entails alternating CDK-driven and destruction driven phases. B-type cyclins drive DNA replication and mitotic entry. Onset of a destructive phase clears B-type cyclins, initiates anaphase onset, and allows for mitotic exit.

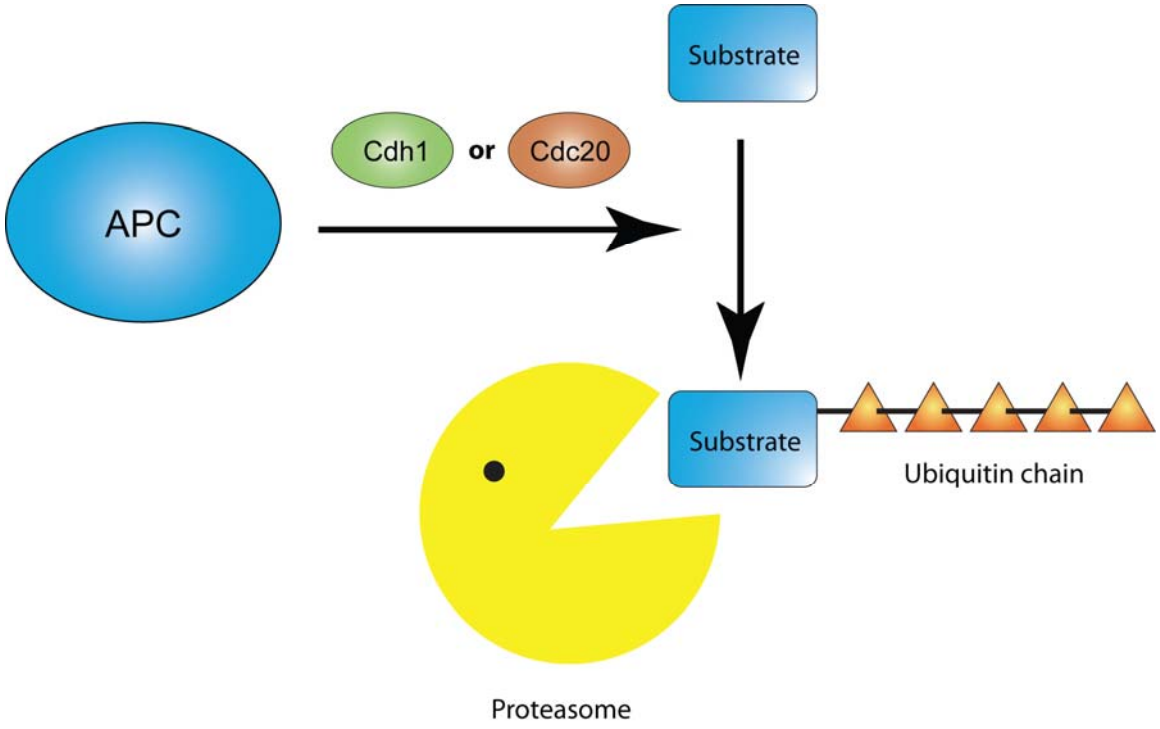

Figure 1.2 The APC ubiquitinates substrates to target them for proteasomal destruction. The APC, in coordination with one of two mitotic activators—Cdc20 and Cdh1—is responsible for the processive transfer of ubiquitin to substrates. The proteasome degrades substrates that have been marked with a polyubiquitin chain.

APC is activated by two temporally separated coactivators, Cdc20 and Cdh1

The APC is active only from anaphase onset through the subsequent G1, although the core complex is present throughout the cell cycle. The conserved coactivators Cdc20 and Cdh1 provide regulation of timing and specificity. APC-Cdc20 begins B-type cyclin degradation and APC-Cdh1 continues it through mitosis and into the ensuing G1 (Irniger and Nasmyth, 1997; Schwab et al., 1997; Shirayama et al., 1999; Wäsch and Cross, 2002; Yeong et al., 2000; Zachariae et al., 1998a).

A major basis for this difference in timing is differential regulation of APC-Cdc20 and APC-Cdh1 by cyclin-CDK activity. APC-Cdc20 is active at high CDK levels, with Cdc20 binding preferentially to CDK-phosphorylated APC (Kramer et al., 2000; Rudner and Murray, 2000). Cdc20 itself is an unstable protein, accumulating late in the cell cycle, followed by mitotic degradation (Prinz et al., 1998; Shirayama et al., 1998; Weinstein, 1997). As B-type cyclin levels decline and the Cdc14 phosphatase (at least in budding yeast) is released from a nucleolar sequestration, the balance between CDK activity and phosphatase activity shifts such that Cdh1 is dephosphorylated on at least some of its 11 CDK sites, which collectively serve to inhibit Cdh1 function (Zachariae et al., 1998a). The second wave of APC-mediated degradation then ensues, dependent on dephosphorylated Cdh1. This activity is responsible for continued mitotic cyclin degradation through G1, until Cdh1 inactivation in the succeeding cell cycle (Amon et al., 1994).

In addition to these temporal differences, Cdc20 and Cdh1 likely have intrinsically different substrate specificities, although they both contribute to mitotic cyclin degradation (Figure 1.3). Cdc20 promotes Pds1 proteolysis, an anaphase inhibitor

that prevents cleavage of cohesin, the protein keeping sister chromatids attached (Cohen-Fix et al., 1996; Shirayama et al., 1999). APC-Cdh1 seems ineffective at promoting Pds1 degradation, but promotes degradation of several spindle proteins and perhaps Cdc20 itself (Hildebrandt and Hoyt, 2001; Huang et al., 2001; Juang et al., 1997; Schwab et al., 1997; Shirayama et al., 1998; Woodbury and Morgan, 2007; Zachariae et al., 1998a). This ordering is logical: the earlier APC-Cdc20 wave will promote anaphase and initial mitotic cyclin proteolysis, promoting APC-Cdh1 activation; APC-Cdh1 then completes mitotic cyclin proteolysis, allowing cytokinesis and other events of mitotic exit, removes Cdc20 to reset the system to G1, and contributes to spindle disassembly by proteolysis of spindle components. This ordering could help ensure that anaphase precedes cytokinesis and spindle disassembly.

Consequences of deleting APC coactivators and core subunits

CDC20 is essential for cell viability, and its absence results in an arrest with unseparated sister chromatids and high Clb2 levels (Sethi et al., 1991; Shirayama et al., 1998). Deletion of the APC-Cdc20 target *PDS1* (securin) allows *cdc20* cells to undergo anaphase (Sethi et al., 1991; Shirayama et al., 1998). Further deletion of *CLB5* results in a viable *cdc20 pds1 clb5* triple mutant, capable of carrying out all essential cell-cycle functions (Shirayama et al., 1999). This defines two critical targets of Cdc20; consistently, both have been reported to be poor APC-Cdh1 substrates (Schwab et al., 1997; Visintin et al., 1997).

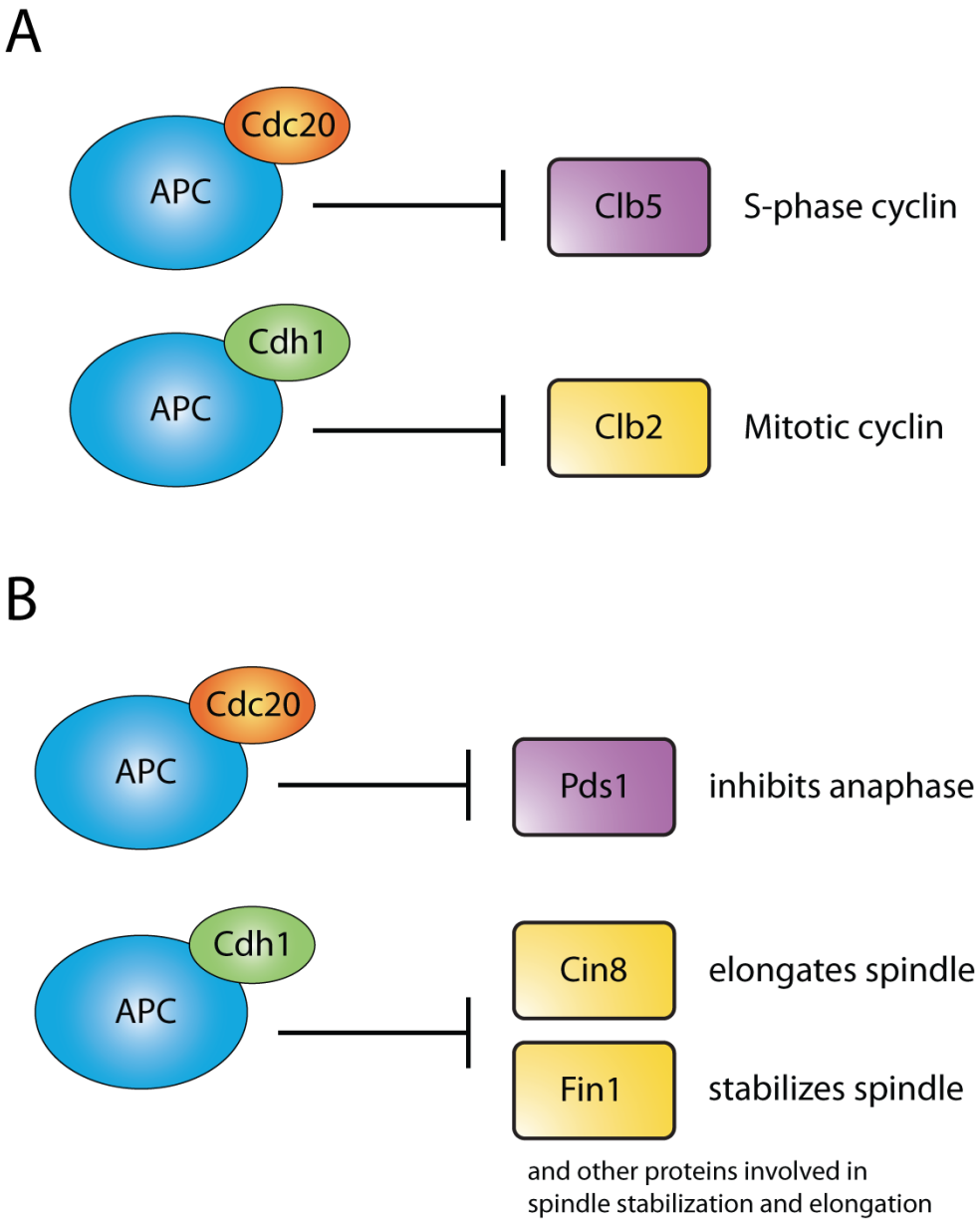

Figure 1.3 The APC is responsible for the destruction of B-type cyclins as well as spindle regulatory proteins **A** APC-Cdc20 targets the S-phase cyclin Clb5 for destruction, and APC-Cdh1 targets the major mitotic cyclin Clb2. APC-Cdh1 is also believed to target the remaining mitotic cyclins—Clb1, 3, 4—as well. **B** APC-Cdc20 targets the anaphase inhibitor Pds1 for degradation, resulting in the onset of anaphase. After spindle elongation, APC-Cdh1 is responsible for degradation of spindle motor proteins such as Cin8, which provide the motor activity for spindle elongation, and spindle stabilizing factors including Fin1. Thus Cdc20 drives the onset of anaphase, and subsequent Cdh1 activity contributes to spindle disassembly after separation of sister chromatids to opposite poles.

In contrast to Cdc20, Cdh1 is not an essential protein. *cdh1* cells exhibit a moderate growth defect, a slight delay in disassembling elongated spindles, and retain Clb2 throughout the cell cycle (Schwab et al., 1997). In G1, Cdh1 activity is partially redundant with Sic1 and the N-terminal region of Cdc6, which both effectively inhibit Clb activity as stoichiometric inhibitors: cells lacking Cdh1, Sic1 and the N-terminal region of Cdc6 are not viable, highlighting the essential role of inhibiting Clb activity in G1(Archambault et al., 2003). However, there is no clearly redundant protein involved in Cdh1's role in spindle disassembly and targeting structural substrates, making the viability of *cdh1* strains somewhat unexpected.

Remarkably, *none* of the APC targets need be degraded at all, if an effective means to regulate Clb activity is present: *apc-null clb5 pds1 10XSIC1* strains (overexpressing the Sic1 Clb inhibitor) are viable (Thornton and Toczyski, 2003). Thus the entire cell cycle can be run without any APC-mediated proteolysis.

APC-Cdh1 and mitotic kinases

Cdh1 was initially cloned as a high copy suppressor of *cdc20-1* at the restrictive temperature. In the absence of Cdh1, the mitotic cyclin Clb2 is present throughout the cell cycle (Schwab et al., 1997). Cdh1 overexpression resulted in an arrest with 2C DNA content and hyperpolarized buds, and with persistence of the S-phase cyclin Clb5 (Schwab et al., 1997). Drosophila *fizzy-related* (a Cdh1 homolog) is responsible for clearing mitotic cyclins. Fzr overexpression inhibits mitosis and results in DNA endoreduplication (Sigrist and Lehner, 1997). Thus APC-Cdh1 may specifically proteolyze mitotic cyclins rather than S-phase cyclins. Consistent with this, in addition to

Clb2, Cdh1 also targets the mitotic cyclin Clb3 (Irniger and Nasmyth, 1997; Zachariae et al., 1998a), and presumably Clb1 and Clb4 (close Clb2 and Clb3 homologs). Clb1,2,3,4 constitute all of the budding yeast mitotic cyclins.

Cdh1 is also responsible for the destruction of Cdc5 (Shirayama et al., 1998), the yeast Polo-like kinase involved in mitotic exit and cytokinesis. Cdc5 localizes to the spindle pole bodies (SPBs) and the mother bud neck, and overexpression results in hyperpolarized buds with multiple septin rings along these buds, and possible SPB over-production (Song et al., 2000). Cdc5 is probably not essential for any processes prior to anaphase, since Cdc5 inactivation results in a late anaphase arrest in temperature sensitive and engineered drug sensitive *cdc5* alleles, as well as by transcriptional shut-off (Hartwell et al., 1973; Snead et al., 2007; Song and Lee, 2001). Cdc5 has been implicated in activation of the APC (Charles et al., 1998), but also in inactivation of APC-Cdh1 (Crasta et al., 2008).

APC-Cdh1 and the mitotic spindle

Cdh1 has been implicated in degrading the spindle-regulatory proteins Ase1, Cin8, Cik1, Fin1 and possibly Kip1 (Benanti et al., 2009; Gordon and Roof, 2001; Hildebrandt and Hoyt, 2001; Juang et al., 1997; van Hemert et al., 2003). Cin8 and Kip1 are plus end kinesins, involved in keeping spindle poles separated (their deletion results in spindle pole bodies coming into approximation with one another) (Hoyt et al., 1992). Ase1 is a spindle midzone protein, involved in spindle stabilization and elongation (Schuyler et al., 2003). Fin1 is an intermediate-filament-like protein that creates

filaments in between the two SPBs (van Hemert et al., 2003), and Cik1 associates with the kinesin Kar3 to regulate the mitotic spindle (Benanti et al., 2009).

Overexpression of unphosphorylated Cdh1 blocks construction of a bipolar mitotic spindle (Crasta et al., 2008). Mitotic spindle construction requires duplication of SPBs (functionally equivalent to metazoan centrosomes), followed by disassembly of the half-bridge connecting them and separation to opposite poles of the nucleus (Figure 1.4A). Subsequently, sister chromatid separation and anaphase spindle elongation separates chromosomes into the progeny (See Figure 1.4B, C). The spindle is then disassembled; each cell inherits a single SPB, which starts the cycle anew. Despite the dependence of destruction of many spindle proteins on Cdh1, spindle disassembly is delayed but not blocked by *cdh1* deletion (Visintin et al., 1997); this delay may decrease fidelity of chromosome segregation (Ross and Cohen-Fix, 2003). Expression of Cdh1-resistant Ase1 results in roughly a ten minute delay in spindle disassembly, comparable to that of *cdh1* cells (Juang et al., 1997; Visintin et al., 1997).

A proposed explanation for the failure of *CDH1*-overexpressing cells to construct a bipolar spindle lies in the fact that the plus end kinesins Cin8, and possibly Kip1, are Cdh1 targets (Crasta et al., 2006; Gordon and Roof, 2001; Hildebrandt and Hoyt, 2001). *cin8* mutants display chromosomal instability and spindle defects, and *cin8 kip1* strains are inviable (Hoyt et al., 1992). Cin8 and Kip1 are implicated in SPB separation, as strain with both *kip1* and the temperature sensitive allele *cin8-3* retain a half-bridge at the restrictive temperature (Hoyt et al., 1992). Mutations in the minus-end directed kinesin Kar3, which opposes the forces generated by Cin8 and Kip1, allow for separation of spindle pole bodies in the absence of Cin8 and Kip3 (Saunders and Hoyt, 1992).

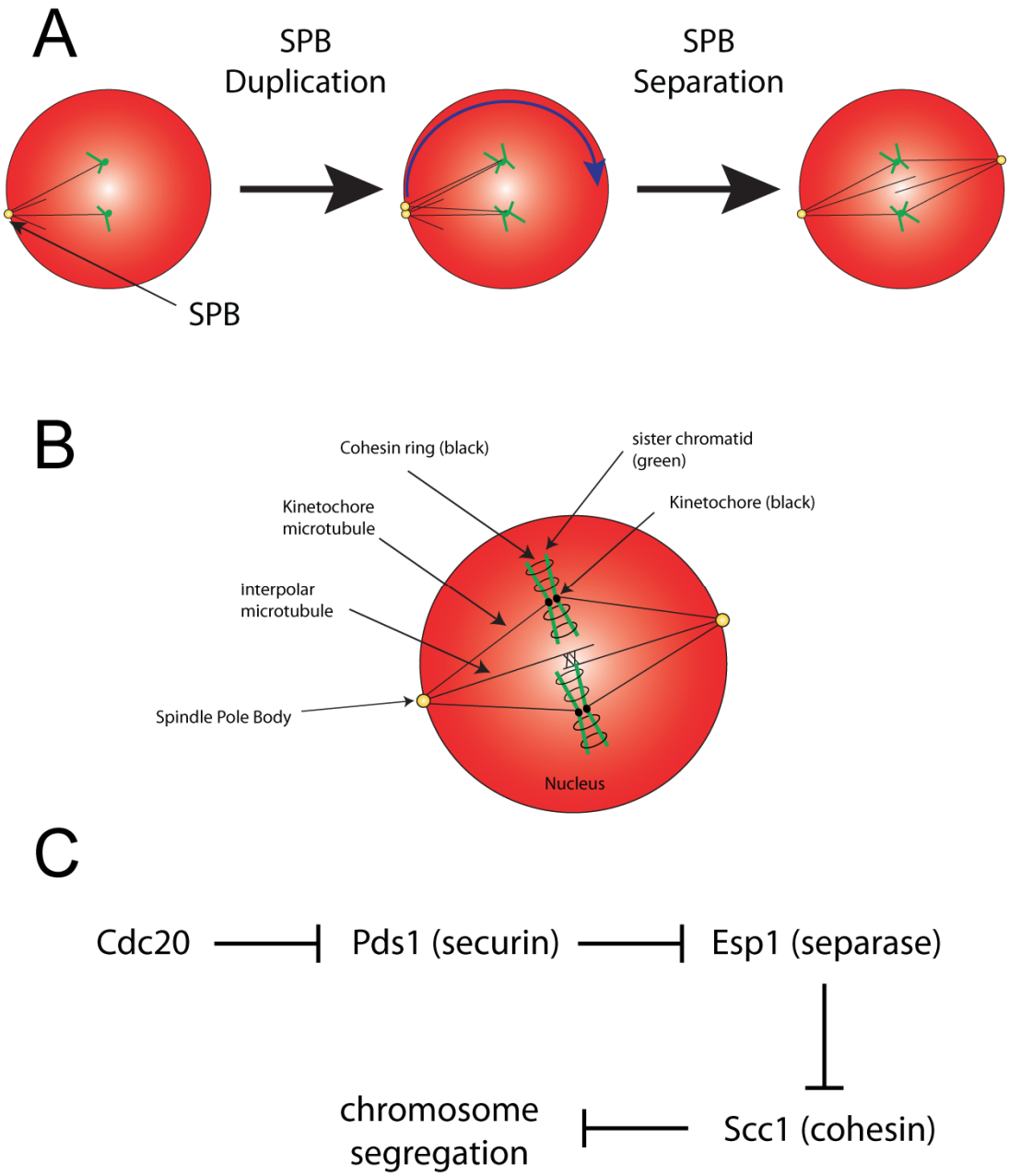

Figure 1.4 Construction and regulation of the mitotic spindle. **A** Bipolar spindle construction requires initial SPB duplication, followed by SPB separation. **B** Schematic structure of the short bipolar spindle: Interpolar microtubules, via motor proteins, push the SPBs apart from one another. Each SPB emanates a kinetochore microtubule to one sister chromatids of each pair, pulling each sister chromatid poleward. The two sister chromatids are attached to each other by cohesin; cohesin cleavage results in the poleward movement of chromatids. **C** Schematic of pathway regulating anaphase onset. Cdc20 activation results in Pds1 (securin) degradation, freeing the enzyme Esp1 (separase) to cleave Scc1 (a major cohesin subunit), which allows for the poleward movement of chromosomes.

Additionally, overexpression of Cin8 is sufficient to separate SPBs in the presence of overexpressed unregulated Cdh1 (Crasta et al., 2006), suggesting that the aberrant degradation of these proteins may account for the ability of unregulated Cdh1 to block spindle formation.

Dynamic Cooperation between CDK and APC-Cdh1 activity

APC-Cdh1 targets both mitotic cyclins and spindle structural components for destruction more or less simultaneously. Additionally, the phosphatase Cdc14, which dephosphorylates CDK targets, is released when Cdh1 is active, and Cdc14 likely contributes directly to Cdh1 activation via Cdh1 dephosphorylation (Visintin et al., 1998). The net result is that dephosphorylation and the degradation of some APC-Cdh1 substrates are temporally coupled. Fin1 is a well characterized example of this, wherein CDK phosphorylates Fin1 and inhibits its localization to the spindle (Woodbury and Morgan, 2007). Dephosphorylation of Fin1 in anaphase targets it to the spindle, where it acts to stabilize the anaphase spindle, and where it is then degraded by APC-Cdh1 during spindle disassembly (Woodbury and Morgan, 2007). CDK phosphorylation has been shown to prevent the association and function of other Cdh1 targets at the spindle midzone (Khmelinskii et al., 2009), so this coordinated regulation may be a general phenomenon.

Substrate Targeting

Specific motifs in substrate proteins target them for APC-mediated ubiquitination: the destruction box (consensus RxxL) (King et al., 1996), recognized by Cdc20 and

Cdh1; the KEN box, which may be more specific for Cdh1 (Pfleger et al., 2001) (but see Burton and Solomon, 2001), and the CRY box Cdh1 recognition sequence (Reis et al., 2006). Thus Cdh1 recognizes unique motifs that Cdc20 does not; in contrast, there are no known Cdc20-specific targeting sequences, although Cdc20 specific substrates exist.

APC targeting mechanisms remain unclear. The core APC has been reported to directly engage the destruction box (Yamano et al., 2004). Alternatively, the N-terminal regions of Cdc20 and Cdh1 have been found to directly interact with substrates (Pfleger et al., 2001), and the WD40 propeller domain of Cdh1 (located in its C-terminal half) to directly interact with the destruction box motif (Kraft et al., 2005). These studies both argue for coactivators conferring substrate specificity on the APC, albeit through different mechanisms, as does biochemical evidence of Cdh1-substrate complexes (Burton et al., 2005; Schwab et al., 2001). An intermediate model has also been proposed, in which both core APC subunits and coactivators contribute to substrate binding (Passmore and Barford, 2005).

Regulation of Cdh1

Cdh1 possess 11 CDK consensus sites, and phosphorylated Cdh1 has significantly reduced ability to interact with the APC (Figure 1.5A) (Jaspersen et al., 1999; Zachariae et al., 1998a). Consistent with this, overexpression of Cdh1-m11, in which the 11 CDK consensus phosphorylation sites are mutated to unphosphorylatable alanine residues, causes cell cycle arrest with low levels of Cdh1-APC targets (Zachariae et al., 1998a). Phosphorylation may also regulate Cdh1 localization: the Msn5 exporter may specifically recognized phosphorylated Cdh1 and transport it from the nucleus to the cytoplasm

(Jaquenoud et al., 2002). Thus in addition to precluding direct APC interaction, Cdh1 phosphorylation may also spatially segregate Cdh1 from relevant substrates and the APC itself, as APC subunits localized thus far have been nuclear (Huh et al., 2003; Sikorski et al., 1993).

Other mechanisms may control Cdh1 activity. Cdc5 (Polo kinase) has been reported to act in concert with CDK phosphorylation to mediate complete Cdh1 inhibition (Crasta et al., 2008). Specifically, Cdc5 has been demonstrated biochemically to be capable of phosphorylating Cdh1 on serines 125 and 259 (Figure 1.5B) (Crasta et al., 2008). It has been proposed, through a series of overexpression studies, that phosphorylation of Cdh1 on these sites is required for complete Cdh1 inactivation, to allow for spindle pole body separation and mitotic spindle assembly. This Cdc5-mediated inhibition of Cdh1 is reported to be essential in the absence of the stoichiometric inhibitor *ACM1* (Crasta et al., 2008) (see below).

Cdh1 in yeast is stable and present throughout the cell cycle (Prinz et al., 1998; Zachariae et al., 1998a). In contrast, vertebrate Cdh1 levels are cell cycle regulated (Kramer et al., 2000); Cdh1 is degraded in S phase by an SCF-complex (Benmaamar and Pagano, 2005), and mediates its own degradation in G0/G1 (Listovsky et al., 2004).

Stoichiometric inhibitors also regulate APC-Cdh1: Acm1 in budding yeast (Figure 1.5C), Rca1 in Drosophila, and Emi1 in vertebrates. Rca1 and Emi1 are F-box proteins that are homologous to each other (Reimann et al., 2001). Acm1 has no obvious sequence homology, but is functionally similar; all are unstable cell-cycle regulated pseudosubstrate inhibitors of APC-Cdh1 that are transcribed in G1/S. *rca1* flies degrade cyclins prematurely and fail to enter mitosis (Grosskortenhaus and Sprenger, 2002).

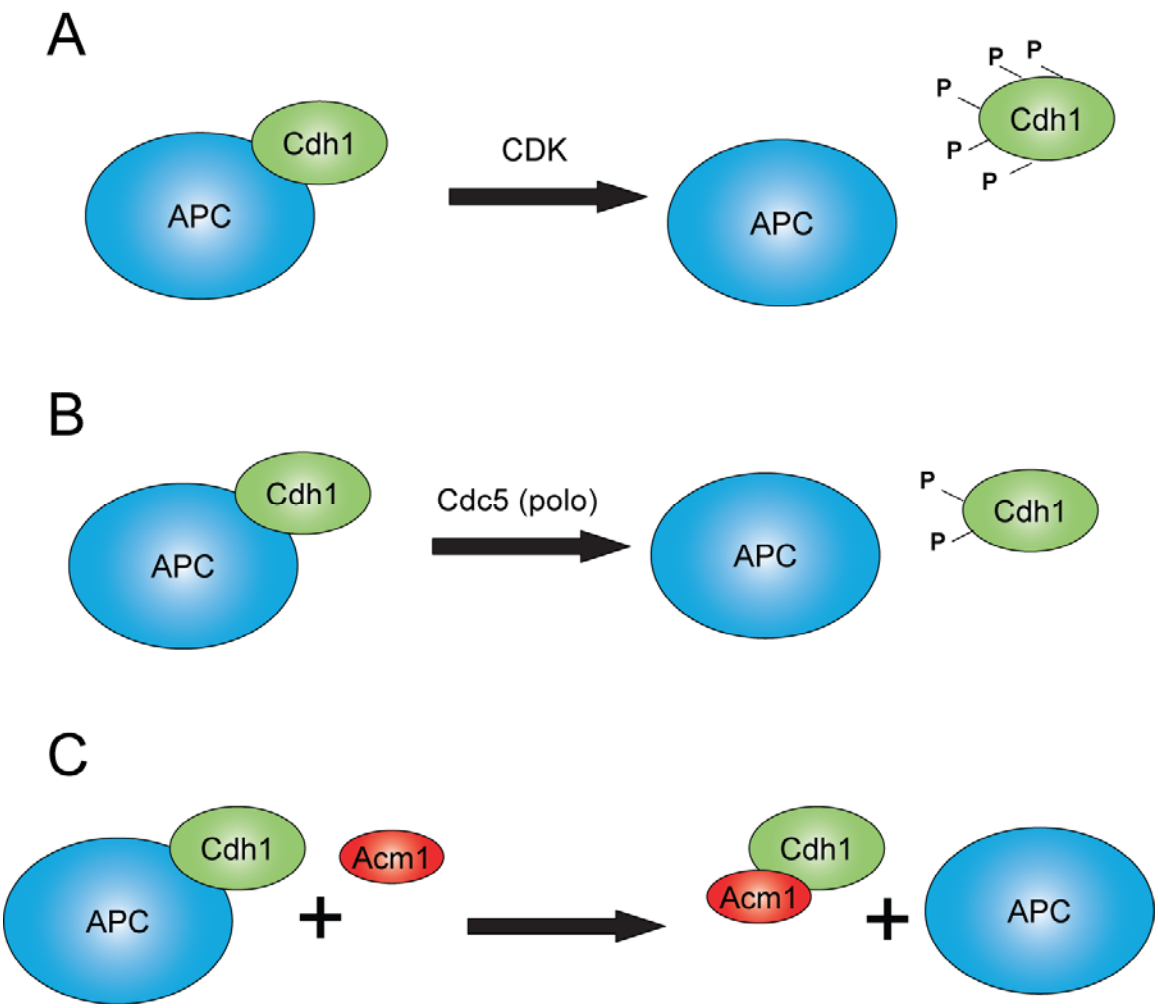

Figure 1.5 Regulatory mechanisms inhibiting Cdh1 activity. **A** CDK activity results in the phosphorylation of Cdh1 on some or all of 11 putative sites. This phosphorylation blocks Cdh1 association with the APC. G1 and S phase cyclins, and possibly early mitotic cyclins, are reported to contribute to this phosphorylation. **B** Cdc5 (polo kinase), appearing late in mitosis, can phosphorylate Cdh1 on at least two residues, and this is reported to block Cdh1 association with the APC. **C** The stoichiometric inhibitor Acm1 is transcribed in G1 and blocks Cdh1 targeting of substrates.

Consistently, Emi1 may inhibit APC-Cdh1 so as to stabilize mitotic cyclins in interphase, promoting mitosis and preventing rereplication (Di Fiore and Pines, 2007). *acm1* deletion has no obvious phenotype, although it exhibits modest synthetic interactions with deficiency in the Swe1 CDK-regulatory kinase (Martinez et al., 2006). Acm1 may be a Cdh1 target (Enquist-Newman et al., 2008), but has also been reported to be destroyed in an APC-independent manner (Hall et al., 2008; Ostapenko et al., 2008).

Regulation by multisite phosphorylation

The presence of 11 putative CDK sites in Cdh1 is a striking example of multisite phosphorylation, a common phenomenon in phosphorylation control (Holt et al., 2009) that features prominently among cell-cycle regulated proteins. Cdh1 can be inhibited by phosphorylation of some or all of its 11 CDK sites; how the various sites contribute and whether this regulation is a critical regulatory mechanism has been unclear. By overexpression of a series of alleles progressively lacking phosphorylation sites beginning with the N-terminus, a seemingly continuous decrease in resultant Clb2 levels was found (Zachariae et al., 1998a), suggesting that all tested clusters of sites contribute approximately additively. Cdh1 phosphorylation decreases sharply upon mitotic exit as mitotic cyclin levels fall and the phosphatase Cdc14 is released, and then increases sharply during progression through G1, based on phosphorylation-dependent gel shifts (Zachariae et al., 1998a); these gel shifts have not been correlated to specific phosphorylations. The function and existence of intermediate phosphorylation states of Cdh1, whether the different sites are functionally distinct from one another, and how the

presence of multiple sites contributes to the regulatory architecture of the APC remains unclear.

A global analysis of CDK substrate phosphorylation sites in budding yeast found evidence for large numbers of poorly evolutionarily conserved clusters of phosphorylation sites in relatively unstructured regions, likely acting through bulk electrostatic effects with some regional specificity (Holt et al., 2009). Indeed, while a high density of N-terminal Cdk sites is conserved throughout eukaryotic evolution, their precise location has diverged even in rather closely related yeast species, consistent with this bulk electrostatic model.

Multisite phosphorylation of the Sic1 CDK inhibitor may control Sic1 proteolysis by a counting mechanism, whereby phosphorylation of any 5 of 9 candidate Cdk sites allows for binding of the SCF activator Cdc4, consequently promoting Sic1 degradation and the progression to S phase (Nash et al., 2001). The apparent precision of this mechanism is hard to square with the bulk electrostatic proposal, and the molecular basis for this specificity remains unclear.

In the case of Sic1, it has been argued that multisite phosphorylation serves both to set a delay and establish a threshold for CDK activity (Nash et al., 2001). Simple mathematical models support this; six fast phosphorylations create a sharp transition with a temporal delay, whereas single fast phosphorylation lacks the temporal delay and a single slow phosphorylation lacks the dynamic range (Deshaies and Ferrell, 2001).

It is not known if Cdh1 is regulated in a similar fashion, or whether functional distinctions exist between the various phosphorylation sites, which might differentially regulate APC interaction and Msn5 interaction.

Kinases responsible for Cdh1 inactivation, and regulatory implications

Numerous kinases have been reported to be involved in the phosphorylation-driven inactivation of Cdh1. Initial studies implicated the G1 cyclins in the inactivation of what we now know is APC-Cdh1 (Amon et al., 1994); more recent work has argued for an additional role for the early expressed B-type cyclins—specifically the S phase Clb5 and the mitotic Clb3 and Clb4 cyclins—in Cdh1 inactivation (Huang et al., 2001; Yeong et al., 2001). However, the relative contribution of G1, S-phase, and mitotic cyclins is unclear. Later mitotic cyclins (Clb1,2) may maintain inhibitory Cdh1 phosphorylation, although this has not been demonstrated directly.

It is important to know the predominant kinase or kinases responsible for inhibitory Cdh1 phosphorylation. As Cdh1 drives mitotic cyclin degradation, if it is itself inactivated by mitotic Clb-CDK activity, this may allow for a positive feedback loop architecture governing Cdh1 activity rooted in Cdh1 phosphorylation. However, while Cdh1 targets the mitotic cyclins Clb2 and Clb3 (Zachariae et al., 1998a), and by homology most likely Clb1 and Clb4, in contrast the S phase cyclin Clb5 is a poor Cdh1 substrate. A physiologically significant role for Clb5 in Cdh1 inactivation would likely couple Cdh1 regulation to a Cdc20-Clb5 negative feedback oscillator (Cross, 2003). Cdc20 is required for cell-cycle appropriate Clb5 destruction (Shirayama et al., 1999), although the SCF has also been reported to degrade it (Bai et al., 1996). Alternatively, as SCF and not the APC is responsible for destruction of the S-phase cyclin Clb6 (Jackson et al., 2006) and the G1 cyclins, their involvement in Cdh1 inactivation would dictate still different circuitry.

Interestingly, deletion of *CLB5* rescues viability of *cdc20 pds1* strains (Shirayama et al., 1999); one interpretation of this is that the deletion of *CLB5* results in a shift of Cdh1 to less phosphorylated and thus less inhibited state that allows for mitotic exit, likely through mitotic Clb destruction (Wäsch and Cross, 2002). The presence of such circuitry does not preclude regulatory phosphorylation by G1 or mitotic cyclins, or still other kinases, which could contribute in an additive or synergistic fashion.

Mapping of Cdh1 phosphorylation sites

Mass spectroscopy has confirmed extensive phosphorylation of Cdh1 in vivo, including both CDK and non-CDK sites (Hall et al., 2004). These included six CDK sites—T12, T157, T173, T176, S239, and S436—as well as possible phosphorylation of S16 and S169 (whose peptides had other potentially phosphorylatable residues, and for which there was not adequate tandem mass spectrometry data for exact site determination). At least nine other non-CDK phosphorylation sites were also detected (Hall et al., 2004). Most Cdh1 molecules contained between four and five phosphates (Hall et al., 2004). Mass spectroscopy on Cdh1 with either CDK or non-CDK sites ablated suggested dependence of non-CDK-site phosphorylation on CDK sites, but not the reverse (Hall et al., 2004). The reported *in vitro* Cdc5 phosphorylation sites S125 and S259 (Crasta et al., 2008) were not detected *in vivo* (Hall et al., 2004). The pattern of Cdh1 phosphorylation does not appear to change from inactivation in S-phase until the end of mitosis (Hall et al., 2004); this may argue against significant CDK inhibition by kinases that are expressed beyond S-phase, such as Cdc5.

Cdh1 in vertebrate development

Cdh1 functions as a G1 stabilizer, and in budding yeast, it is required for proper pheromone-induced G1 arrest (Schwab et al., 1997). G1 stabilization may allow Cdh1 to function as a developmental regulator in metazoans. In neurons, Cdh1 targets Id2 (Inhibitor of Differentiation 2) for destruction, coupling cell cycle exit and differentiation/axonal growth (Lasorella et al., 2006). Cdh1 has been implicated in the differentiation of non-neural tissues as well (Li et al., 2007), and thus could couple cell cycle exit and differentiation.

Rationale for the present study

This thesis examines how APC-Cdh1 is regulated, and the consequences of misregulating its activity. All studies are done in the budding yeast *Saccharomyces cerevisiae*, a haploid eukaryote whose cell cycle is well characterized and substantially conserved with higher eukaryotes. Genetic manipulation of *S. cerevisiae* is extensively developed, including homologous recombination that allows for precise alterations of endogenous genes.

Most previous work on Cdh1 has relied heavily on overexpression, resulting in conflicts over mechanisms and significance of APC-Cdh1 regulation. Here we employ exact gene replacements and careful cell biological characterization to clarify key mechanisms of Cdh1 regulation, and to dissect the consequences of its misregulation.

CHAPTER TWO

Requirements and reasons for effective APC-Cdh1 inhibition

Inhibitory CDK phosphorylation of Cdh1 is essential

CDH1-m11, which lacks all CDK phosphorylation sites (Figure 2.1), is lethal when overexpressed (Zachariae et al., 1998a) but has been reported to allow viability when carried on a plasmid under control of its endogenous promoter, suggesting the former result to be an artifact of overexpression (Jaquenoud et al., 2002) . To determine rigorously whether CDK-mediated Cdh1 phosphorylation was required for viability at endogenous expression levels, we sought to create an exact chromosomal gene replacement of *CDH1* with *CDH1-m11.* We used a recombination-based approach, in which two copies of *cdh1-m11*, each rendered non-functional by insertion of different selectable markers at different positions, were arranged in tandem at the endogenous locus. Recombination between the two copies can be selected for, and recombinants simply scored for retention of the insertional markers. *CDH1-m11* exact gene replacements should lack both markers (Figure 2.2). No recombinants yielding uninterrupted *CDH1-m11* were obtained (Figure 2.2). The critical region for this recombination did yield frequent recombinants using a control allele, comprised of two similarly interrupted *cdh1-m11* alleles in the opposite order. Recombinants using the control allele will all be non-functional due to retention of insertional marker(s). These results suggested that intact *CDH1-m11* is severely deleterious as an exact gene replacement.

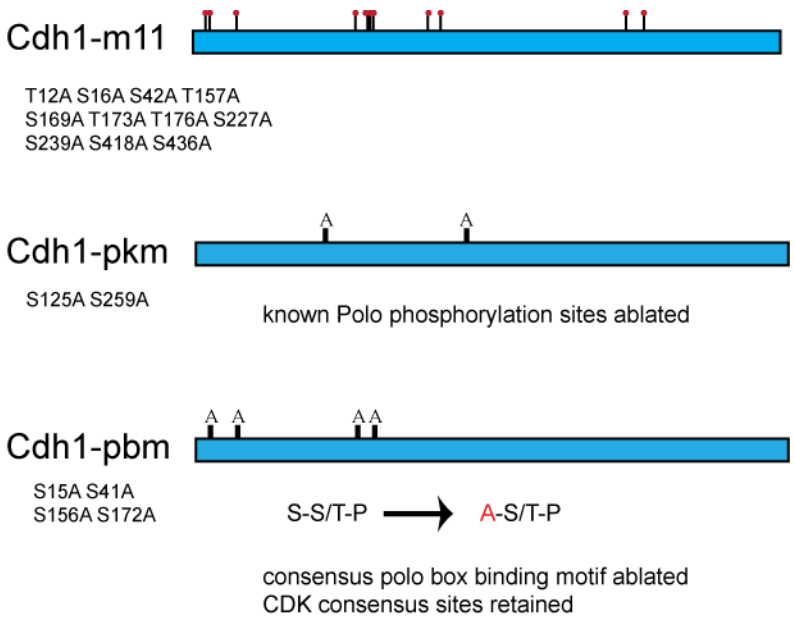

Figure 2.1 *CDH1* alleles constructed for this chapter. *CDH1-m11* (top) has the eleven putative CDK phosphorylation sites mutated to alanines (red dots), such that the resultant protein is unphosphorylatable by CDK. *CDH1-pkm* (middle) has the two known Cdc5 (Polo-like kinase) sites mutated to alanine. *CDH1-pbm* (bottom) codes for an alanine substitution in the first residue of the polo binding box, such that it ablates the polo binding box itself while maintaining the neighboring CDK consensus site.

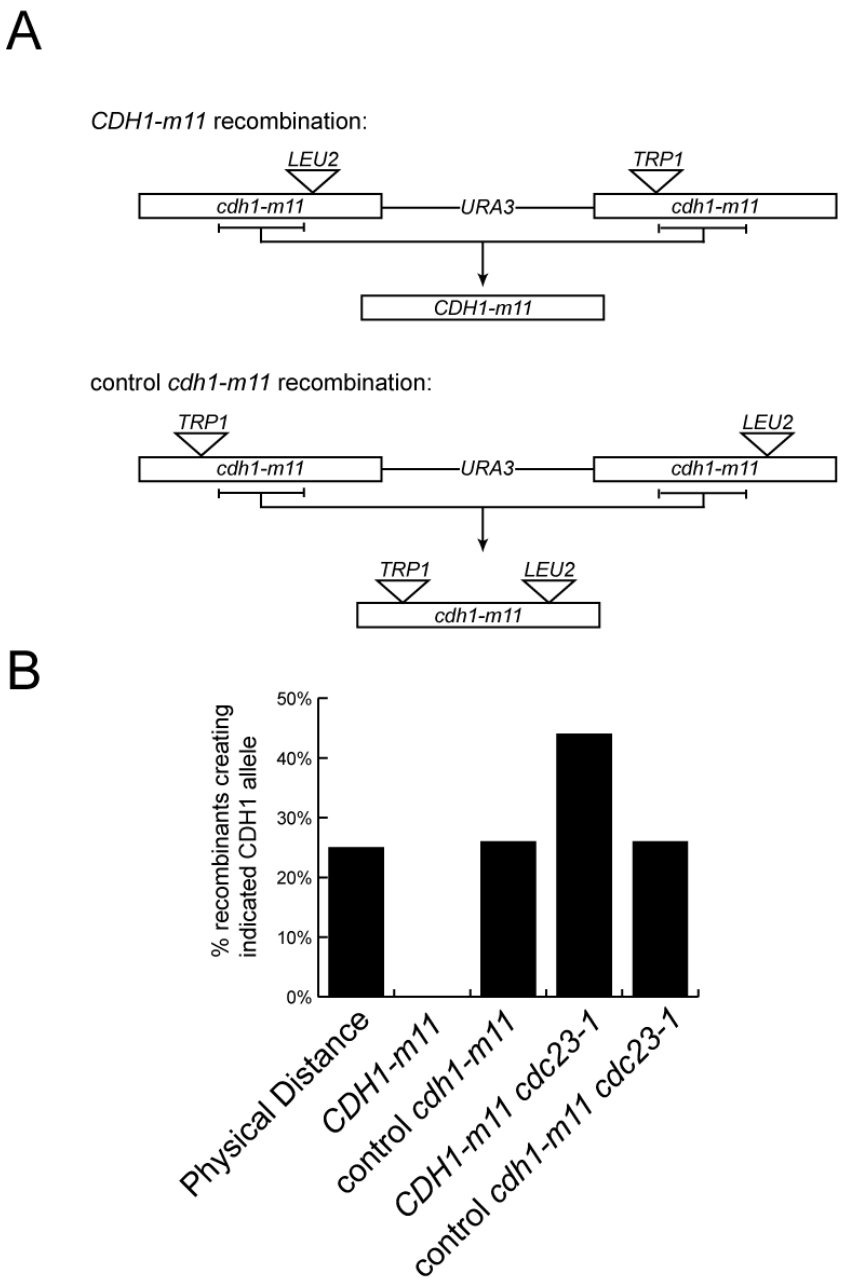

Figure 2.2 Cdh1 inhibition requires CDK phosphorylation. **A**. Recombination-based strategy used to obtain *CDH1-m11* as an exact gene replacement (top), and control recombination (bottom). Horizontal bracket indicates region of recombination that recreates either *CDH1-m11* or the doubly-interrupted control *cdh1-m11*. **B.** Percentage of *CDH1-m11* or control disrupted *cdh1-m11* alleles recovered as determined by selectable markers. Intact *CDH1-m11* was not recovered in the presence of a wild type APC.

CDH1-m11 gene replacement could be deleterious due to unregulated APC activation; however, previous studies have suggested an APC-independent mechanism for lethality of overexpressed Cdh1-m11 (Thornton et al., 2006). Cdc23 is an essential subunit of the APC; *cdc23-1* is hypomorphic for APC-Cdh1 activity even at the permissive temperature (Schwab et al., 2001). In contrast to failure of recovery of *CDH1-m11* recombinants in a *CDC23* background, *CDH1-m11 cdc23-1* recombinants were readily obtained (Figure 2.2), and confirmed to be exact by mapping and sequencing of PCR products from the recombinants. When we attempted to cross these recombinants to *CDC23* strains, doubly heterozygous diploids were not obtainable, suggesting that *CDC23* and *CDH1-m11* made a dominantly lethal combination and that the lethality of *CDH1-m11* is APC dependent.

This result enabled us to perform a high copy suppressor screen for *CDH1-m11*, by transforming a wild type strain with a genomic library, crossing the pool of transformants to a *CDH1-m11 cdc23-1* strain at the permissive temperature, and selecting for viable diploids. High-copy *ACM1* was isolated multiple times in independent clones from the genomic library, but no other strong positives were obtained. We found that we could readily construct *GAL-ACM1 CDH1-m11* strains that were viable on galactose medium (*GAL-ACM1* on, Acm1 overexpressed) but inviable on glucose medium (*GAL-ACM1* off, only endogenous levels of Acm1 present) (Figure 2.3). We carried out a high-copy plasmid suppression screen for viability of such a strain on glucose medium, once again obtaining only multiple *ACM1* clones. These results suggest (but do not prove) that Acm1 may be the only regulator able to restrain activity of unphosphorylated Cdh1.

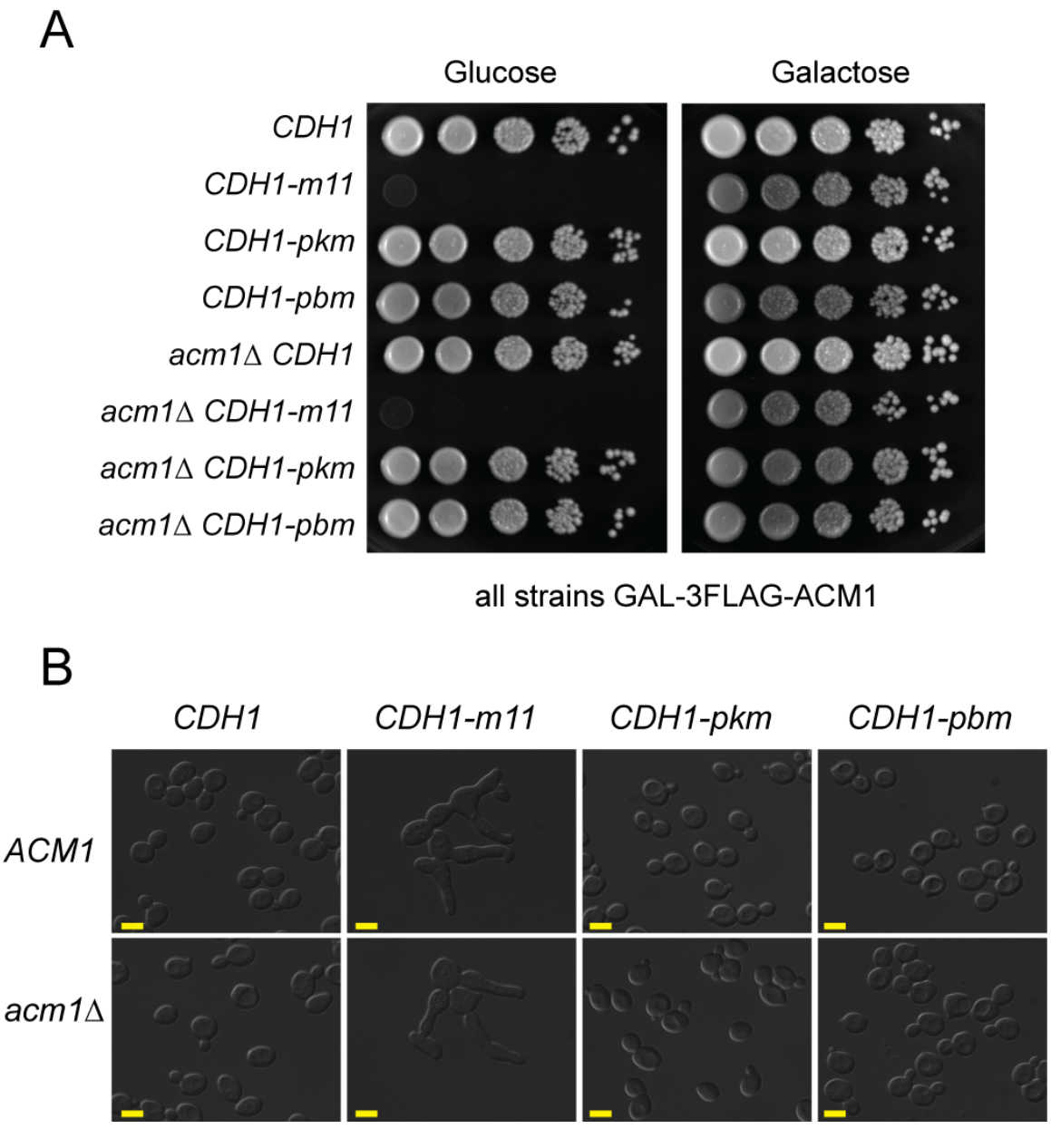

Figure 2.3 Cdh1 inhibition does not require Cdc5 phosphorylation or Acm1. **A.** Tenfold serial dilutions performed on strains containing galactose-inducible Acm1 and the indicated *CDH1* exact gene replacements. **B.** DIC images of strains from (A) after 8 hours in glucose. Note the hyperpolarized growth present only in *CDH1-m11* strains. Scale bars are 5 microns.

Cdc5 phosphorylation of Cdh1 is not required for cell viability

Cdc5 has been reported to act in concert with CDK phosphorylation to mediate complete Cdh1 inhibition (Crasta et al., 2008). Cdc5 can phosphorylate Cdh1 on serines 125 and 259 (Crasta et al., 2008). It has been proposed that phosphorylation of Cdh1 on these sites is required for complete Cdh1 inactivation, to allow for spindle pole body separation and mitotic spindle assembly. Furthermore, Cdc5-mediated inhibition of Cdh1 was reported to be essential in the absence of *ACM1* (Crasta et al., 2008). However, these experiments were all carried out under conditions of overexpression. Therefore, we created an exact gene replacement ablating these two known sites of Cdc5 phosphorylation ('*CDH1-pkm*') (Figure 2.1). We initially introduced this gene replacement into a *cdc23-1* background (see above), and confirmed the structure of the CDH1-pkm allele by sequencing of PCR products. We then crossed this allele into a *CDC23 GAL-ACM1* background. The resulting *CDH1-pkm GAL-ACM1 CDC23* strains were not dependent on *ACM1* overexpression for viability, as evidenced by complete viability upon shutoff of *GAL-ACM1* (Figure 2.3), and Mendelian recovery of fully viable *CDH1-pkm CDC23* segregants lacking *GAL-ACM1* (data not shown).

It has been argued that endogenous Acm1 restrains Cdh1 in the absence of Cdc5 phosphorylation (Crasta et al., 2008). However, *CDH1-pkm acm1* strains were viable with no obvious growth or morphological defects. Efficient degradation of the major mitotic cyclin Clb2 is Cdh1-dependent (Schwab et al., 1997; Visintin et al., 1997), and *CDH1-pkm acm1* strains accumulate and destroy Clb2 with normal kinetics (Figure 2.4). It was reported that the lethality of Cdh1 lacking Cdc5 phosphorylation sites was the result of an inability to separate SPBs. However, we observed wild-type proportions of

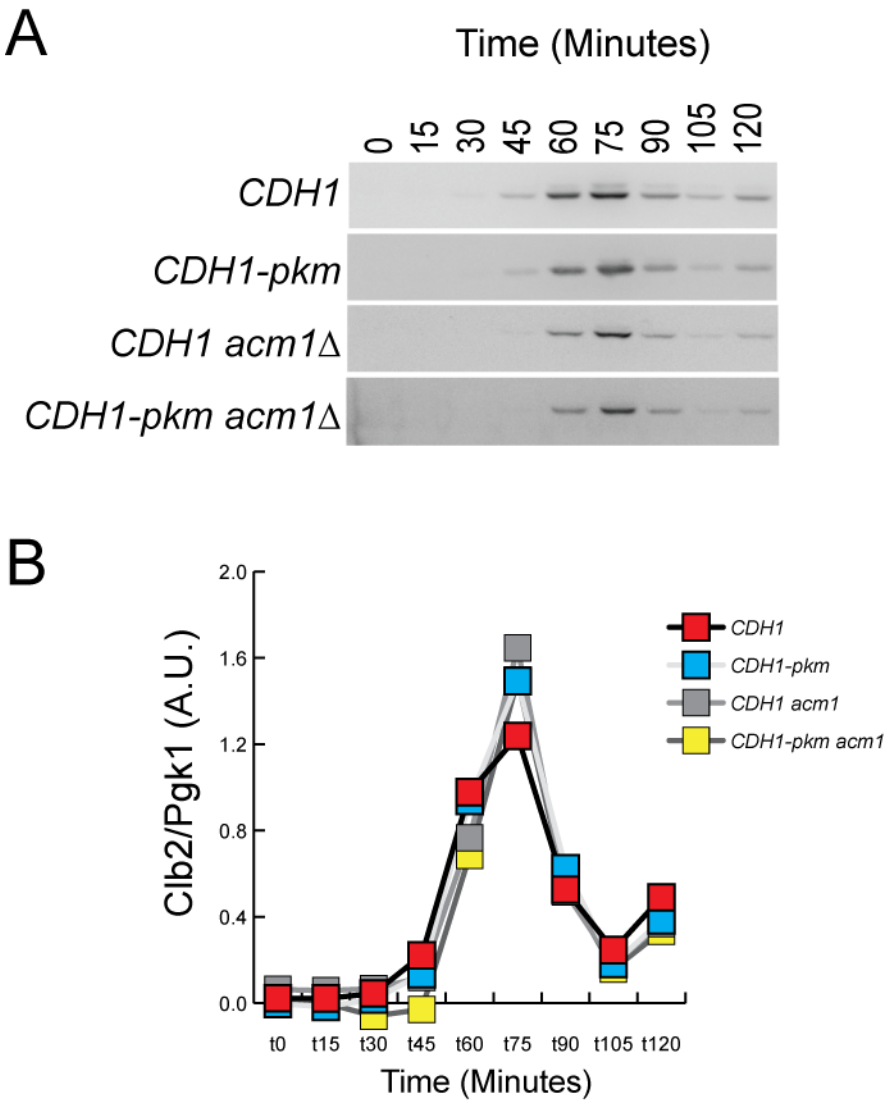

Figure 2.4 Clb2 oscillation is not altered in *CDH1-pkm* cells. **A** Time course of cells of the indicated genotype released from an α-factor block, and immunoblotted against Clb2. **B** Quantification of Clb2 levels from strains in A, normalized to Pgk1.

cells with separated and unseparated SPBs in asynchronous cultures of *CDH1-pkm acm1* strains (Figure 2.5).

These results rule out any significant role in Cdh1 inhibition for Cdc5 phosphorylation of S125 and S259, the only known Cdc5 sites in Cdh1. However, there could be other unidentified Cdc5 sites. While phosphorylation of S125 and S259 was not detected in a mass spectrometry survey, phosphorylation of numerous other non-CDK sites was observed (Hall et al., 2004). Cdc5-dependent phosphorylation of diverse targets requires polo box binding motifs (PBBs) in the substrate. PBBs have the consensus sequence S-pS/pT-P, with the required phosphorylation frequently created by proline-directed CDK activity (Elia et al., 2003). There are four such sites in Cdh1, which were collectively demonstrated to promote binding of Cdc5 to CDK-phosphorylated Cdh1(Crasta et al., 2008). Therefore, we constructed a *CDH1* allele in which the initial serines in the four PBBs were mutated to alanines (Figure 2.1). This manipulation is predicted to block Cdc5 binding but not CDK phosphorylation (since the initial S is not part of the CDK consensus S/T-P). This allele, *CDH1-pbm*, thus may uncouple CDK from Cdc5 phosphorylation. Previous experiments eliminated the PBB by mutating the CDK sites themselves, which makes results ambiguous as to whether Cdc5 or CDK is the relevant kinase being prevented from phosphorylating Cdh1 (Crasta et al., 2008).

Using the same strategy as described above for *CDH1-pkm*, we constructed an exact gene replacement of *CDH1* with *CDH1-pbm*, and found that this allele had no discernible cell-cycle phenotype and no dependence on *ACM1* for viability (Figure 2.3).

Overall, our results from endogenous expression levels of Cdh1 do not support a significant cell-cycle role for Cdc5-dependent phosphorylation of Cdh1, at endogenous

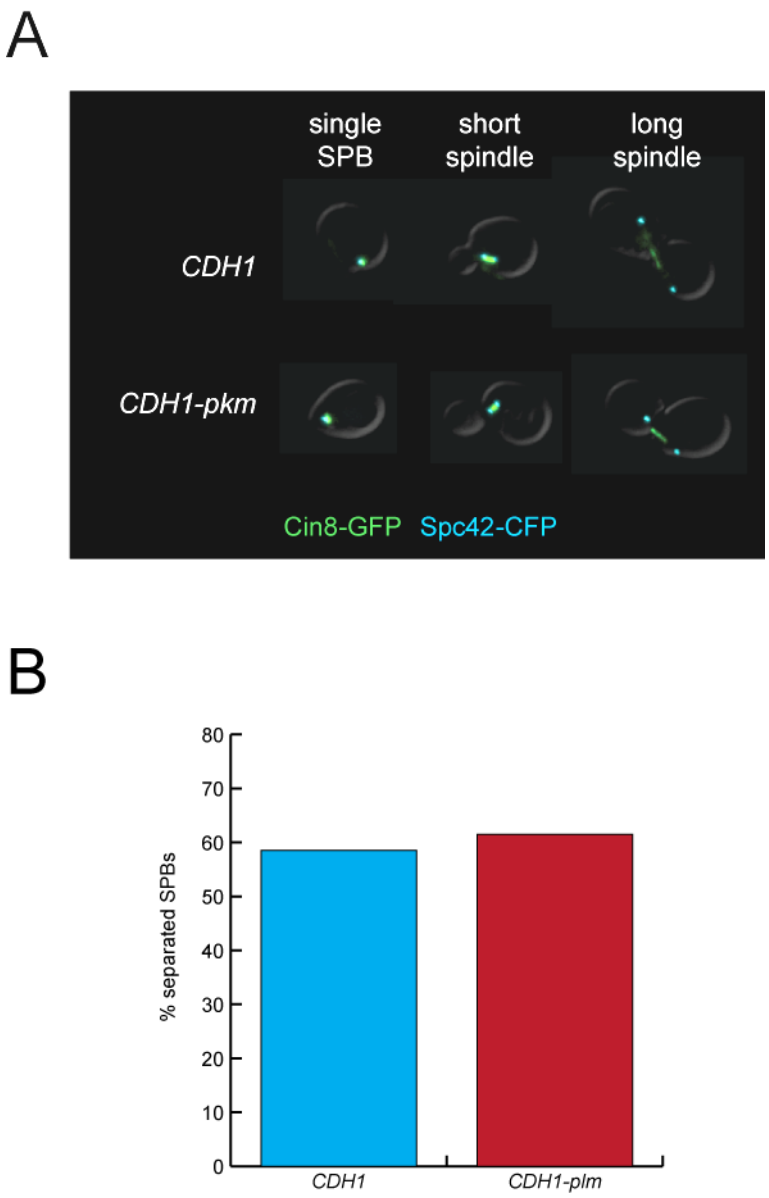

Figure 2.5 Bipolar spindle assembly is not altered in *CDH1-pkm* cells. **A** *CDH1-pkm* strains form morphologically normal long and short spindles, images from fixed cells from an asynchronous population **B** Percentage of asynchronous *CDH1* and *CDH1-pkm* cells with separated SPBs.

expression levels, in sharp contrast to the essentiality of CDK-dependent phosphorylation of Cdh1. We cannot formally exclude the possibility that there are other sites of Cdc5 phosphorylation and/or other non-consensus PBBs; however previous biochemical work argues against this (Crasta et al., 2008).

CDH1-m11 at the endogenous locus results in first-cell-cycle arrest with replicated DNA, hyperpolarized bud growth, low levels of Cdh1 target proteins, and a heterogeneous spindle pole body phenotype

To determine the lethal phenotype of cells expressing Cdh1-m11 (CDK-unphosphorylatable) at endogenous levels, we arrested *GALL-HA-ACM1 CDH1-m11* cells (*GALL* is a weakened version of the *GAL1* promoter (Mumberg et al., 1994)) in G1 using α-factor in galactose medium. We transferred the cells to glucose medium to turn off the *GALL* promoter and deplete HA-Acm1, and then released the α-factor block. By immunoblot, HA-Acm1 was greatly reduced in α-factor as expected (Enquist-Newman et al., 2008; Hall et al., 2008; Ostapenko et al., 2008), and undetectable after glucose incubation. Both *CDH1-m11* and *CDH1* control cells released synchronously and with comparable kinetics from the α-factor block, as indicated by bud emergence and expression of Clb5 (Figure 2.6). Clb5 is an early-expressed B-type cyclin that promotes DNA replication, and that is not sensitive to Cdh1 (Figure 2.6B); consistent with timely Clb5 accumulation, kinetics of DNA replication in *CDH1-m11* and *CDH1* cells were indistinguishable (Fig 2.6C). Clb5 levels then declined, remaining at approximately a quarter of peak in the arrested *CDH1-m11* cells.

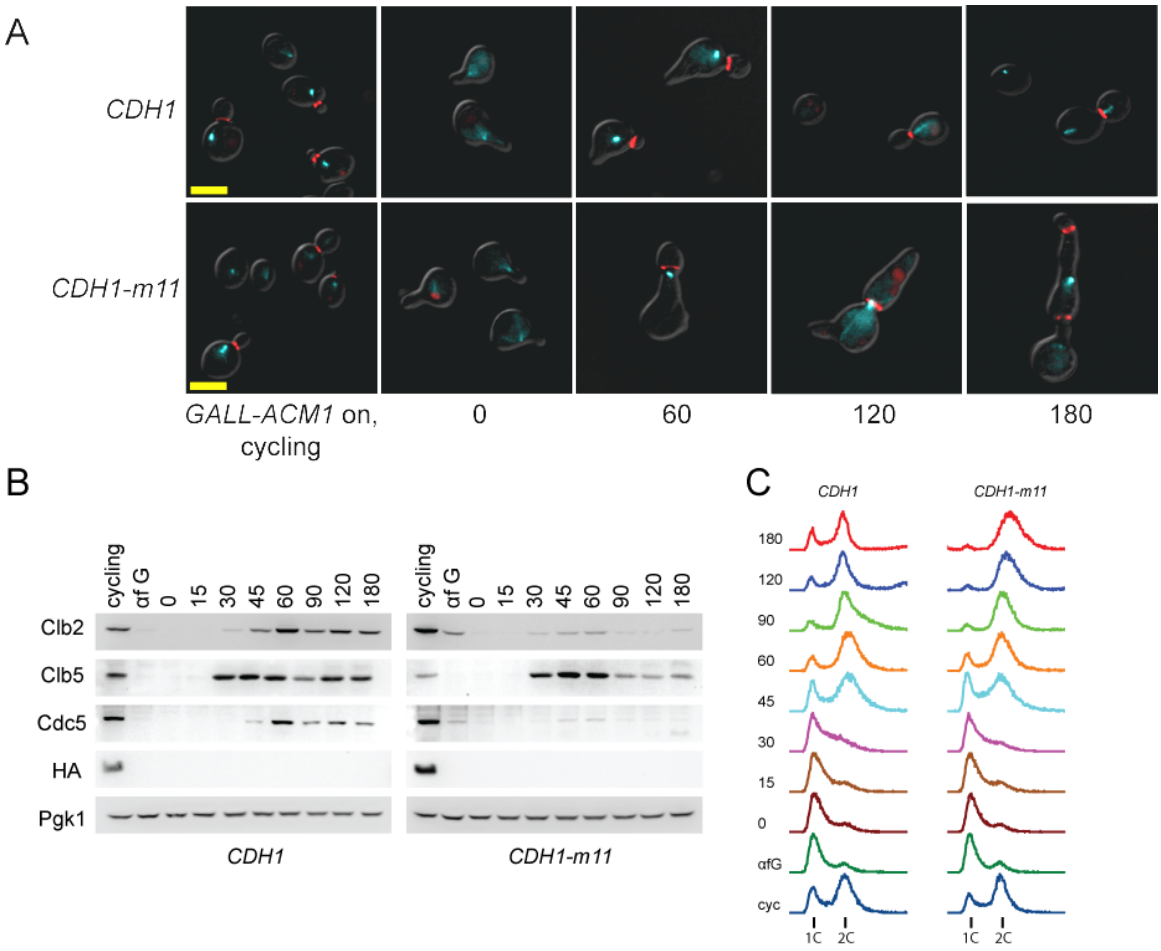

Figure 2.6 *CDH1-m11* results in a first-cycle arrest. **A** *CDH1-m11* or *CDH1* cells (both *GALL-HA-ACM1*) were arrested in G1 with α-factor, depleted of HA-Acm1, and synchronously released. Fluorescence microscopy of Myo-mCherry (red) marking the bud neck, and Tub1-CFP (cyan) were taken at the indicated timepoints after release from α-factor. *CDH1-m11* cells multiply bud as indicated by multiple Myo1 rings. Tubulin signal varies in appearance from a point to a short bar, but elongated spindles are not observed. Scale bar is 5 microns. **B** Immunoblots of cells as in (A) detecting the indicated proteins. Pgk1 is a loading control. 'afG' cells are in α-factor prior to glucose introduction. **C** Bulk DNA flow cytometry of cells as in (A).

In contrast, accumulation of the later-expressed mitotic cyclin Clb2 was significantly reduced in *CDH1-m11* cells, with about a 15-fold reduction in peak Clb2 levels compared to *CDH1* controls. This is consistent with effective Cdh1 deregulation by the CDK site mutations, since Clb2 is a known Cdh1 target. Clb2 expression drives a switch from polarized to isotropic bud growth, and this is blocked in *CDH1-m11* cells (Figure 2.6A). Accumulation of Cdc5, another known Cdh1 target, was similarly reduced in *CDH1-m11* cells. Interestingly, the timing of initial accumulation of both Clb2 and Cdc5 was similar in *CDH1* and *CDH1-m11* cells.

CDH1-m11 cells do not undergo anaphase or cytokinesis. They continue polarized bud growth, and rebud as evidenced by accumulation of fluorescent Myo1-mCherry (a bud site marker) at a novel location along the initial hyperpolarized bud (Figure 2.6A) and/or by a new bud. Spindle morphogenesis appeared defective: Tub1(beta-tubulin)-CFP revealed a range of morphologies from single dots to short bars was detected (Figure 2.6A).

To more accurately examine spindle morphogenesis, we used *SPC42-CFP* and *TUB1-GFP* to label the spindle pole body and microtubules. In these double-labeled cells, an intact bipolar spindle will appear as two distinct blue Spc42-CFP signals connected by a bridge of green Tub1-GFP (Spc42-CFP and Tub1-GFP fluorescent signals were sufficiently spectrally separated to make this determination). Such spindles were almost uniformly observed in *CDH1* controls; at 60 minutes after release over 80% of cells had clearly separated SPBs. In contrast, 70% of *CDH1-m11* cells had a single focus of Spc42-CFP signal (Figure 2.7). We expect, from previous work, that this single Spc42 signal represents duplicated but unseparated SPBs (Crasta et al., 2008; Fitch et al.,

1992). Consistent results were obtained with *SPC42-CFP* alone, as well as with *SPC29-YFP* and untagged *SPC42*, suggesting that the tags did not significantly affect the results.

30% of *CDH1-m11* cells contained short bipolar spindles that did not progress through anaphase. We considered several mechanisms that could account for anaphase failure. If the spindles are aberrant in structure or kinetochore attachment this could trigger the spindle assembly checkpoint to prevent anaphase. However, deletion of the critical checkpoint component *MAD2* had no effect on spindle assembly or function in *CDH1-m11* cells (Figure 2.8).

A failure of cohesin cleavage not dependent upon checkpoint activation could also explain failure of anaphase. Cdh1 has been reported to target Cdc20 for destruction in vivo. Cdc20 promotes anaphase by degradation of the separase inhibitor Pds1, allowing cleavage of the cohesin complex subunit Scc1; sister chromatids can then separate upon loss of cohesion. Failure to accumulate sufficient Cdc20, if it results in an inability to clear Pds1, could account for persistent short bipolar spindles. We find that *CDH1-m11* cells fail to accumulate Cdc20 (Figure 2.9A).

If failure to accumulate Cdc20 accounts for anaphase failure, then Pds1 should remain at high levels in *CDH1-m11* cells. Indeed, we find that Pds1 remains present at near-peak levels at the *CDH1-m11* induced block (Figure 2.9B). Thus Pds1 accumulation and consequent failure of cohesin cleavage could account for anaphase failure. Consistent with this idea, *scc1-73,* a temperature sensitive allele of a cohesin complex subunit, promotes increased spacing between SPBs at the restrictive temperature in *CDH1-m11* cells, indicating that inability to cleave cohesin contributes to the short bipolar spindle phenotype (Figure 2.10).

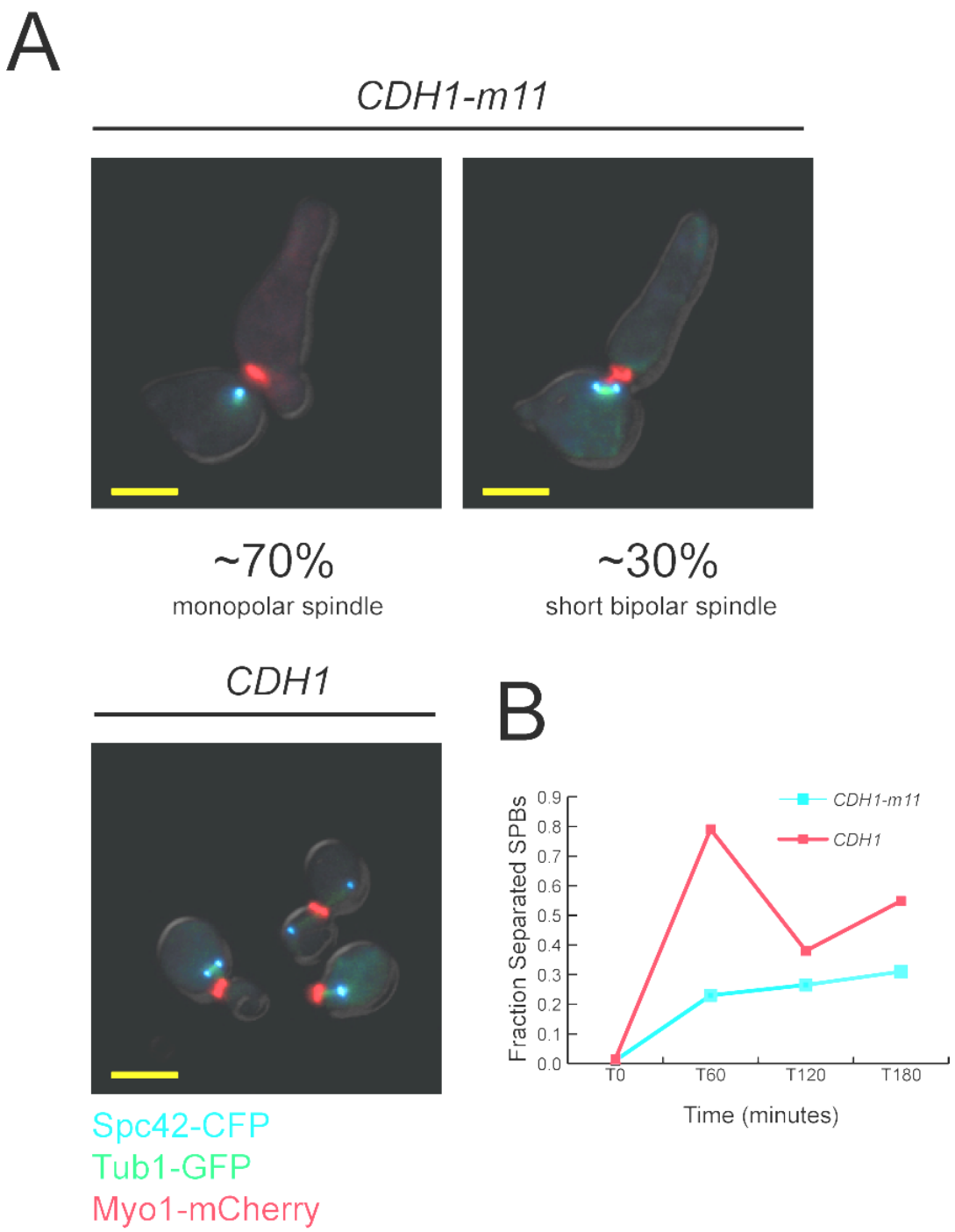

Figure 2.7 *CDH1-m11* cells have a variable spindle pole body phenotype. **A** Fluorescence microscopy for Spc42-CFP (cyan) Tub1-GFP (green) and Myo1-mCherry (red); 30% of *CDH1-m11* cells form bipolar spindles, as indicated by two separate Spc42 dots connected by intervening tubulin-GFP. Strains were treated as in Figure 2, images taken 180 minutes after release. Scale bar: 5 microns. **B** Percentage of cells from (A) with separated spindle pole bodies at the indicated time points.

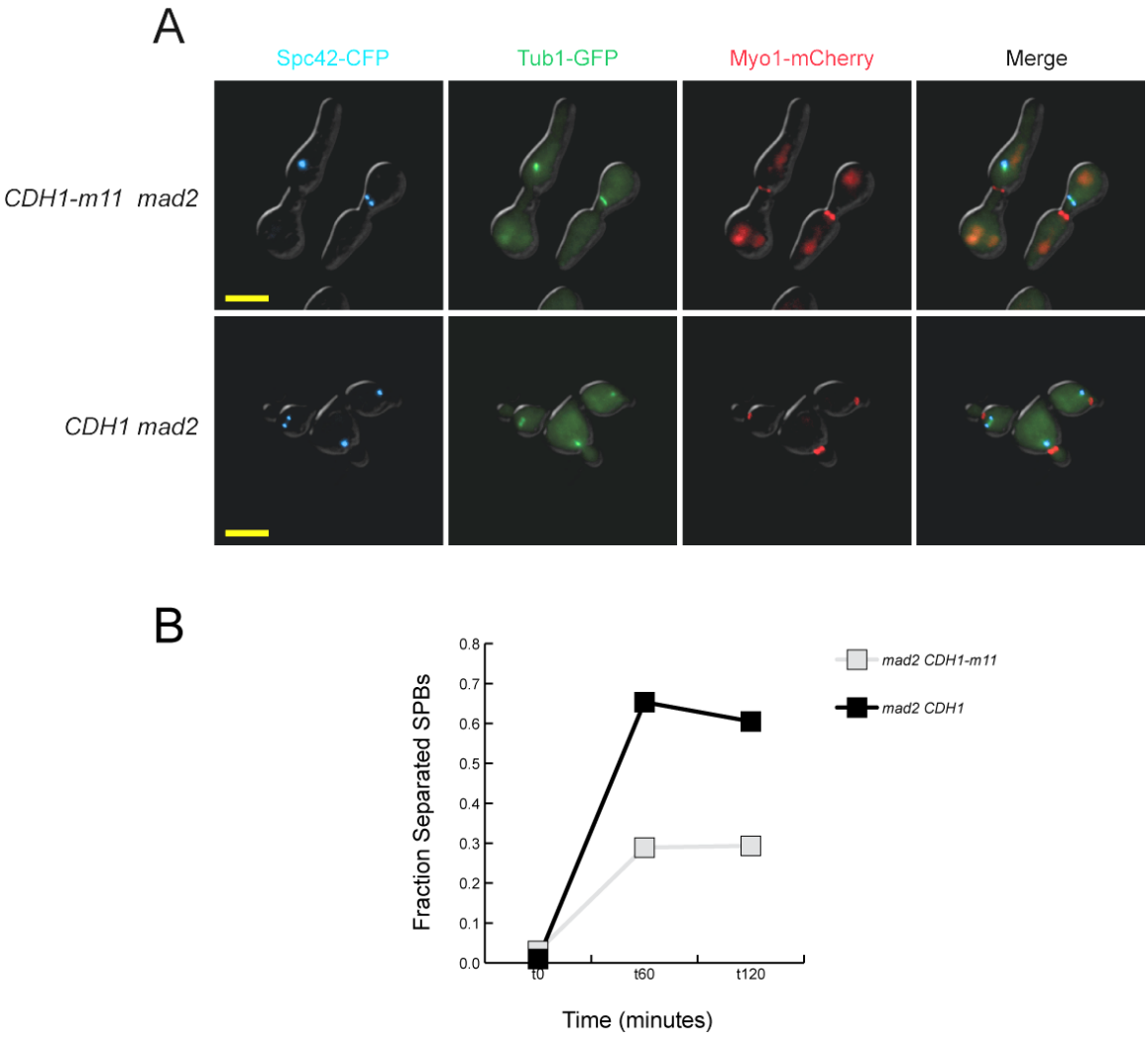

Figure 2.8 Maintenance of short bipolar spindles in *CDH1-m11* cells is not dependent on *MAD2* **A** Micrographs of *mad2 CDH1-m11* or *mad2 CDH1* strains 120 minutes after release from α-factor. Scale bars are 5 microns. **B** Percentage of cells from (A) with separated spindle pole bodies at the indicated time points. Anaphase spindles were not observed.

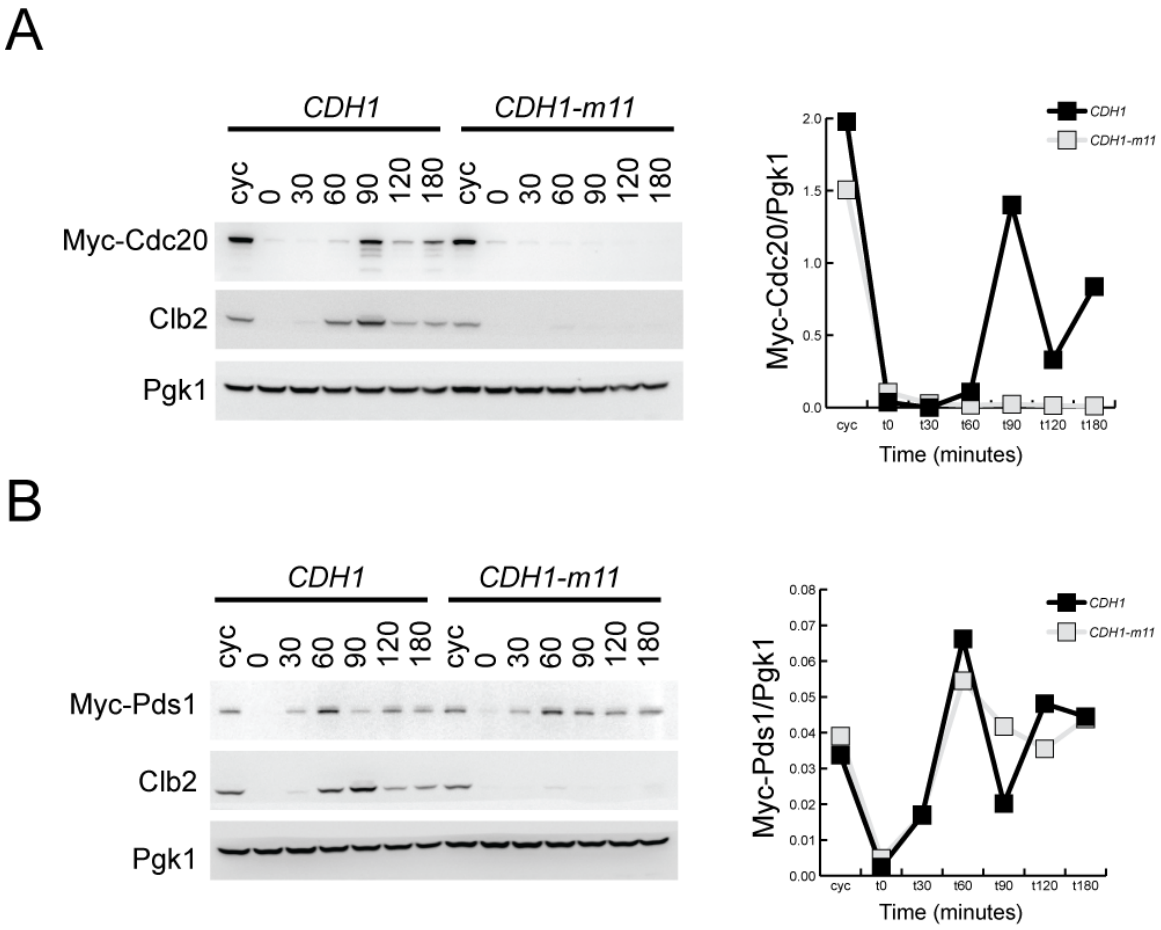

Figure 2.9 *CDH1-m11* cells accumulate Pds1 but not Cdc20 **A** Immunoblots against strains synchronously released from α-factor with endogenously tagged Cdc20 and either *CDH1* or *CD1-m11*, and right, quantification of normalized Myc-Cdc20 levels from immunoblots. **B** Left: immunoblots against strains synchronously released from α-factor with endogenously tagged Pds1 and either *CDH1* or *CDH1-m11*; right, quantification of Myc-Pds1 levels standardized to Pgk1 loading control.

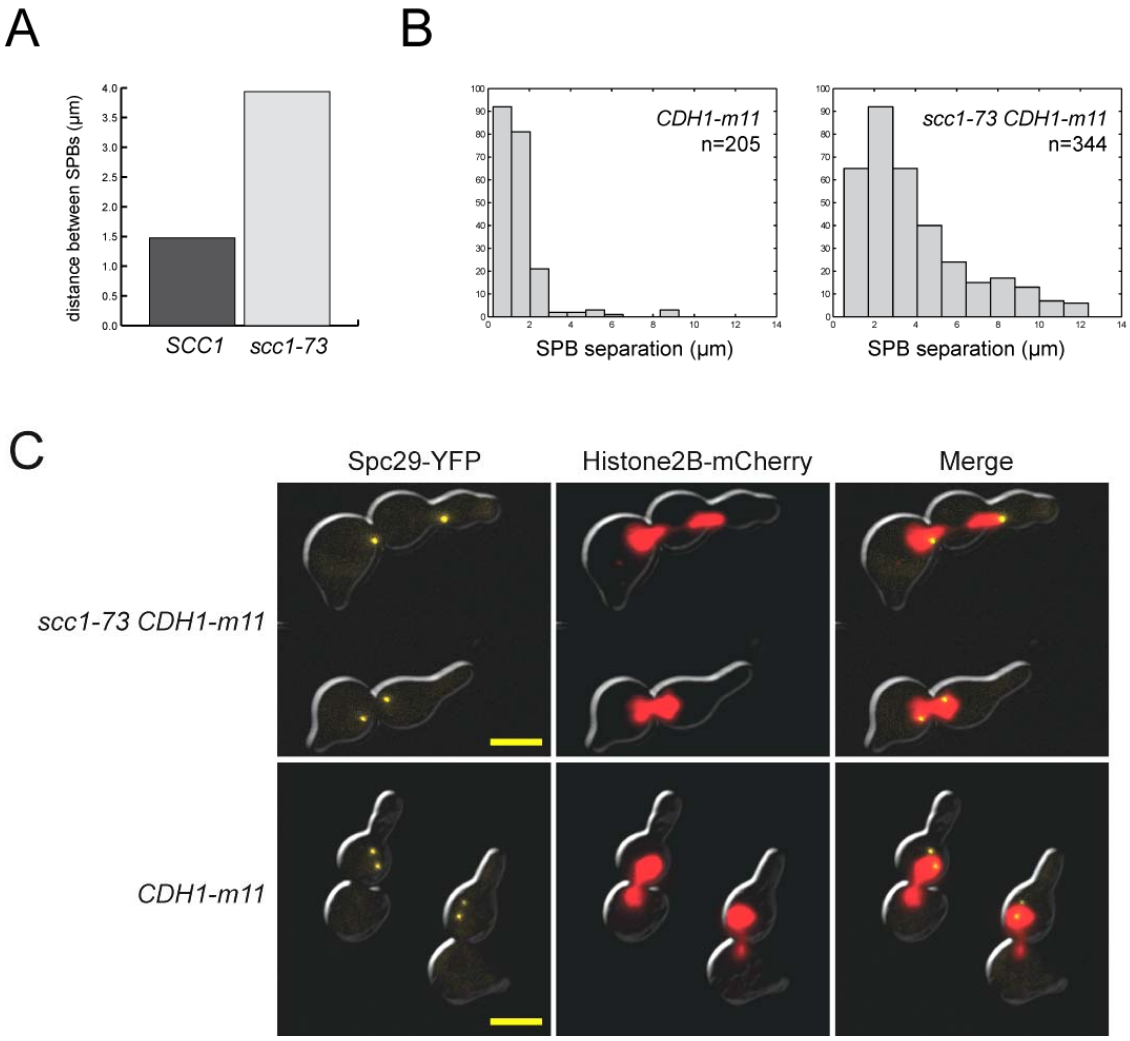

Figure 2.10 *CDH1-m11* cells lengthen their spindles upon cohesin inactivation. **A** Average distance between SPBs in *CDH1-m11 SCC1* and *CDH1-m11 scc1-73* cells at the restrictive temperature, two hours after α-factor release. B. Histogram of the length distribution of spindles in the cells from (A). **C** Fluorescence microscopy of strains from (A) observing the SPB protein Spc29-YFP (yellow) and nuclear Histone2B-mCherry (red).

Cdc20 was reported to promote Pds1 proteolysis much more effectively than mitotic cyclin proteolysis, and Cdh1 was reported to have the opposite specificity (Visintin et al., 1997). Our results are consistent with this idea, since Pds1 persists in the face of unregulated Cdh1-m11. Surprisingly, Pds1 is efficiently targeted by purified APC-Cdh1 in vitro (Rodrigo-Brenni and Morgan, 2007; Thornton et al., 2006), suggesting some additional level of control of proteolysis in vivo.

We noted grossly abnormal nuclear morphology, as monitored with histone H2B-mCherry, in *CDH1-m11* cells, whether or not they contained a bipolar spindle (Figure 2.12). Time-lapse microscopy shows H2B-mCherry signal 'meandering' along the hyperpolarized bud and the mother cell body. Microscopic observations of fixed cells with labeled SPBs and tubulin suggested that this aberrant nuclear migration may be dependent on astral microtubules, since extended mCherry signal frequently coincided with long microtubules that were not terminated with an SPB (Figure 2.11). We do not know the reason for this phenotype, which has not been described previously to our knowledge.

Spindle Pole Body separation in CDH1-m11 cells is dependent on endogenous *ACM1*

The heterogeneous spindle pole body phenotype of *CDH1-m11* cells suggested the possibility that the level of APC-Cdh1 activity in these cells is close to a threshold for spindle morphogenesis. We reasoned that endogenous Acm1 might titrate a sufficient level of Cdh1-m11 to keep the system near this threshold. Consistent with this idea, *CDH1-m11 acm1* cells completely failed to separate spindle pole bodies: <1% of cells, compared to ~30% in *ACM1* cells (Figure 2.12A, B).

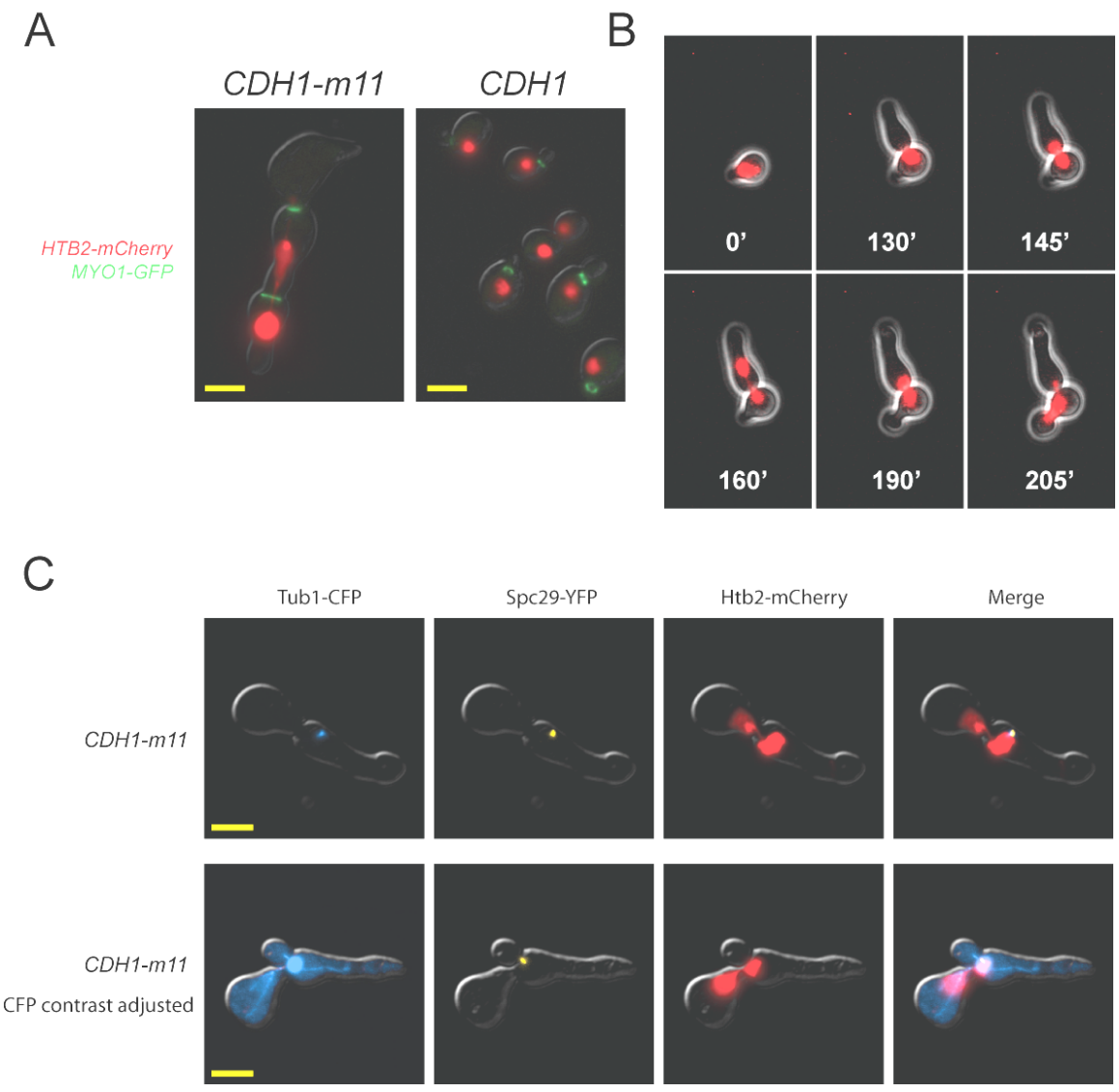

Figure 2.11 *CDH1-m11* results in aberrant nuclear division in the absence of SPB separation. **A** Micrographs of fixed *CDH1-m11* or *CDH1* cells 3 hours after release from α-factor, Htb2-mCherry (red) and Myo1-GFP (green) Scale bars are 5 microns. **B** Frames from time lapse microscopy of the same strain at the indicated times after release from α-factor imaged for Histone-mCherry. Note the ability to divide Histone-mCherry asymmetrically, as well as the subsequent fusion of the two connected nuclear blobs. **C** *CDH1-m11* strains with Spc29-YFP marking the spindle pole body as well as Tub1-CFP and Htb2-mCherry were released from α-factor, with the depicted images taken 3 hours after release. Aberrant nuclear morphology with unseparated spindle pole bodies are apparent. Adjusted CFP-channel contrast (bottom) reveals microtubule structures possibly responsible for aberrant nuclear migration and/or division. Scale bars are 5 microns.

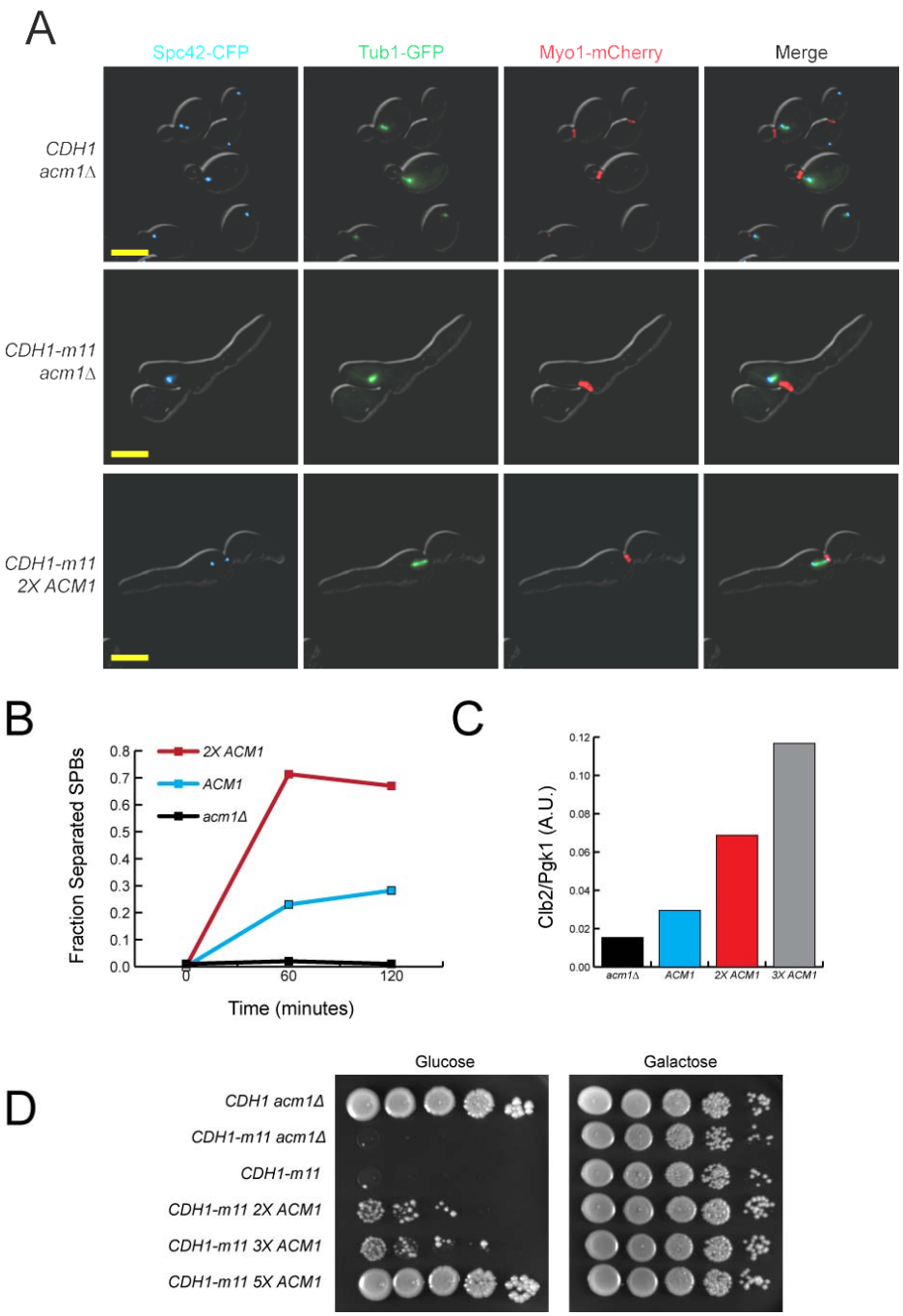

Figure 2.12 The *CDH1-m11* strain spindle pole body phenotype is modulated by endogenous *ACM1*. **A** Fluorescence microscopy of indicated genotypes performed as in Figure 2.7. In *CDH1-m11 acm1* cells, tubulin can be seen emanating from SPBs, but separated SPBs are not observed. *2XACM1 CDH1-m11* cells separate spindle pole bodies and form bipolar spindles. **B** Percentage of synchronized *acm1*Δ, wild type (1X *ACM1*), and 2X *ACM1* cells displaying separated spindle pole bodies at indicated timepoints. **C** Clb2 levels for indicated genotypes at 60 minutes after release from α-factor, standardized to Pgk1 loading control. **D** Tenfold dilution assay for *ACM1* allelic series of strains, as in (A); note that less than 1% of *2XACM1 CDH1-m11* cells form colonies.

If Cdh1-m11 is near a threshold for inhibition by Acm1, then increasing *ACM1* gene dosage should strongly increase APC-Cdh1 inhibition. To test this, we integrated a genomic segment containing *ACM1* at the *URA3* locus in a *GALL-ACM1 CDH1-m11* background. We assessed *ACM1* copy number by quantitative PCR, and found clones with two, three or five copies of *ACM1* (including the endogenous locus). Five copies of *ACM1* fully rescued viability of *CDH1-m11* cells, consistent with the high-copy plasmid suppression results described above. However, 2 or 3 copies were essentially insufficient for rescue (approximately three to four logs drop in viability upon shutoff of *GAL-ACM1* expression) (Figure 2.12D).

Despite lack of rescue of overall viability, *2X ACM1 CDH1-m11 GALL-ACM1* cells were almost all able to form a short bipolar spindle upon *GALL-ACM1* shutoff (Figure 2.12A, B). Strikingly, these cells nevertheless almost quantitatively failed to progress to anaphase.

These results suggest that multiple events in spindle morphogenesis and function are inhibited by Cdh1-m11, since failure of short spindle formation could be quantitatively uncoupled from subsequent anaphase failure by increase *ACM1* gene dosage. It is likely that graded increases in Acm1 levels are accompanied by graded inhibition of Cdh1-m11, as Clb2 levels in *CDH1-m11* strains correlates with *ACM1* copy number (Figure 2.12C). This suggests that different events regulated by Cdh1 have distinct thresholds for inhibition, presumably due to different sensitivity of Cdh1 proteolysis targets.

Restoring levels of the Cdh1 target kinesin Cin8 does not restore spindle pole body separation in *CDH1-m11* cells

Previous work suggested that failure to produce a bipolar spindle without restraint of Cdh1 activity was due specifically to degradation of plus-end kinesins Cin8 and Kip1, since a short bipolar spindle could be obtained by overexpression of undegradable Cin8 in the absence of Cdc28 activity, (which is required for inhibition of APC-Cdh1) (Crasta et al., 2006). We sought to test this idea more directly, with endogenous levels of expression of both Cdh1-m11 and undegradable Cin8. We used the *CIN8-alaKEN* allele (Hildebrandt and Hoyt, 2001), in which the KEN box required for Cdh1-mediated Cin8 degradation was mutated to AAA. Myc-tagged alleles of either *CIN8* or *CIN8-alaKEN* were placed at the endogenous locus (with an untagged *CIN8* allele downstream) in *CDH1-m11 GAL-ACM1* strains. By Western blot, Myc-Cin8 was readily detected in wild-type cells and was found at lower levels in *CDH1-m11* cells after *GAL-ACM1* shutoff compared to *CDH1* controls; Myc-Cin8-alaKEN was detected in comparable levels in both backgrounds (Figure 2.13C). These results are expected since the KEN mutation prevents Cdh1-dependent proteolysis of Cin8 (Hildebrandt and Hoyt, 2001). Consistently, we found similar results using the *CIN8-KED* mutation to inactivate the Cin8 KEN box (Hildebrandt and Hoyt, 2001). Thus, reduction of Cin8 in *CDH1-m11* cells is specifically due to Cdh1-Cin8 interaction via the Cin8 KEN box.

Despite restoration of Cin8 protein levels by the *alaKEN* mutation, *MYC-CIN8-alaKEN* had essentially no effect on the terminal spindle phenotype of Cdh1-m11 cells compared to *MYC-CIN8* or *CIN8* controls (Figure 2.13A, B). The Myc tag on Cin8 was shown previously to be fully compatible with Cin8 function (Hildebrandt and Hoyt,

2001). Therefore, restoration of Cin8 at physiological levels to *Cdh1-m11* cells is not sufficient to allow bipolar spindle formation, strongly suggesting the existence of other Cdh1 targets that are required for bipolar spindle formation. Previous results suggesting that restoring Cin8 might be sufficient for bipolar spindle formation (Crasta et al., 2006) could be explained by the idea that overexpressed Cin8 could exert a strong pulling or polymerizing force between the two SPBs, or could be due to a lack of equivalence between the hypomorphic *CDC28* allele and complete failure of Cdh1 phosphorylation.

Consequences of restoring mitotic cyclins to a Cdh1-m11 block

The Cdh1-m11 arrest is associated with destruction of cell cycle regulators (mitotic cyclins, Cdc5) as well as spindle components (see above). Mitotic cyclins modulate numerous cell cycle processes. Some cell cycle defects in *CDH1-m11* cells could be due specifically and solely to mitotic cyclin proteolysis. To test this, we placed Clb2-kd, an undegradable version of Clb2 lacking both KEN and destruction boxes and therefore immune to APC-mediated proteolysis (Wäsch and Cross, 2002) under the control of the *MET3* promoter, and turned on expression by methionine deprivation in synchronized *CDH1-m11* cells, after they were released from α-factor and allowed to bud. Strikingly, the presence of *CLB2-kd* in *CDH1-m11* cells largely eliminated the *CDH1-m11* hyperpolarized bud growth phenotype (Figure 2.14, 15). Cdc5 protein does not reappear after Clb2-kd expression, suggesting that APC-Cdh1-m11 remains active in the presence of undegradable Clb2.

In addition, Clb2-kd had striking though variable effects on SPB and tubulin morphology. The majority of *CDH1-m11* cells in which Clb2-kd was expressed had at

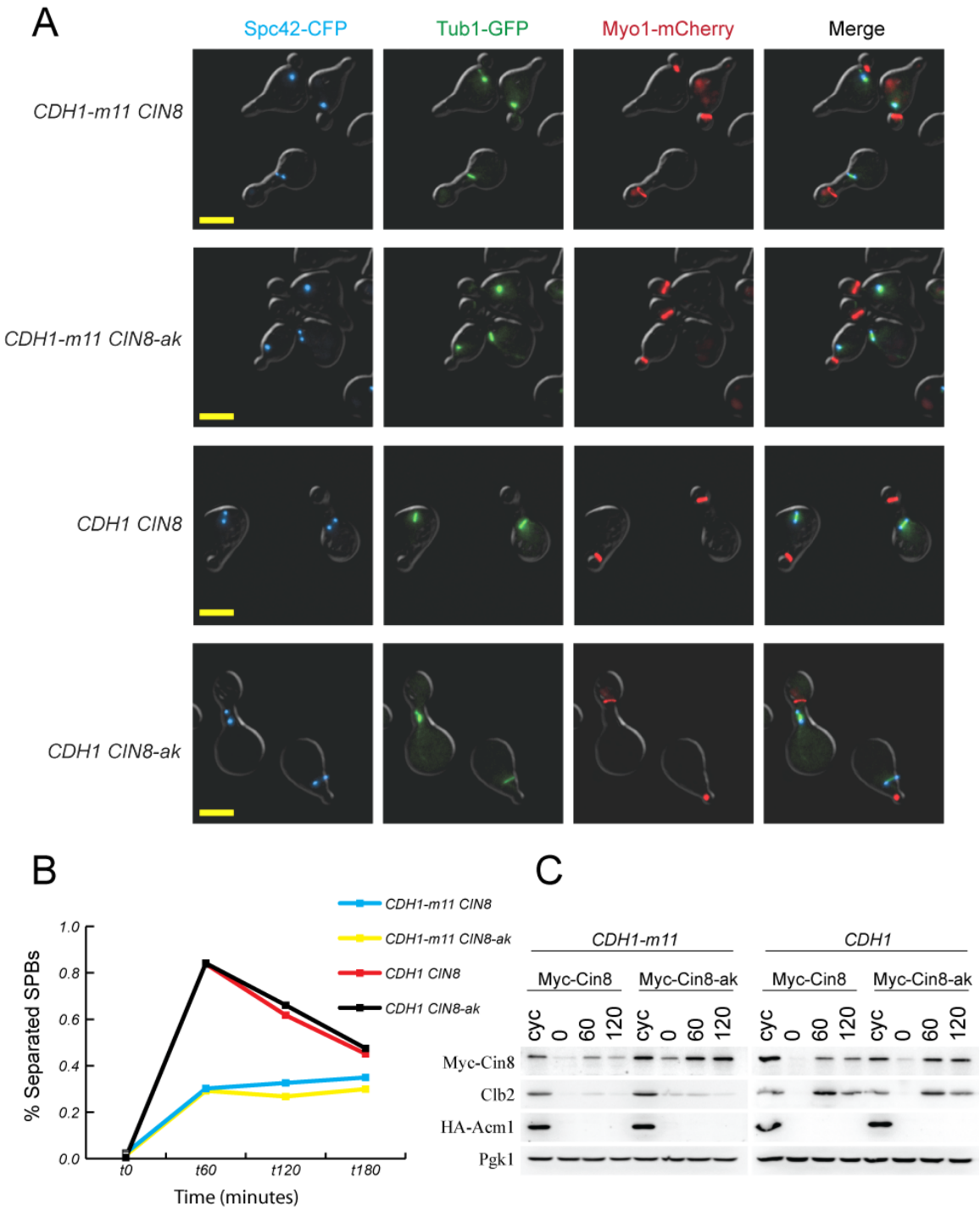

Figure 2.13 Cdh1-resistant *CIN8* does not promote bipolar spindle assembly in *CDH1-m11* cells **A** Fluorescence microscopy of cells with *MYC-CIN8* or Cdh1-resistant *MYC-CIN8-ak* (coding for Myc-Cin8-alaKEN, with KEN box residues mutated to alanine), 60 minutes after release from α-factor block. Scale bars are 5 microns. **B** Quantification of SPB separation of cells from **A** at indicated timepoints from α-factor release. **C** Immunoblots of released cells. Clb2 and exogenous HA-Acm1 are degraded normally. Cin8-ak is resistant to Cdh1-m11 mediated proteolysis.

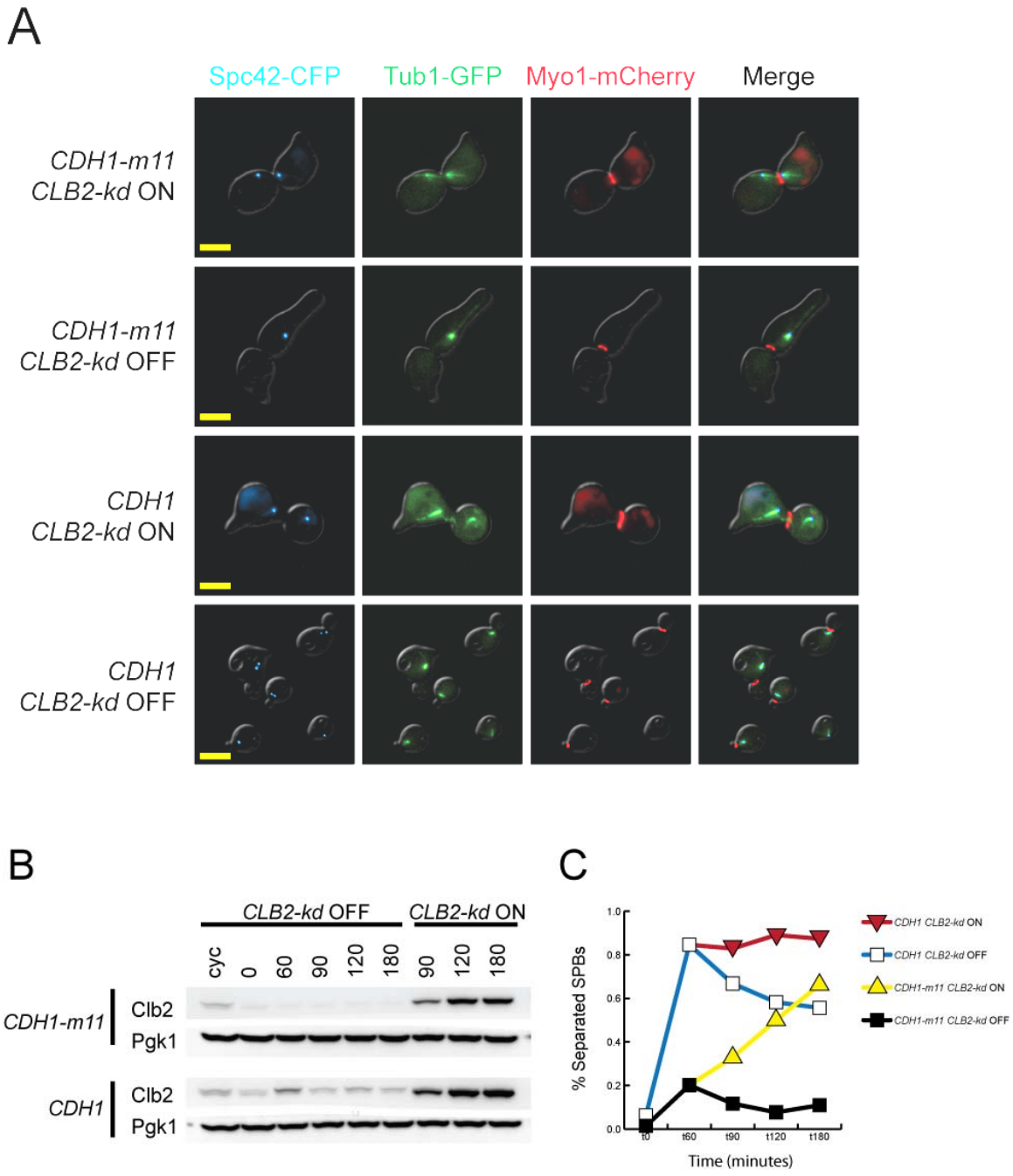

Figure 2.14 Restoration of mitotic cyclin Clb2 promotes bipolar spindle pole body separation in *CDH1-m11* cells. **A** *MET3pr-Clb2-kd* cells, with either *CDH1* or *CDH1-m11*, were synchronized in α-factor, released, and Clb2-kd induced 60 minutes after release; images were obtained 180 minutes after α-factor release. Scale bars: 5 microns. **B** Clb2 immunoblot for cells in A. Clb2 antibody detects both endogenous Clb2 and Clb2-kd. Pgk1 serves as a loading control. **C** Quantification of cells with separated SPBs from (**A)**.

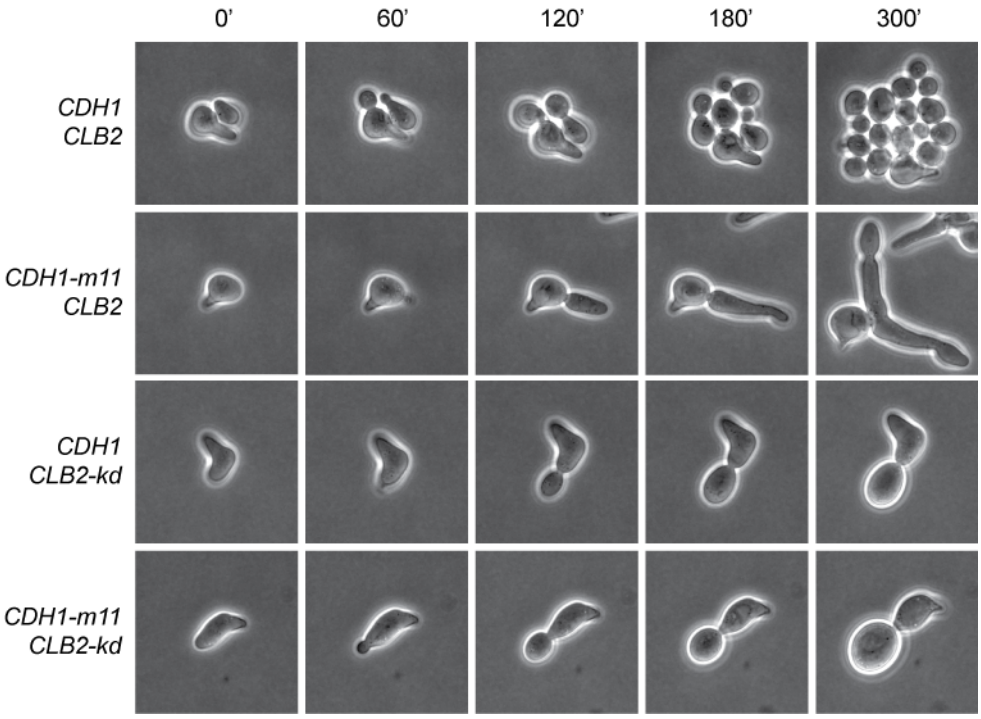

Figure 2.15 Restoration of mitotic cyclin Clb2 restores isotropic growth in *CDH1-m11* cells. Single-cell time-lapse microscopy of strains of the indicated genotypes (all exact gene replacements), with minutes after release from α-factor indicated.

least two foci of SPC42-CFP signal, instead of the single signal predominantly observed in controls without Clb2-kd (Figure 2.14). This effect was detectable when Clb2-kd levels were similar to those attained with Clb2-kd expressed from the endogenous locus, (this level was attained transiently, 30 minutes after induction; fully induced Clb2-kd levels from the *MET3* promoter plateau at approximately threefold the level of Clb2-kd under its endogenous promoter).

Spc42-CFP foci in *CDH1-m11 MET3-CLB2-kd* cells were sometimes associated with intervening Tub1-GFP signal, as in a normal metaphase spindle; in other cells, little or no polymerized tubulin could be detected. Various other abnormal structures were observed, including multiple (three or more) Spc42-CFP foci. The total signal intensity of Spc42-CFP foci in these cells at 180 minutes after release was approximately half that of either *CDH1-m11* cells not expressing Clb2-kd or the same cells prior to Clb2-kd induction. This suggests that duplicated SPBs separate in response to Clb2-kd expression, resulting in two foci, that each with a level of Spc42 comparable to a normal SPB (Figure 2.16). Therefore, failure of SPB separation in *CDH1-m11* cells might be specifically due to Cdh1-mediated degradation of Clb2 and other mitotic cyclins. Nevertheless, reintroduction of Clb2 into *CDH1-m11* cells by this method results in severe disruption of normal spindle morphogenesis in most cells, perhaps due to alterations in microtubule dynamics (Higuchi and Uhlmann, 2005). Normal spindle morphogenesis requires not only mitotic cyclin stabilization but also stabilization of other proteins, likely including spindle morphogenesis proteins such as Cin8, Ase1 and Fin1; we have not tested the effects simultaneous stabilization of multiple APC-Cdh1 substrates in *CDH1-m11* cells.

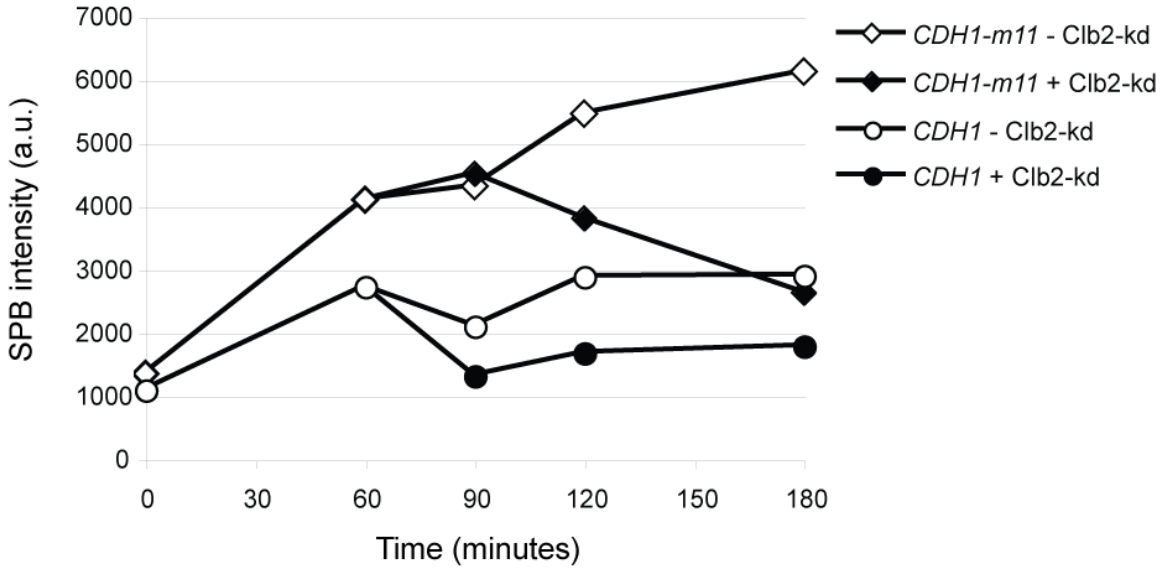

Figure 2.16 *CLB2-kd* induction in *CDH1-m11* cells approximately halves the intensity of fluorescent SPB foci. SPB intensity, assessed by an automated analysis, of the CFP-channel images from the experiment described and depicted in Figure 2.14, for indicated time points. At least 200 cells were analyzed and averaged for each data point.

As noted above, Clb2-kd under the *MET3* promoter was not much overexpressed in this experiment compared to the level of Clb2-kd expressed from the endogenous locus. Consistent with this, comparable effects on cell polarity and spindle morphogenesis were obtained in *CDH1-m11* cells bearing an exact endogenous gene replacement of *CLB2* with *CLB2-kd* using single cell time-lapse analysis (Figure 2.15); however, these cells were partially defective in the α-factor block-release protocol, precluding clear quantification of bulk cultures.

Thus, restoration of a physiological level of mitotic cyclins to strains with constitutively active APC-Cdh1 results in restoration of near-normal bud morphology, and also results in SPB separation. Mitotic cyclin degradation is not responsible for all spindle phenotypes of *CDH1-m11* cells, though, because spindle structure and microtubule dynamics likely are profoundly perturbed due to persistent APC-Cdh1 activity even in the presence of stable mitotic cyclins.

Discussion

CDK phosphorylation is essential to restrain lethal activities of Cdh1

Cdh1 is highly active in destruction of many important proteins, so multiple mechanisms of Cdh1 regulation might be expected. CDK-mediated phosphorylation of Cdh1 inhibits Cdh1-APC interaction, and also promotes export of Cdh1 from the nucleus. The Acm1 protein is a stoichiometric Cdh1 inhibitor, most likely blocking access of even unphosphorylated Cdh1 to the APC. Finally, Cdc5 (polo kinase) has been proposed to phosphorylate and inhibit Cdh1.

Here, we address the relative functional significance of CDK phosphorylation, Acm1 binding, and Cdc5 phosphorylation in control of Cdh1, at endogenous expression levels, using exact gene replacement. We find that CDK phosphorylation is essential. Acm1 is not essential for effective Cdh1 regulation, but Acm1 binding contributes a buffering capacity. We cannot detect a contribution of Cdc5 phosphorylation to Cdh1 regulation by the assays we have used.

The essentiality of CDK phosphorylation for Cdh1 regulation could be due to a phosphorylation requirement for blockage of Cdh1-APC interaction, for Msn5 interaction and nuclear export, or both. Our experiments do not distinguish between these possibilities, although nuclear export is unlikely to be required for Cdh1 inhibition, as Msn5 is not essential.

Our results show the benefits of exact gene replacement for accurate analysis. Overexpression of wild-type Cdh1 is lethal at sufficient levels, so lethality of any overexpressed mutant form of Cdh1 is necessarily ambiguous with respect to normal cell physiology. A previous mention of viability of *CDH1-m11* when present on a low-copy plasmid with the endogenous promoter (Jaquenoud et al., 2002) is on its face inconsistent with our results; however, we have found that including a 5' untranslated fragment extending even into the next gene (*ERP6*) as a promoter for *CDH1* on a low-copy plasmid is insufficient for effective complementation of *cdh1* defects. Plasmid-borne genes could potentially be underexpressed due to a truncated promoter or unknown effects of vector context; they clearly also can be overexpressed due to copy number or other effects. Even stable integration of translocated copies of genes has the potential to mislead since such approaches invariably introduce unnatural neighboring sequences

(vector or chromosomal) that could affect expression. In gene replacement ('knock-in') studies in animals, it has been recognized that removal of vector and marker sequences is required for unambiguous results (Wang et al., 1999)

CDH1-m11 as an exact gene replacement yields a tight first-cycle arrest with uniform bud morphology and replicated DNA; this result identifies CDK phosphorylation as a critical physiological Cdh1 regulator. In contrast to results with *CDH1-m11* overexpressors, the spindle phenotype of *CDH1-m11* cells is heterogeneous; this result may have interesting consequences for the role of Acm1 (see below).

Heterozygous *CDH1-m11/CDH1 GAL-ACM1* diploids, while inviable upon shutoff of *GAL-ACM1*, nevertheless undergo efficient meiosis and sporulation without *ACM1* overexpression. This may be due to alternate Cdh1 inhibitory mechanisms that functions during the meiotic cell cycle; for example, the meiotic kinase Ime2 is capable of inhibiting Cdh1 on an alternate set of phosphorylatable residues (Holt et al., 2007).

Cdh1 interferes with spindle morphogenesis at multiple steps

While the most prominent spindle defect in *CDH1-m11* cells is failure to make a short bipolar spindle, a significant minority of these cells do make a short spindle, as do almost all *CDH1-m11 2X ACM1* cells. *CDH1-m11* cells with a short spindle (with or without doubled *ACM1* gene dosage) nevertheless fail to undergo anaphase. Our results suggest that this is likely due to failure of Pds1 proteolysis and resulting failure of cohesin cleavage.

The failure of Pds1 proteolysis may be the consequence of severely depleted Cdc20 levels in *CDH1-m11* cells. APC-Cdh1 is required for efficient Cdc20 degradation

(Huang et al., 2001; Shirayama et al., 1998), although Cdc20 may also be degraded in an APC-independent manner (Goh et al., 2000). We tested whether mutation of the two identified Cdc20 destruction boxes (Shirayama et al., 1998) would restore spindle morphogenesis to *CDH1-m11* cells, with negative results; however, removing these two Cdc20 destruction boxes has a relatively minor effect on cell-cycle-regulated Cdc20 accumulation (Prinz et al., 1998). Cdc20 may contain additional unidentified sequences targeting it for Cdh1-dependent degradation. In a following chapter, we examine Cdh1- and destruction box-dependence of Cdc20 degradation.

Cdh1-m11 might also alter *CDC20* transcription. Other factors contributing to anaphase failure in spindle-bearing *CDH1-m11* cells could include proteolysis of other motor proteins or spindle components due to Cdh1-m11 activity; activation of the spindle checkpoint does not appear responsible.

We have tested the hypothesis that one missing component for spindle morphogenesis is the mitotic cyclin Clb2, since mitotic cyclins are required for spindle morphogenesis (Fitch et al., 1992). Indeed, introducing undegradable Clb2 into *CDH1-m11* cells results in apparent spindle pole body separation, with a proportion of cells displaying anaphase spindle-length separations. This is not a complete explanation, though, since introducing undegradable Clb2 into *CDH1-m11* cells resulted in disrupted or absent spindle morphology despite SPB separation in most cells.

It has been proposed, based on overexpression studies, that Cdh1-dependent degradation of plus-end-directed motors, especially Cin8, could explain the requirement to inhibit Cdh1 for bipolar spindle morphogenesis. Our results, at endogenous expression levels, fail to confirm this hypothesis. Cin8 is indeed efficiently degraded in *CDH1-m11*

cells, and introducing the undegradable Cin8-KED or Cin8-alaKEN blocks this degradation as expected (Hildebrandt and Hoyt, 2001). Nevertheless, undegradable Cin8 was completely ineffective at restoring bipolar spindle formation to *CDH1-m11* cells. Cin8 degradation may nevertheless contribute to failure of spindle formation in these cells, since plus-end-directed motors are required for this process. One possible explanation is that the Cdh1 target Ase1 controls the physiological localization of Cin8; Ase1 proteolysis may prevent proper targeting of the stabilized Cin8 to the mitotic spindle (Khmelinskii et al., 2009).

Acm1 as a physiological buffer

Curiously, endogenous levels of *ACM1* allow bipolar spindle formation in a minority of *CDH1-m11* cells, since deletion of *ACM1* eliminates these spindles; in contrast, doubling *ACM1* copy number results in bipolar spindle formation in nearly all *CDH1-m11* cells. Thus Acm1 appears to be rather accurately titrated to a level just insufficient to inactivate completely unphosphorylated Cdh1, when both proteins are expressed at endogenous levels. It is interesting to consider possible dynamic consequences of this effect. Acm1 levels are tightly cell-cycle-regulated by changes in transcription and protein stability. Acm1 levels higher than those in wild-type cells might sporadically allow premature bipolar spindle formation, before full inactivation of Cdh1 by complete CDK phosphorylation (since available evidence suggests that partial phosphorylation results in partial Cdh1 activity (Zachariae et al., 1998a)). Lower levels than wild-type, in contrast, could put a demand on the system for much more efficient and quantitative Cdh1 phosphorylation than would otherwise be required.

These considerations cannot imply an essential role for regulation of Acm1 levels, since both strong overexpression and deletion are tolerated with little or no overt phenotype. Subtle effects of *ACM1* deletion or overexpression on fidelity of chromosome transmission have not been examined to our knowledge; perhaps even occasional chromosome mis-segregation has provided a sufficient selection to titrate Acm1 levels appropriately.

Substrate Specificity of Cdh1

The APC coactivators Cdc20 and Cdh1 target an overlapping set of proteins for proteasomal destruction; this substrate specificity likely contributes to the orderly progression through anaphase and exit from mitosis. The mechanism by which this specificity is achieved remains contested. As Cdh1 activity is effectively inhibited until late anaphase, it has been unclear whether failure of overexpressed Cdh1 to degrade targets such as Pds1 was the consequence of true substrate specificity or merely efficient pre-anaphase inhibition of Cdh1 activity. The ability of purified APC-Cdh1 to efficiently ubiquitinate Pds1 (Thornton et al., 2006) argued for the latter case. The arrest of *CDH1-m11* strains, in which Cdc20 does not accumulate, allows for a clean analysis of the proteolytic consequences of unrestrained Cdh1 activity in the context of an otherwise normal cell cycle. Here we find that APC-Cdh1 is highly effective at clearing Clb2, Cdc5 and Cdc20, but far less capable of clearing Pds1 and Clb5. This suggests that, *in vivo*, some physiological mechanism exists preventing Cdh1 from efficiently clearing Pds1. Possibilities include direct biochemical regulation not recapitulated in the purified system, or activation of transcriptional circuitry sufficient to replenish the depleted

proteins. This is possible, since *CDH1-m11* cells likely have unrestrained SBF activity, resulting in accumulation of SBF transcriptional targets such as the G1 cyclin Cln2 (Cross et al., 2002); *PDS1* is in the SBF regulon (Spellman et al., 1998), which is inactivated by the Cdh1 target Clb2 (Amon et al., 1993). Further, Clb2 promotes its own transcription as well as that of *CDC20* (Amon et al., 1993; Zhu et al., 2000). Such transcriptional circuitry could help ensure the proper order and function of APC coactivators; delayed inactivation of Cdh1 during a normal cell cycle could result in greater transcription of the G1 and S-phase cyclins that serve to inactive Cdh1, while inhibiting anaphase through Pds1 synthesis.

Clb2-Cdh1 mutual antagonism

In the case of spindle morphogenesis, Cdh1 acts at various thresholds, and most likely acts on multiple targets, to prevent final successful anaphase. Mitotic cyclins are capable of restoring a separated spindle pole body phenotype in the context of *CDH1-m11*; however these do not predominantly appear to be physiologically normal spindles, as evidenced by abnormal tubulin fluorescence and the frequent occurrence of more than two SPB foci. This suggests that balance between Cdh1 and Clb2 permits specific steps such as spindle pole body separation to occur, with multiple other interactions and couplings present to orchestrate specific aspects of spindle physiology, including tubulin dynamics and spindle maintenance. Complex dynamics have been described at the spindle midzone regulated by both APC-Cdh1 targets and net CDK phosphorylation (Fridman et al., 2009; Higuchi and Uhlmann, 2005; Khmelinskii et al., 2009) In contrast, the hyperpolarized bud growth phenotype characteristic of *CDH1-m11* cells is likely a

simple and direct consequence of removal of the mitotic cyclin Clb2, since its restoration to *CDH1-m11* cells eliminates hyperpolarized bud growth in favor of isotropic growth. This presumably occurs either because Clb2 directly promotes isotropic growth, or because Clb2 inhibits expression of genes such as the G1 cyclin *CLN2* that are directly driving polarized bud growth (Amon et al., 1994; Lew and Reed, 1993)

The add-back approach

Our strategy in this study, to first deregulate Cdh1 at the endogenous level, and then to add back single Cdh1 targets by introducing undegradable alleles expressed at endogenous levels, allows accurate dissection of the mechanism of action of even a highly pleiotropic regulator such as Cdh1. In the case of bud morphogenesis, the situation is simple: the hyperpolarized bud phenotype is essentially due to a single target, Clb2. Spindle morphogenesis is clearly much more complicated, but nevertheless, we are able to implicate mitotic cyclins as major regulators sufficient for significant spindle morphogenesis in the absence of other Cdh1 targets. It may be possible through restoration of Cdh1-resistant targets such as Clb3 and Ase1 to permit mitosis in the face of constitutive APC-Cdh1 activity, thus defining a (not necessarily unique) set of essential Cdh1 targets. More generally, with appropriate variations, this strategy should be applicable to dissection of the action of other complex regulators.

CHAPTER THREE

Dissection of Cdh1 multisite phosphorylation

Recombinational strategy to create partially phosphorylatable alleles of *CDH1*

A variant on the recombinational strategy used to introduce *CDH1-m11* into the chromosome (Chapter 2) was designed to introduce exact untagged chromosomal gene replacements of *CDH1* alleles mutated for varying subsets of phosphorylation sites. Specifically, an allele pair comprised of *cdh1-m11* and *cdh1,* each rendered non-functional by insertion of different selectable markers at different positions, were arranged in tandem at the endogenous locus in both possible orientations (Figure 3.1). The *URA3* gene is placed between the two *cdh1* copies, so that FOA-selected 'popout' homologous recombination will result in the isolation of CDK phosphorylation site mutants, ablating contiguous sites beginning at either the N or C terminus of *CDH1* dependent on whether the 5' or 3' allele was the CDK-unphosphorylatable *CDH1-m11* (Figure 3.1A).

Isolation of partially phosphorylatable *CDH1* alleles

In a wild-type background, the yield of recombinants ablating the N-terminal sites was reduced compared to expectations from physical distance (Figure 3.1B). Recombination occurs readily within this same interval to recreate a wild type *CDH1* allele. Similarly, recombination is in direct proportion to physical distance if the tandem alleles are constructed so all possible products are interrupted (see Figure 2.2). The

A

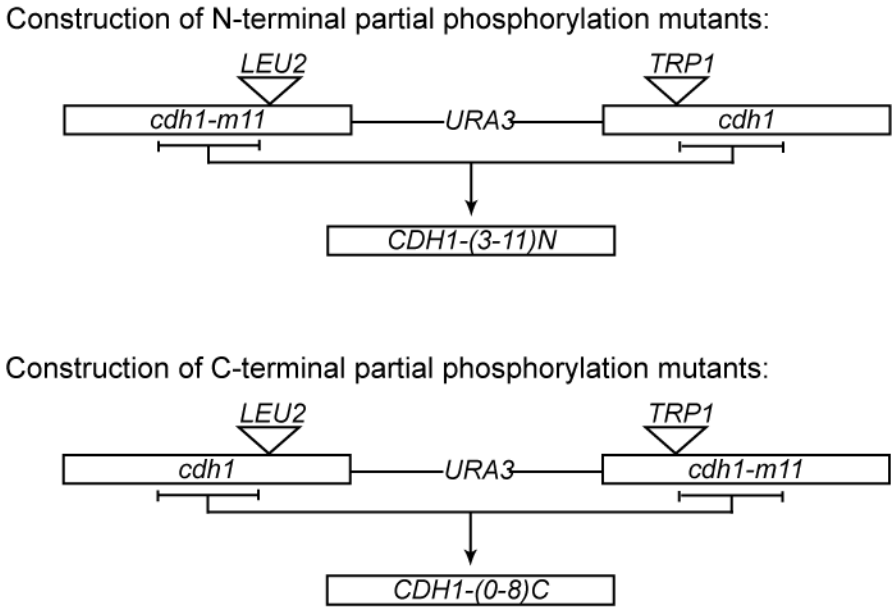

B

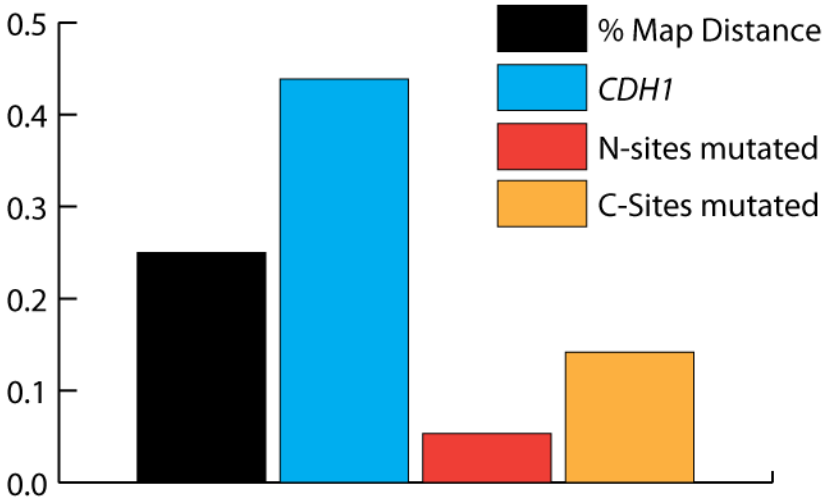

Figure 3.1 Recombinational approach to obtain *CDH1* partial phosphorylation mutants. **A** Recombination based strategy used to obtain N-terminal (top) and C-terminal (bottom) partially phosphorylatable alleles as an exact gene replacements. Horizontal bracket indicates region of recombination that results in an uninterrupted exact gene replacement. **B** Percentage of recombinations of the loci from (A) occurring within the region marked by the horizontal bracket, determined by loss of selectable markers. *CDH1* strain were as in (A) except the locus contained two tandem wild type *CDH1* alleles.

distributional shift away from functional alleles was weaker for the C-terminally ablated sites, providing an initial suggestion that the N-terminal sites are particularly important in regulating *CDH1* activity (Figure 3.1B).

Further, sequencing of viable recovered N-terminal mutants showed that all clones had less than four phosphorylation sites ablated. Given the proximity of the fourth site to the *TRP1* marker, the expectation from the physical distance is that most N-terminal recombinants should have at least four sites ablated. However, clones with fewer than the expected minimal three sites were frequent, likely from gene conversion since in some cases the wild-type sites were interspersed between mutant sites. Such events are presumably rare, and likely reflect selection against N-terminal mutations. Recovered viable C-terminal mutants revealed little or no such bias. This suggested that the N-terminal sites have a greater weight in inhibiting Cdh1 activity, with N-terminal mutations being highly deleterious.

Exact gene replacement with the lethal CDK-unphosphorylatable *CDH1-m11* allele was obtained in a *cdc23-1* background hypomorphic for the APC (see Chapter 2). Therefore, we repeated the construction of partially phosphorylatable *CDH1* alleles in a *cdc23-1* background. Recombinant *CDH1* alleles were obtained at frequencies higher than those in *CDC23* strains, although still reduced as compared to physical distance or the control recombination. The reason for this is unclear, although poorer homology owing to the mutations ablating the phosphorylation sites on one of the alleles may be contributory. The ratio of N-terminal mutants obtained in a *cdc23-1* background is roughly threefold higher than with a wild type APC, whereas C-terminal mutants are nearly at parity (Figure 3.2A). Sequencing revealed N-terminal mutations ranging from 3

to 11 sites, and C terminal mutations ranging from 0 to 8 sites (Figure 3.2B). As with *CDH1-m11*, this argues that the decreased recovery of some of these strains in a *CDC23* background was the consequence of aberrant APC activation.

Inviability of *CDH1* mutants defective for N-terminal phosphorylation sites is APC dependent and suppressible by conditional *ACM1* overexpression

The *CDH1* alleles obtained in *cdc23-1* cells (see Figure 3.2B) were crossed into a *CDC23 GAL1pr-3FLAG-ACM1* ('*GAL-ACM1*') background, so that the effects of these alleles in the context of a wild type APC could be observed (see Chapter 2). Viability of strains with partially phosphorylatable *CDH1* alleles was assessed by shutoff of *ACM1* expression (Figure 3.3A). In the N-terminal series, *CDH1-4N* was the least phosphorylatable construct compatible with viability, whereas none of the C-terminal mutations including the maximal *CDH1-8C* noticeably impaired colony formation. The morphology of these cells at six hours after *GAL-ACM1* shutoff was assessed by DIC microscopy (Figure 3.3B). Viable strains were predominantly morphologically normal; inviable strains displayed hyperpolarized growth similar to that found in *CDH1-m11* strains (see Chapter 2).

We analyzed growth rates, Clb2 levels, and DNA content for viable *CDH1* mutant cells in the absence of *ACM1* overexpression. The N terminal mutants *CDH1-3N* and *CDH1-4N* strains had lower cycling Clb2 levels, and slightly longer doubling times; C-terminal mutant cells were similar to wild-type (Figure 3.4A, B). DNA content, assessed by FACS, was comparable among strains with the various *CDH1* alleles (Figure 3.4C).

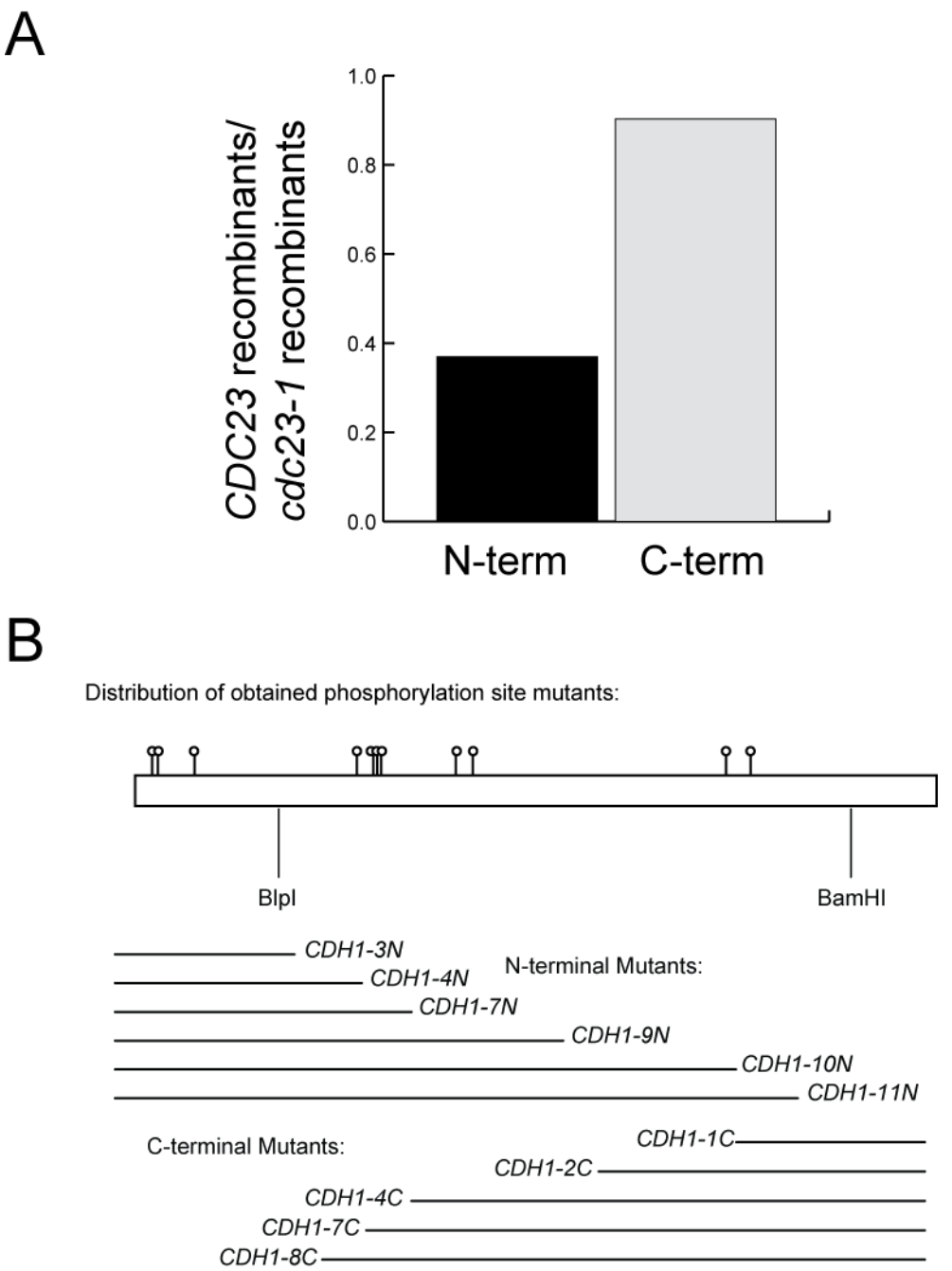

Figure 3.2 The hypomorphic APC subunit allele *cdc23-1* allows for isolation of a wide range of partially phosphorylatable *CDH1* recombinants. **A** *cdc23-1*, which is permissive for *CDH1-m11* (see Chapter 2), increases the recovery of N-terminally but not C-terminally mutated *CDH1* alleles relative to *CDC23* strains. **B** *CDH1* phosphorylation site mutant alleles obtained in a *cdc23-1* background. Circles represent putative CDK sites. Horizontal bars indicate regions of *CDH1* whose CDK sites have been mutated to alanines.

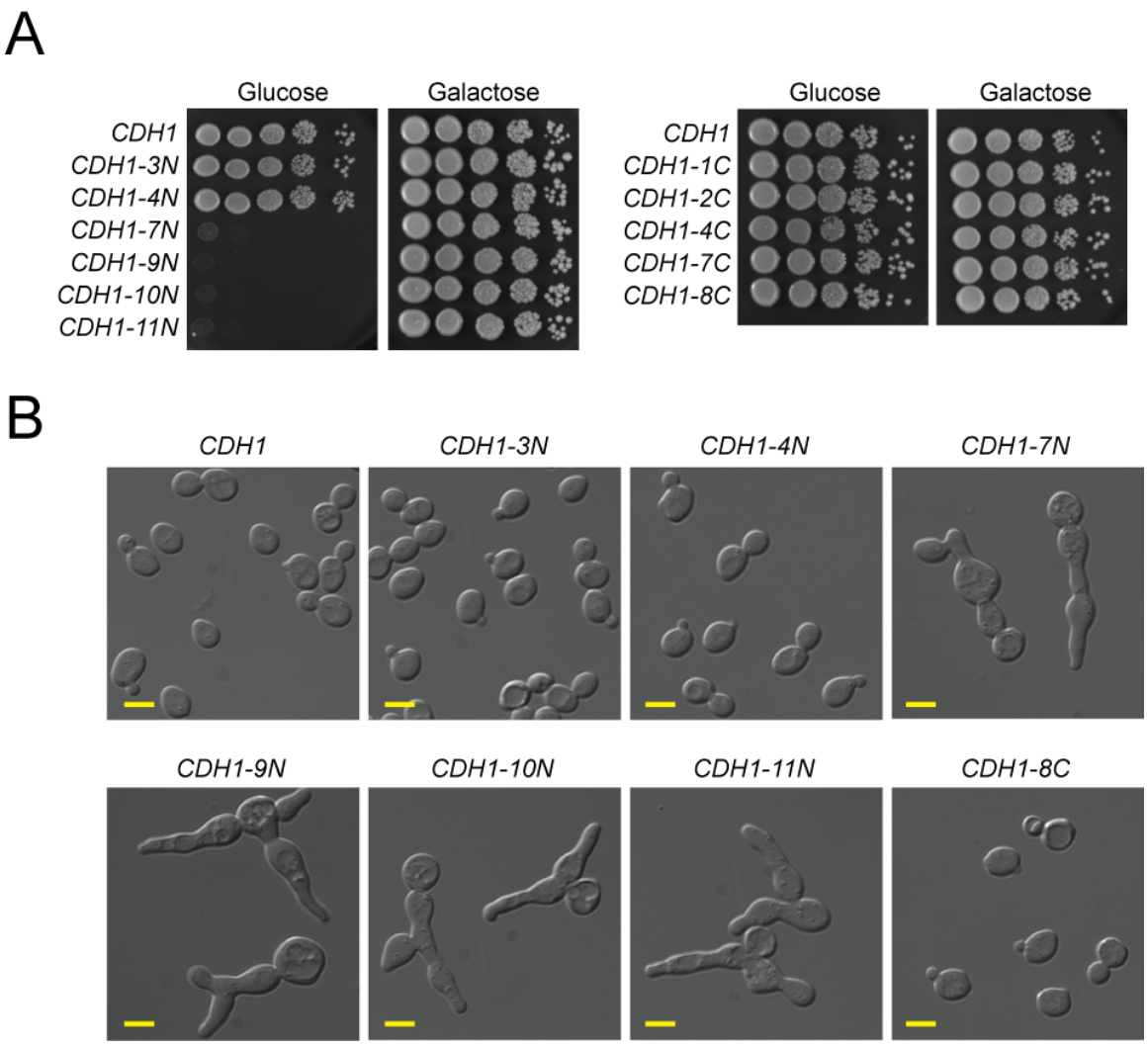

Figure 3.3 CDK regulation of *CDH1* does not work by a strict counting mechanism. **A** Tenfold dilutions of the indicated alleles of *CDH1* (exact gene replacements) all with *GAL-ACM1* were grown in galactose medium and plated onto glucose or galactose-containg plates. **B** Strains from (A) were grown in galactose, shifted to glucose media for six hours (*GAL-ACM1* off), and DIC images taken. Scale bars are 5 microns.

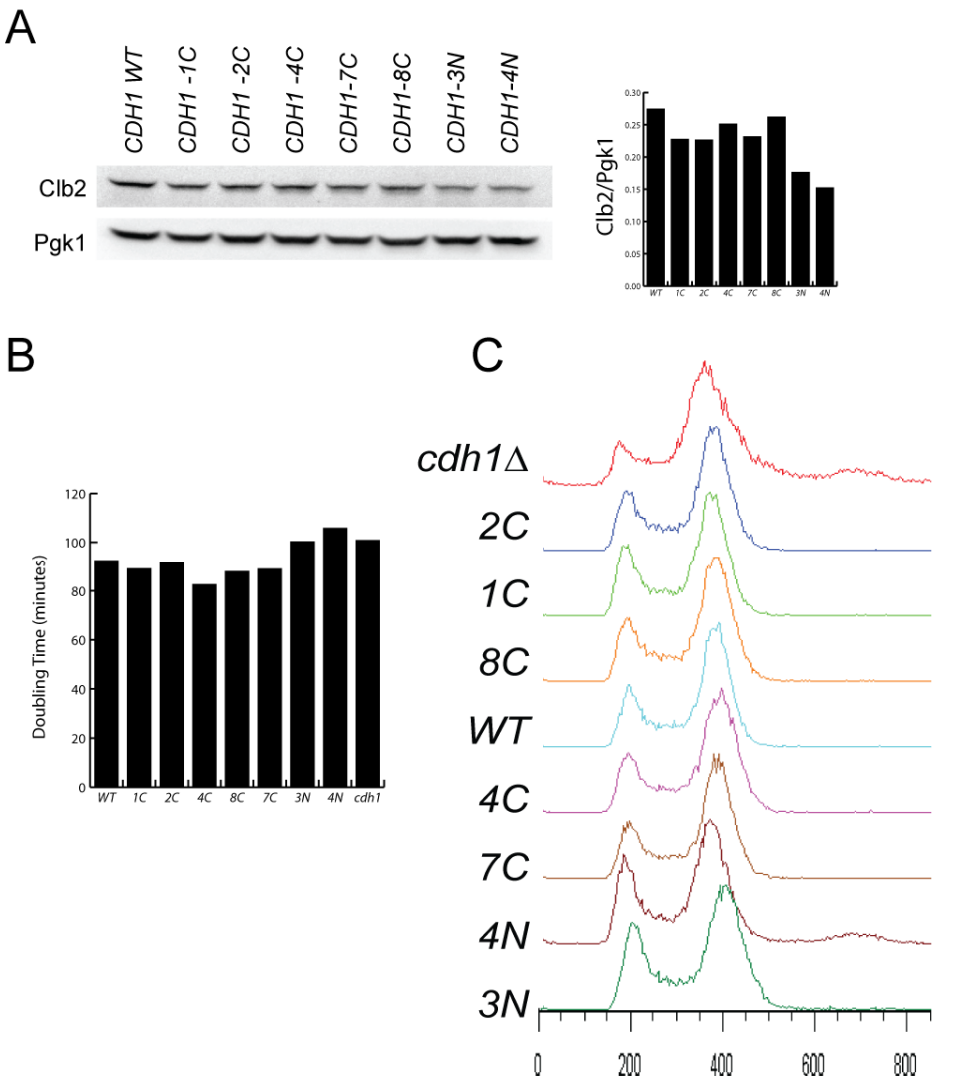

Figure 3.4 Phenotype of *CDH1* alleles compatible with viability **A** Strains with the indicated *CDH1* alleles (those resulting in strains viable in the absence of *ACM1* overexpression), were grown to log phase in glucose and Clb2 levels determined by western blot, using Pgk1 as a loading control (left). Graph on right quantifies immunoblot intensity, column names indicate the specific *CDH1* allele. **B** Growth rates of the strains from (A) were measured **C** FACS to assess DNA content was performed on the strains in (A)

N-terminal mutants display synthetic interactions with S-phase cyclins

The kinase(s) responsible for inactivating Cdh1 in late G1/S phase remain unclear, and arguments have been made for Clb3, 4, 5 and G1 cyclins playing a significant role in the inactivation of APC-Cdh1 (see Introduction). We first sought to test for genetic evidence of S-phase cyclin contribution to Cdh1 inactivation. We introduced the various partially phosphorylatable alleles into a *clb5 clb6 GAL-ACM1* background, and then tested for viability upon *GAL-ACM1* shutoff. The logic of this approach is that if Clb5/6 are uniquely responsible for phosphorylating some site(s), then the absence of Clb5/6 should phenocopy the lack of those sites. For example, if Clb5/6 uniquely phosphorylate the C-terminal sites, then the *CDH1-4N* mutant should cause inviability in a *clb5,6* background because it is equivalent (with respect to Cdh1 phosphorylation) to the completely unphosphorylatable and lethal *CDH1-m11*.

CDH1-4N strains were inviable in the absence of *CLB5/6*, whereas there was no obvious loss of viability of *CDH1-7C* cells (Figure 3.5), consistent with the hypothesis above. When tested with individual cyclin deletions, the predominant synthetic interaction was with *CLB5*; *clb6 CDH1-4N* strains were viable independent of Acm1 overexpression (Figure 3.5). This argues genetically for an interaction between *CLB5* and *CDH1*, possibly a direct one in which Clb5 phosphorylation serves to inhibit Cdh1 activity, and in the absence of the N-terminal 4 sites, C-terminal Clb5-dependent phosphorylation of Cdh1 becomes essential. This suggests that Clb5 is particularly important for phosphorylation of some or all of the remaining 7 C-terminal sites to effectively restrain APC-Cdh1 activity (although other interpretations are possible), and that Clb5/6 cannot be uniquely required for phosphorylation of the N-terminal 4 sites.

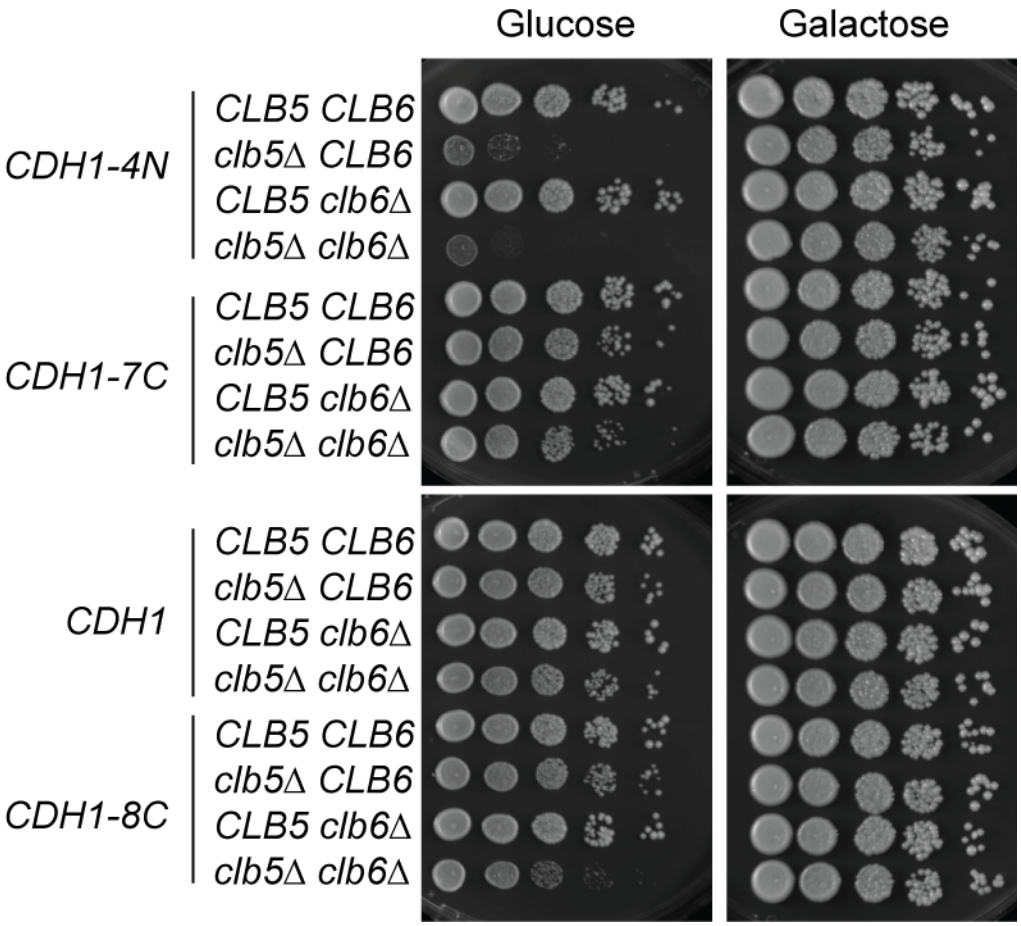

Figure 3.5 Synthetic interactions between S-phase cyclins and *CDH1* phosphorylation mutants. *CDH1-4N* but not *CDH1-7C* strains are dependent upon *CLB5* for viability. Tenfold dilutions of strains of the indicated genotypes, all with *GAL-ACM1* were spotted onto glucose or galactose plates.

Preliminarily, inviable cells in this experiment display the typical high Cdh1 activity phenotype with hyperpolarized growth characteristic of *CDH1-m11* exact gene replacement. *clb5 clb6 CDH1* strains display modestly hyperpolarized growth relative to wild type (data not shown); this may be due a decrease in the ability to inhibit APC-Cdh1 activity on the N-terminal sites and/or a delay in the inactivation of the G1 regulon (which is Clb-CDK dependent).

In contrast, *CDH1-4N clb3 clb4* and *CDH1-7C clb3 clb4* strains were found to be viable (data not shown), suggesting that Clb5/6 may be more significant in Cdh1 inhibition than Clb3/4. This could be consistent with the earlier expression of Clb5/6 than Clb3/4, or could reflect intrinsic substrate preference of Clb5/6 for Cdh1. It could also reflect the ability of Cdh1 to proteolyze Clb3/4 but not Clb5/6, so that Clb5/6 are 'immune starters' for Cdh1 inactivation.

Acm1 is essential to block activity of partially phosphorylated Cdh1

Three regulatory mechanisms have thus far been described for CDK-coupled inhibition of Cdh1 activity: CDK phosphorylation directly inhibiting the biochemical interaction of Cdh1 with the APC, CDK causing the nuclear export of Cdh1 by the Msn5 transporter, and lastly binding of Cdh1 to Acm1, which precludes APC interaction; this mechanism interacts with CDK activity not through Cdh1 phosphorylation but rather through regulated degradation and localization of the Cdh1 inhibitor Acm1 (Enquist-Newman et al., 2008; Hall et al., 2008; Martinez et al., 2006). To test whether blocking specific phosphorylation sites in Cdh1 revealed specific interactions with these pathways, the various alleles were placed in an *acm1 MSN5*, *ACM1 msn5*, or *acm1 msn5*

backgrounds. Deletion of *ACM1* alone results in no obvious phenotype (Martinez et al., 2006); *msn5* deletion has pleiotropic effects owing to its role in nuclear transport, but *MSN5* is not essential (Akada et al., 1996; Kaffman et al., 1998). *acm1 msn5* cells are viable and morphologically normal.

ACM1 becomes essential in the context of N-terminal phosphorylation site ablations (Figure 3.6A). *CDH1-4N* cells were inviable in the absence of *ACM1*, while *CDH1-7C acm1* cells were fully viable. Deletion of *MSN5* was found to act as an enhancer of several *acm1 CDH1*-phosphomutant phenotypes (see Figure 3.7), but was not itself synthetically lethal with any partially phosphorylatable *CDH1* allele.

These results suggest a regulatory hierarchy, with CDK phosphorylation of N-terminal sites and then C-terminal Cdh1 sites, Acm1 inhibition and Msn5-dependent nuclear export in decreasing order of importance.

Genetic interactions between the Four N-terminal Cdh1 sites and *ACM1*

The synthetic lethality between *CDH1-4N* and *acm1* led us to analyze the first four sites in greater detail. No single site was essential in the absence of ACM1 and/or *MSN5* (Figure 3.6B). Combinations of mutations of the N-terminal 4 sites varied from strict dependence upon endogenous *ACM1*, to full viability even in an *acm1 msn5* background (Figure 3.7). Some were viable in an *acm1* but not an *acm1 msn5* background, indicating an ancillary or potential role for Msn5 regulation. Each individual site had phenotypic consequences to its mutation in some assay, implying that these 4 potential sites can all actually be phosphorylated, with regulatory consequences. S42 appears to be the most significant, and T12 the least, of these 4 sites.

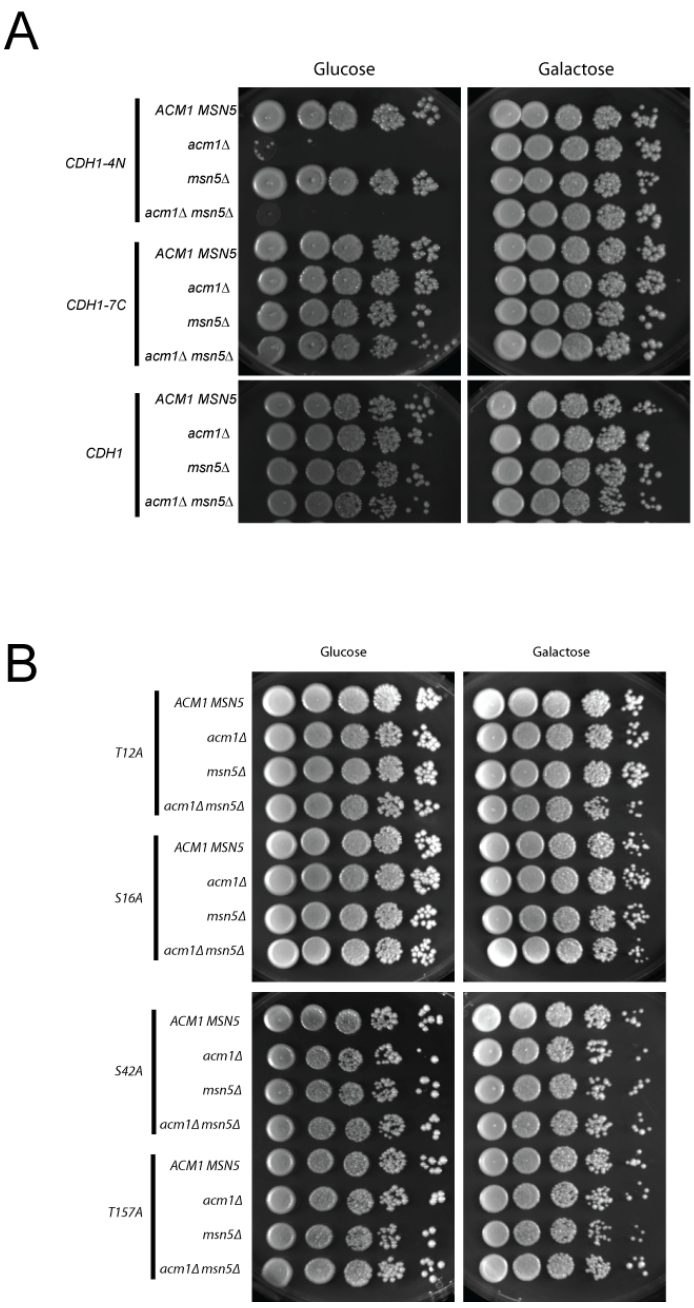

Figure 3.6 Strains lacking N-terminal phosphorylation sites of *CDH1* are dependent upon *ACM1* for viability, but no individual site is essential **A** *CDH1-4N* but not *CDH1-7C* strains are dependent upon *ACM1* for viability. Tenfold dilutions of strains of the indicated genotypes, all with *GAL-ACM1*, were spotted onto glucose or galactose plates. **B** *acm1* strains are not dependent upon phosphorlyation on any single specific site for viability. Tenfold dilutions of strains of the indicated genotypes, all with *GAL-ACM1*, were spotted onto glucose or galactose plates.

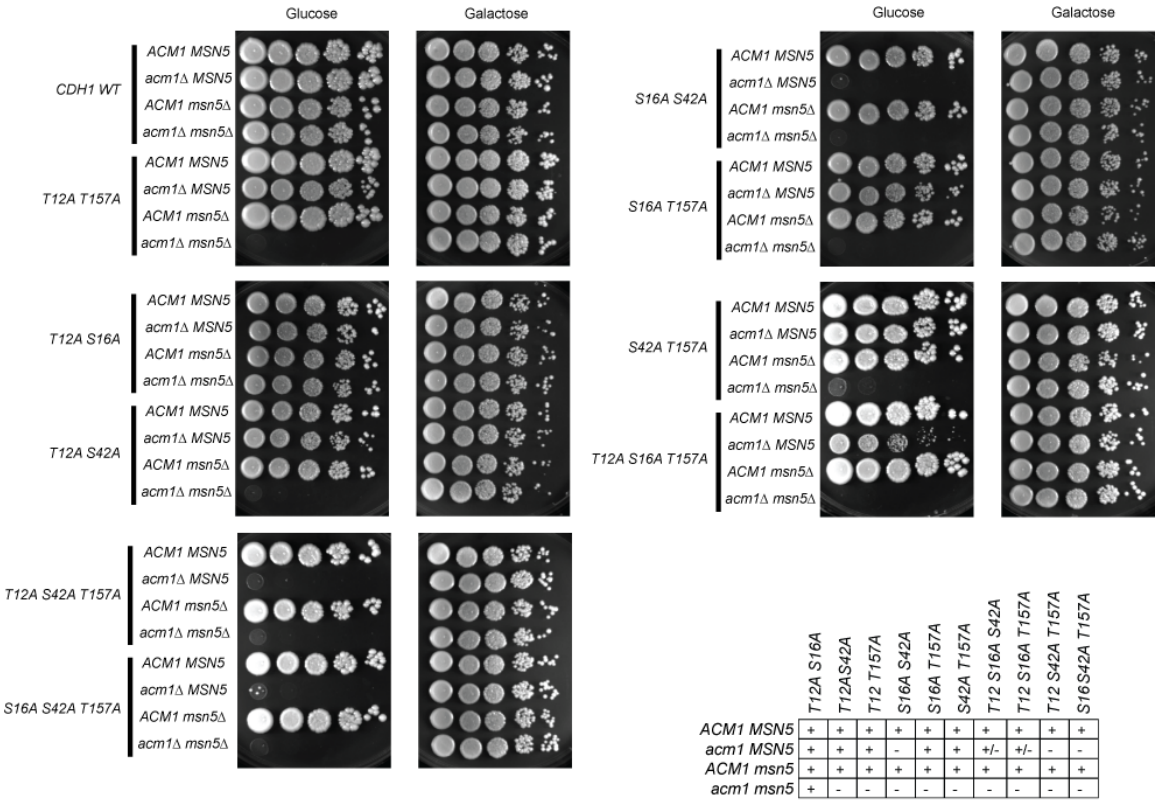

Figure 3.7 Synthetic interactions of the first four *CDH1* phosphorylation sites with *acm1* and *msn5*. Assessed by tenfold dilution assays in *GAL-ACM1* containing strains. *CDH1* allele plated is indicated in left column. Table qualitatively summarizes the synthetic lethalities, with *CDH1* genotype on the x axis. '+' is fully viable, '+/-' is intermediate ability to form colonies, and '–' is strictly inviable on glucose.

Analysis of strains with partially unphosphorylatable Cdh1 by time lapse microscopy

The dependence of partial site mutants on normally dispensable regulatory machinery suggested that strains with these mutations might exhibit sporadic severe cell cycle problems, despite the absence of a severe bulk culture phenotype. The logic of this idea is that fully phosphorylatable Cdh1 is protected with high redundancy, and occasional failure of complete phosphorylation could be compensated by high Acm1; conversely, occasional low Acm1 levels would be benign because of usually efficient Cdh1 phosphorylation. The partially phosphorylatable versions have lost one of these safety mechanisms and so might reveal defects stochastically within a culture.

To test this, we employed time-lapse quantitative fluorescent microscopy, using the nuclear marker *HTB2*-mCherry as well as a functional GFP-Clb2 fusion protein, which is degraded by Cdh1. In all strains, most cell cycles were normal, with progression through mitosis and accumulation and removal of Clb2 occurring with normal dynamics. Approximately 3% of wild type *CDH1* and 5% of *CDH1-7C* strains displayed abnormal mitoses, invariably of the form of a delay at a stage with a bilobed nucleus and relatively high Clb2-GFP, most of which eventually completed anaphase during the imaged period. Previous experience with such sporadic blocks in time-lapse microscopy of wild-type cells suggests that they are due to DNA damage, possibly induced by illumination for GFP detection (Bean et al., 2006).

CDH1-4N strains had a significantly higher frequency (24%) of aberrant cell cycles. These were heterogeneous, including arrests of the type noted above and also sequential aberrant mitoses (including abortive mitoses without nuclear division, mitoses

with very low accumulation of Clb2, and multibudded mitoses with nuclei passing through three cell bodies (see Figure 3.8B for example)).

Discussion

Recombinational construction of an exact gene replacement series of mutants

We describe a novel approach to creating a series of exact gene replacements, useful for the creation and analysis of intermediately modified forms of genes with numerous known modifications. It allows for the inference of modifications that are selected against, as well as efficient recovery of a diversity of viable mutants. In our case, eleven intermediately phosphorylatable alleles of *CDH1* were created by homologous recombination. The nature of this allelic construction precludes the possibility of altered gene function owing to the presence of alternate exogenous sequences, selection markers, flanking vector sequences, or an otherwise modified chromosomal milieu, and is thus advantageous for the reasons discussed for the *CDH1-m11* exact gene replacement.

Cdh1 inhibition cannot be reduced to counting phosphorylations

Multisite phosphorylation in the stoichiometric B-type cyclin inhibitor Sic1 appears to work by a strict counting mechanism, whereby six site need to be phosphorylated to be targeted for degradation by SCF-Cdc4 (Nash et al., 2001). Given the prevalence of multisite phosphorylation, it is important to determine if this conclusion is general. In Sic1, there is a clear distinction in efficiency and strength of the different phosphorylation sites, but this does not alter the general requirement for six sites (Nash et

al., 2001; Petroski and Deshaies, 2003; Verma et al., 1997). Cdh1 functionally overlaps with Sic1, in that it opposes mitotic B-type cyclins from late anaphase through the subsequent G1. However, our evidence argues against a counting mechanism regulating Cdh1 activity, since ablation of 8 C-terminal sites is viable without any discernible phenotype, whereas ablation of 3 or 4 N-terminal sites results in a discernible phenotype, and ablation of 7 is incompatible with viability. One obvious concern would be that the 'phosphorylation sites' ablated are not actual kinase substrates *in vivo*, and thus of little physiologic relevance. However, previous mass spectroscopic date places five of the six conclusively demonstrated phosphorylated sites among the 8 C-terminal sites that are not essential (Hall et al., 2004), and our genetic data clearly imply that all of the N-terminal sites are also phosphorylated (see above).

No single CDK site on Cdh1 is essential

Previous studies of the phosphorylation sites of Cdh1 have been restricted to a single allelic series ablating phosphorylation sites starting from the N-terminus, placed under a partial GAL promoter. It was not possible to infer from this result whether one particular site beyond the first site is in fact essential to prevent the activation of Cdh1. Here, we find that there is not any one specific site that necessarily must be phosphorylated by CDK, as both the *CDH1-4N* and *CDH1-8C* alleles are viable in the presence of a fully functional APC. There are also not any two adjacent sites which necessarily must be phosphorylated for viability, which could be relevant for some models of local high charge (Holt et al., 2009; Strickfaden et al., 2007).

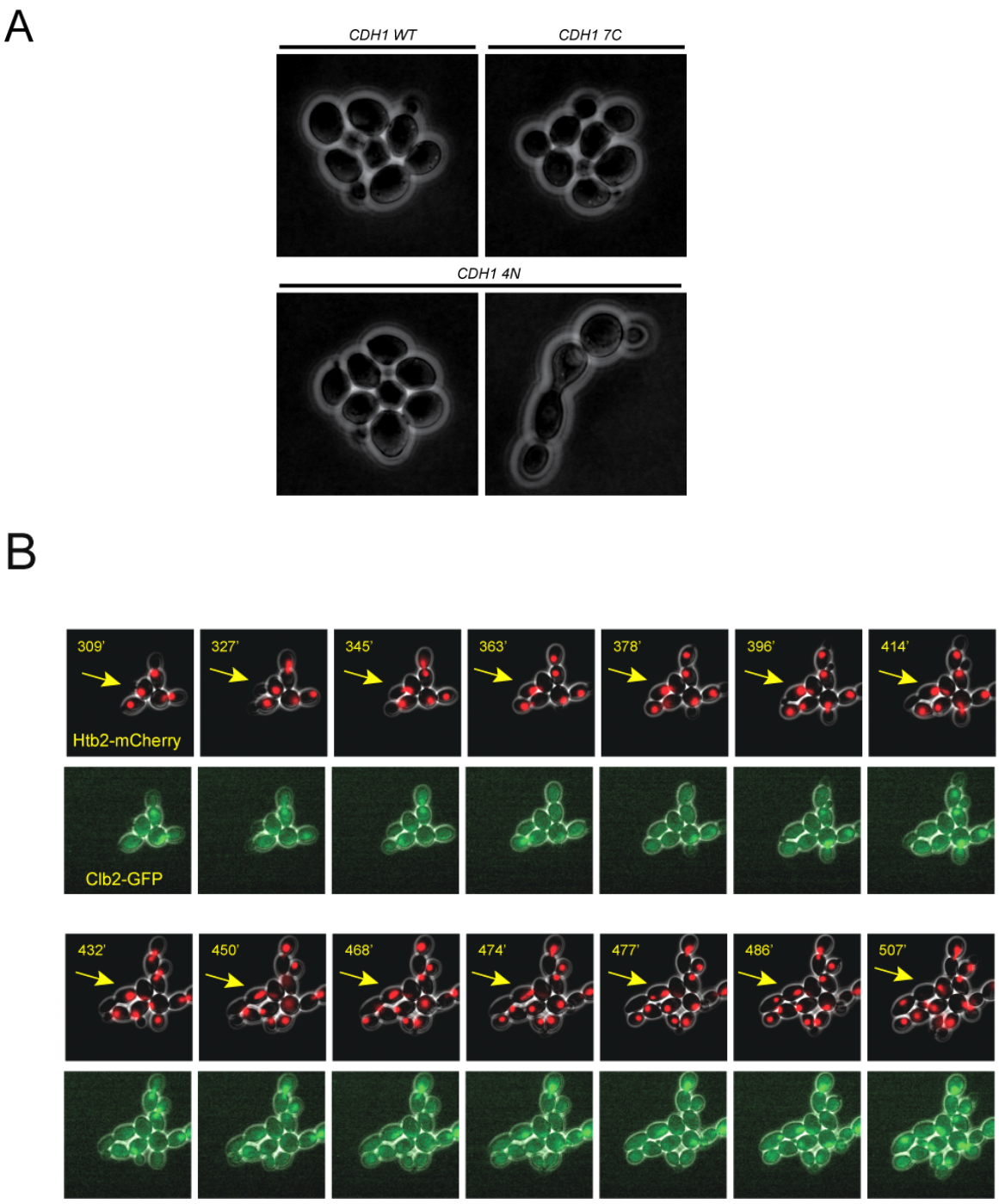

Figure 3.8 Single cell time lapse imaging of *CDH1* mutants **A** Phase images of microcolonies formed by cells of the indicated genotypes. Note *CDH1-4N* strain ability to form both morphologically normal and aberrant cells, a property not found in *CDH1* or *CDH1-7C*. **B** Aberrant mitoses in *CDH1-4N* cells. Time lapse imaging of GFP-Clb2 (green) and Histone-mCherry (red) marking the nucleus. Yellow arrow points to a hyperpolarized cell which initially fails to undergo nuclear divison, and subsequently rebuds and divides its nucleus between three cell bodies.

N-terminal and C-terminal Phosphorylation sites are functionally distinct

Ablation of three or four N-terminal sites resulted in lowered cycling Clb2 levels and slightly slowed growth. *CDH1-4N* cells were dependent upon endogenous *ACM1* for viability, and *CDH1-4N acm1* cells arrest similarly to *CDH1-m11 ACM1* cells. Additionally, a minority of *CDH1-4N* cells demonstrated characteristics consistent with an inability to restrain APC-Cdh1 activity, including hyperpolarized growth, low GFP-Clb2 accumulation, and aberrant nuclear separation, similar to that seen in *CDH1-m11* strains but not in *CDH1* or *CDH1-8C* strains.

Implications for specific CDK inhibition of APC-Cdh1 activity

The G1 cyclins Cln1,2,3, and the early-expressed B-type cyclins Clb5, and Clb3/4 have been reported to be responsible for inhibitory phosphorylation of Cdh1. We explored the possibility that ablation of a subset of contiguous sites would result in the remaining sites dependent upon a specific class of cyclins for inhibitory phosphorylation. Consistent with an important role for Clb5 in inactivating Cdh1, *CDH1-4N* strains are dependent upon *CLB5* for viability. *CLB6* has weaker genetic interactions, consistent with a less central role in *CDH1* inhibition. We do not find strong synthetic interactions between the tested CDH1 alleles and the early mitotic cyclins *CLB3* and *CLB4*. Genetic tests with G1 cyclins have not yet been performed.

Nuclear Export of Cdh1 may play an ancillary role in regulation

CDK phosphorylation both blocks biochemical association of Cdh1 with the APC and promotes its nuclear export, which may sequester it from nuclear targets. Different

sites could be responsible for these two actions. This idea results in the following genetic prediction: if mutation of some Cdh1 sites resulted in constitutive APC activation, but Msn5 interacted with a different set of sites for nuclear export, and this export was sufficient to restrain Cdh1, then deleting *MSN5* and mutating these sites in combination should be lethal. To test this we crossed all partially phosphorylatable Cdh1 alleles to an *msn5* strain, and found that none of them were dependent on *MSN5* for viability. This argues against nuclear export being a critical regulator of Cdh1 activity. We were thus not able to find a partially phosphorylatable allele of Cdh1 which was critically dependent upon Msn5, suggesting that there was no partially phosphorylatable allele created that was exportable from the nucleus but which would otherwise constitutively activate the APC. This result does not support the ability of Msn5-dependent transport to strongly restrain Cdh1 activity, although we obviously did not test all 2^{11} combinations of sites, and it also could be that identical sites are responsible for regulating interaction with both the APC and Msn5. Still, Msn5 nuclear export can contribute to Cdh1 inhibition, as shown by an *MSN5* requirement in *acm1* strains mutated for some Cdh1 CDK sites. Further experiments are planned to test this directly (see future directions).

General implications for regulation by multisite phosphorylation

Here we present an analysis of the relative contributions of subsets of phosphorylation sites for the core cell cycle regulator Cdh1. S-phase cyclins and *ACM1* are essential for the viability of cells carrying specific CDK-unphosphorylatable *CDH1* alleles as exact gene replacements. We infer the sites to be partially redundant, but phosphorylation of at least some (non-unique) subset of the sites is essential. We do not

find evidence for a strict counting mechanism, as has been seen with Sic1 (Deshaies and Ferrell, 2001), nor clearly separable functions as evident in Pho4 (Komeili and O'Shea, 1999). Rather, we seem to find differing phosphorylation sites to have marginal effects of differing magnitudes. It could be that parsing out the contributions of individual site(s) to Msn5 interaction or APC interaction would reveal a more specific pattern than can be seen so far just examining mutant viability in wild-type or compromised backgrounds. It could also be that much of the effect of Cdh1 phosphorylation comes from bulk electrostatic effects with some regional specificity, a proposed pattern in many cases of multisite phosphorylation (Holt et al., 2009).

Future Directions

This work offers insights into the regulation of Cdh1 by multisite phosphorylation, but much remains to be done.

Testing for synthetic interactions with G1 cyclin deletions may offer insights into the regulatory architecture of Cdh1. The *cln1 cln2* double mutant is viable, and often display defects owing to lack of G1 cyclins such as failure to bud (Skotheim et al., 2008), If G1 cyclins are solely responsible for the inhibitory phosphorylation of Cdh1 on a genetically separable subset of CDK sites, in the presence of *CDH1* allele possessing only these sites it is possible that a *cln1 cln2* mutant, with lowered G1 cyclin activity, will result in unrestrained Cdh1 activity preventing adequate accumulation of mitotic cyclins.

One implication of the present study is that nuclear export by Msn5 is not a critical regulator of Cdh1 activity. The construction of GFP-tagged partially phosphorylatable alleles will allow for direct assessment of localization and possibly the

determination of sites responsible for nuclear localization; subsequent work could determine if any such site(s) are also required for regulation of direct Cdh1-APC interaction.

A more detailed characterization of the arrest phenotype of cells lacking greater than 4 N-terminal phosphorylation sites—specifically *CDH1-7N*, *9N*, and *10N*—will reveal whether these alleles result in arrests with graded levels of Clb2, or whether either cyclins or Cdh1 ultimately prevails. The prevalence, activity and significance of partially phosphorylated Cdh1 species during the cell cycle is not known, and the behavior of these alleles may offer insights into the nature of such species. If all less phosphorylatable alleles result in similarly low Clb2 levels, the implication is that a marginal phosphorylation event may result in a sharp transition in APC-Cdh1 activity—that is, in the absence of complete inhibitory phosphorylation, APC-Cdh1 may simply be fully on. If graded decreases in Clb2 levels are found, this may be suggestive of either graded APC-Cdh1 activity in individual cells or stochastic but binary APC-Cdh1 activity in a bulk population. Such stochastic switch-like APC activity has been observed with *fzr*, the Drosophila *CDH1* homolog: analysis of increasingly weak alleles revealed a corresponding increase in the fraction of epidermal cells displaying unscheduled high level reaccumulation of mitotic cyclins; this result contrasts with the linear expectation of steadily increasing intermediate levels, and is suggestive of a dynamic relationship. Quantitative single cell time lapse microscopy will allow us to look for bistability by measuring GFP-Clb2 levels in individual arrested cells with partially phosphorylatable *CDH1*. If APC-Cdh1 activity is strictly bistable, and all alleles incompatible with viability are constitutively active, then both the terminal GFP-Clb2 level, and the

progression to that level, ought to be the same in the context of the various alleles. In the case of stochastic inactivation, it is possible that the fraction of cells with high level GFP-Clb2 will correlate with the number of remaining phosphorylatable residues on Cdh1; the mechanism for such a high CDK level arrest in this context would have to be determined. Alternatively, if APC-Cdh1 activity is graded in individual cells, then intermediate levels of GFP-Clb2 may be observable which are sufficient to maintain phosphorylation of remaining Cdh1 sites so as to sustain graded APC activity, but insufficient for proper mitotic progression.

Time lapse microscopy will also allow us to infer the APC dynamics of single cells with partially phosphorylatable *CDH1* alleles. This has been done preliminarily: sporadic cytologically aberrant mitoses were observed in *CDH1-4N* cells, frequently associated with very low Clb2-GFP levels. Precise measurements may allow for an assessment of whether individual cells either have delayed APC-Cdh1 inactivation in late G1 or premature activation during mitotic exit as indicated by shifts in the GFP-Clb2 trace; such a result would be consistent with APC-Cdh1 switch-like behavior, in which removal of potential phosphorylation sites biases the switch to the 'on' position. It is also conceivable that timing will be essentially unaltered but peak GFP-Clb2 levels damped, which would imply a graded activity of partially phosphorylated Cdh1. In this way, the analysis of single cells may allow for inferences into the regulatory architecture of Cdh1 multisite phosphorylation.

CHAPTER FOUR

Regulated degradation of the APC coactivator Cdc20

Temporal separation of APC-Cdc20 and APC-Cdh1 activity is thought to promote ordering of degradation of APC substrates (see Introduction). Not only must Cdh1 activity be restrained until mitotic exit (see Chapter 2), but it is likely that Cdc20 must be inactivated for the subsequent cell cycle. Inability to inactivate Cdc20 would impede securin accumulation, impairing separase regulation, and constitutive Cdc20 could also block accumulation of the major S-phase cyclin Clb5.

Three mechanisms are known to contribute to Cdc20 inactivation: the dephosphorylation of the APC (Kramer et al., 2000; Rudner and Murray, 2000), transcriptional shutoff (Prinz et al., 1998), and the destruction of Cdc20 itself (Prinz et al., 1998; Shirayama et al., 1998; Weinstein, 1997). The following is an attempt to clarify the literature with regards to the regulated destruction of Cdc20.

Destruction boxes of Cdc20 both contribute to its degradation

Cdc20 has two destruction boxes thought to target it for destruction (Shirayama et al., 1998). It has been argued based on the stabilization of overexpressed alleles deleted for the region containing destruction boxes that both destruction boxes contribute to Cdc20 degradation in G1 (Prinz et al., 1998; Shirayama et al., 1998). One study also found residual APC-dependent but destruction-box independent Cdc20 instability throughout the entire cell cycle (Prinz et al., 1998). Another study argued that degradation of Cdc20 was dependent only on the first destruction box (Goh et al., 2000),

and was cell-cycle-regulated (highest in G1), but was independent of APC activity. These substantially contradictory results hamper understanding of this potentially important regulatory event.

We sought to test the consequences of removing Cdc20 destruction boxes on protein stability through the ablation of either each destruction box individually, or both simultaneously, in the context of the endogenous locus and promoter. This is in contrast to all previous work on Cdc20 destruction box function, which was carried out with overexpression. An 18-myc tag was placed at the N-terminus so that protein levels could be followed, and the destruction box consensus site RxxL was mutated to AxxA so as to prevent APC engagement of the destruction box without possible inadvertent consequences from deletions, as were used in much previous work (Figure 4.1). *CDC20-db1* ablates the first destruction box, *CDC20-db2* the second, and *CDC20-db3* both. These alleles were fully functional, as they replaced the endogenous copy of *CDC20*, which is an essential gene. Additionally, they were also viable in the absence of *CDH1*, a genetic background known to be sensitive to hypoactive APC-Cdc20 (Cross, 2003). Cells were synchronized in α-factor and released, with Myc-Cdc20 accumulation monitored by western blotting against Myc (Figure 4.2). Both destruction boxes contributed to Cdc20 degradation, and the effects of mutating both of them were significantly greater than the mutation of either one alone.

Cdc20 protein levels remained cell cycle regulated even with mutated destruction boxes. The Cdc20 destruction boxes were required for clearance of Cdc20 in α-factor blocked cells (most clearly seen with the double db mutant Cdc20-db3). Cdc20-db3 reproducibly declined shortly after release from the α-factor block, followed by a rise to a

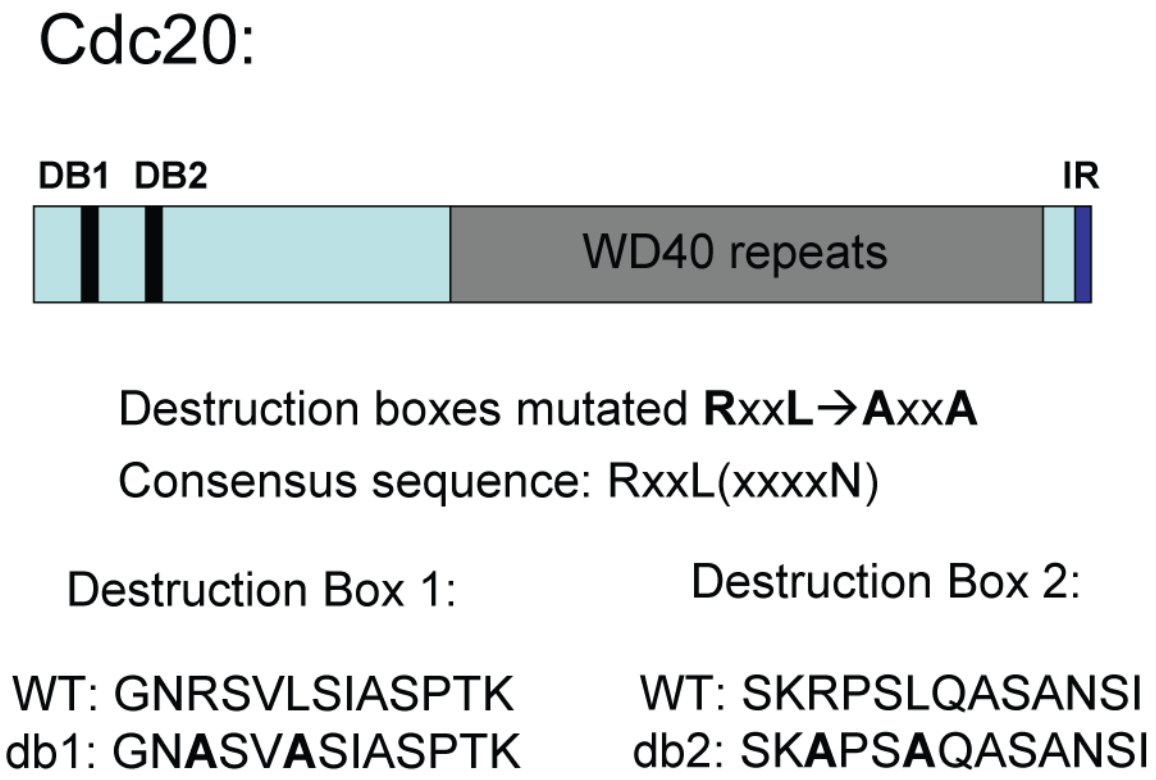

Figure 4.1 Schematic of Cdc20 and destruction box mutants. Two destruction boxes are found in the N-terminus (DB1 and DB2), with DB1 neighboring a potential CDK site of unknown function. The alanine substitutions ablating these destruction boxes in the *CDC20-db* alleles are indicated below.

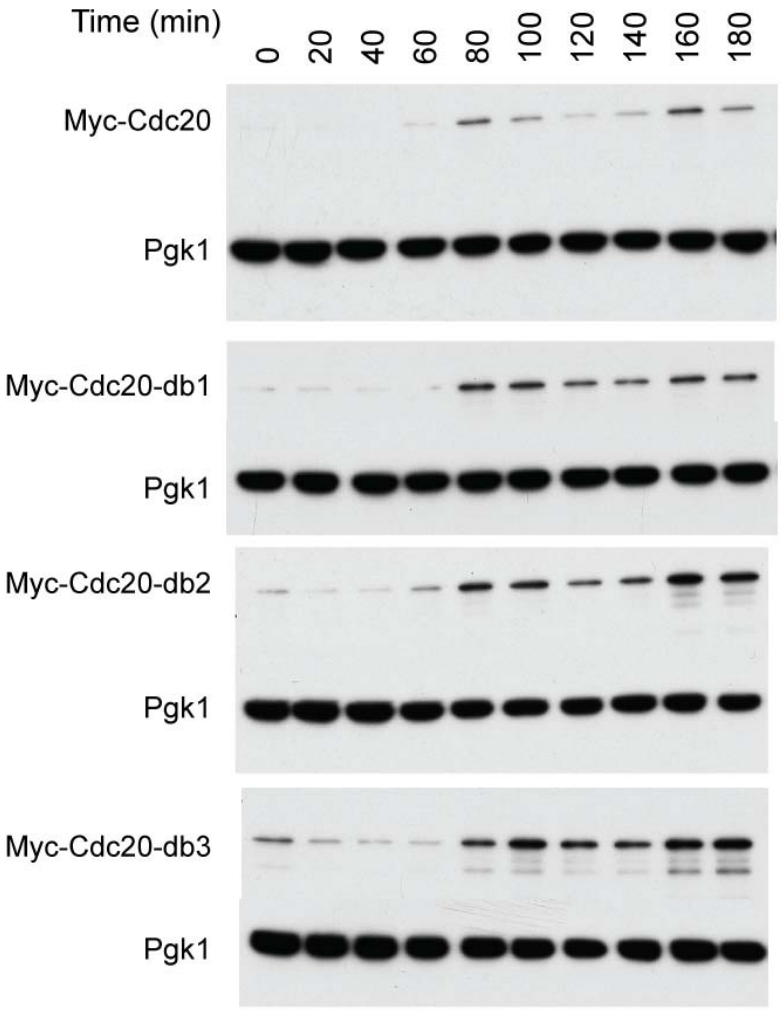

Figure 4.2 Destruction boxes contribute to, but are not solely responsible for, the destruction of Cdc20. Strains bearing *18MYC*-tagged *CDC20* with either destruction box 1 (db1), destruction box 2 (db2), or both destruction boxes (db3) ablated were synchronized with α-factor and released. Immunoblots against Myc are shown, with Pgk1 serving as a loading control.

higher peak level around the time of mitosis. (A similar effect was detectable with wild-type Cdc20, despite the extremely low initial levels which presumably resulted from efficient destruction-box-dependent proteolysis.) *CDC20* transcription is low at α-factor arrest, and only increases late in the cell cycle (Spellman et al., 1998); thus, the decline in Cdc20 levels shortly after release from the α-factor block is probably not the consequence of transcriptional downregulation. Rather, Cdc20 appears to be actively destroyed by some process as cells progress through G1 into S. This degradation is destruction box-independent, and is unlikely to be APC-Cdh1 mediated, as Cdh1 activity is very high in α-factor-blocked cells and declines upon release.

To allow for direct comparison of Cdc20 levels from the α-factor release, identical time points were loaded on the same gel to avoid gel-to-gel variability in intensity. The destruction box dependent degradation in α-factor was confirmed (Figure 4.3A). Interestingly, the destruction boxes had no effect on Cdc20 at 40 minutes and 80 minutes after release; at 120 minutes post-release destruction box-dependent degradation became apparent based on higher Cdc20 levels in the absence of destruction boxes.

Overexpression of *CDC20* lacking destruction boxes has been reported to interfere with S-phase progression (presumably mediated through sustained APC-Cdc20 ubiquitination of the S-phase cyclin Clb5) (Huang et al., 2001). However, with *CDC20-db3* expressed at endogenous levels we observe no S-phase or division delay (Figure 4.3B), so this reported effect is likely a consequence of overexpression.

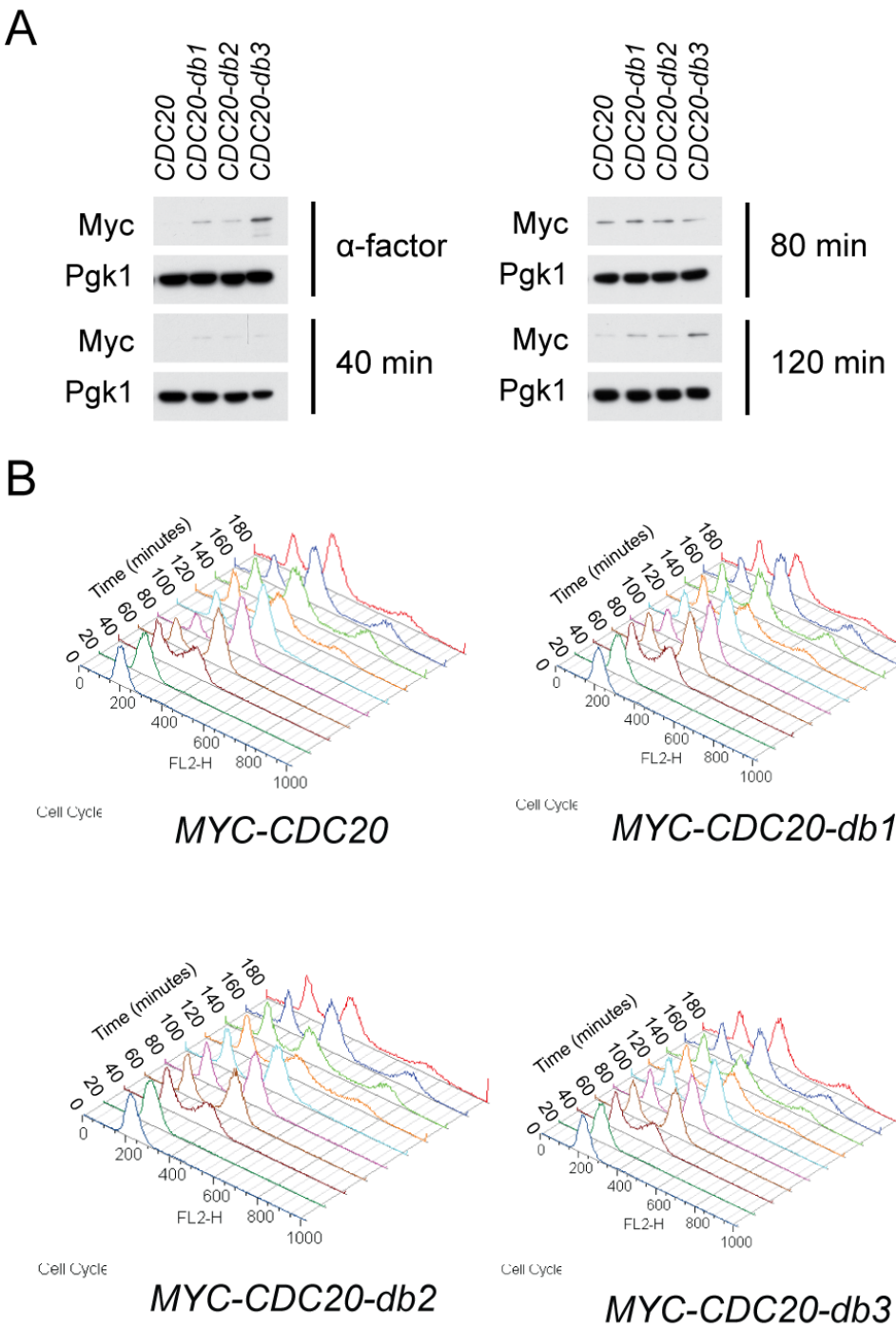

Figure 4.3 Ablation of destruction boxes particularly stabilizes Cdc20 in α-factor, but does not affect DNA replication kinetics. **A** Samples from Figure 4.2 for each *CDC20* allele at indicated timepoints were loaded next to one another on the same gel and blotted against. **B** FACS analysis of DNA content from samples taken in parallel with those from Figure 4.2. No differences are discernible with respect to progression through S-phase, or at other points, amongst the different *CDC20* alleles.

Overexpression of *CDH1* fails to clear Cdc20

APC-Cdh1 activity has been reported to restrain Cdc20 accumulation until early S-phase (Huang et al., 2001). We found Cdc20 to be nearly completely removed in α-factor-blocked cells, but this removal was only partially destruction-box dependent. α-factor-blocked cells contain high APC-Cdh1 activity, which could account for Cdc20 clearance in these cells. Therefore, we tested whether Cdh1 overexpression in cycling cells is able to clear Cdc20 expressed from the endogenous locus. Overexpressed *CDH1* had little effect on Cdc20 levels, and while *CDH1-m11* was able to reduce the level of Cdc20, this effect was incomplete even after two hours of *CDH1-m11* induction (Figure 4.4). This time of induction of *GAL-CDH1-m11* results in massive overexpression of Cdh1-m11 (Zachariae 1998a; data not shown). This indicates that Cdh1, even when both overexpressed and highly active, is not capable of efficiently clearing Cdc20, and suggests that the effective clearance of Cdc20 in α-factor-blocked cells is due at least in part to Cdh1-independent activities.

Cdc20 levels are increased but still cell cycle regulated in the absence of *CDH1*

We examined the effect of endogenous Cdh1 on Cdc20 levels. Using centrifugal elutriation, we separated cycling *cdh1* and wild-type cells into different cell cycle fractions based on cell size (this change in procedure was necessary because *cdh1* cells fail to arrest properly in response to α-factor). *cdh1* cells have higher levels of Cdc20 than *CDH1* cells, particularly in G1; however, Cdc20 declines to a low level in *cdh1* cells as they progress through S-phase (Figure 4.5), before increasing later in the cell cycle. This is consistent with both *CDH1*-dependent and *CDH1*-independent mechanisms being

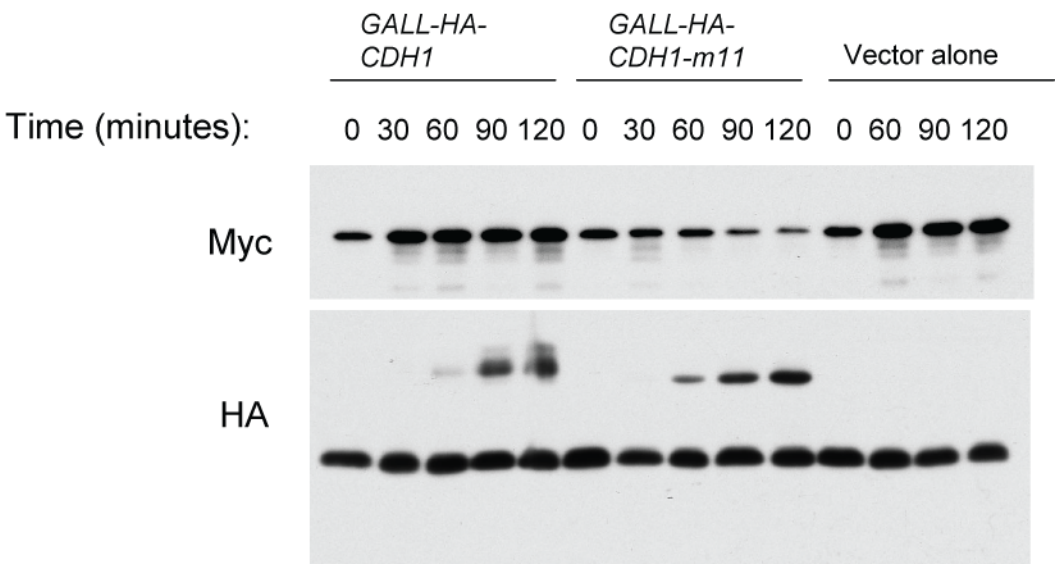

Figure 4.4 Overexpressed *CDH1-m11* lowers Cdc20 levels, but does not clear it. Either *HA-CDH1* or *HA-CDH1-m11* was induced using deoxycorticosterone in cycling strains with a GAL4-Mineralocorticoid receptor fusion (containing the DNA binding domain of the former, and ligand binding domain of the latter, rendering GAL responsive genes inducible by exogenous mineralocorticoids). Levels of endogenously expressed 18MYC-Cdc20 and HA-Cdh1 were followed by immunoblot, with a nonspecific band reactive with the anti-HA antibody serving as a loading control.

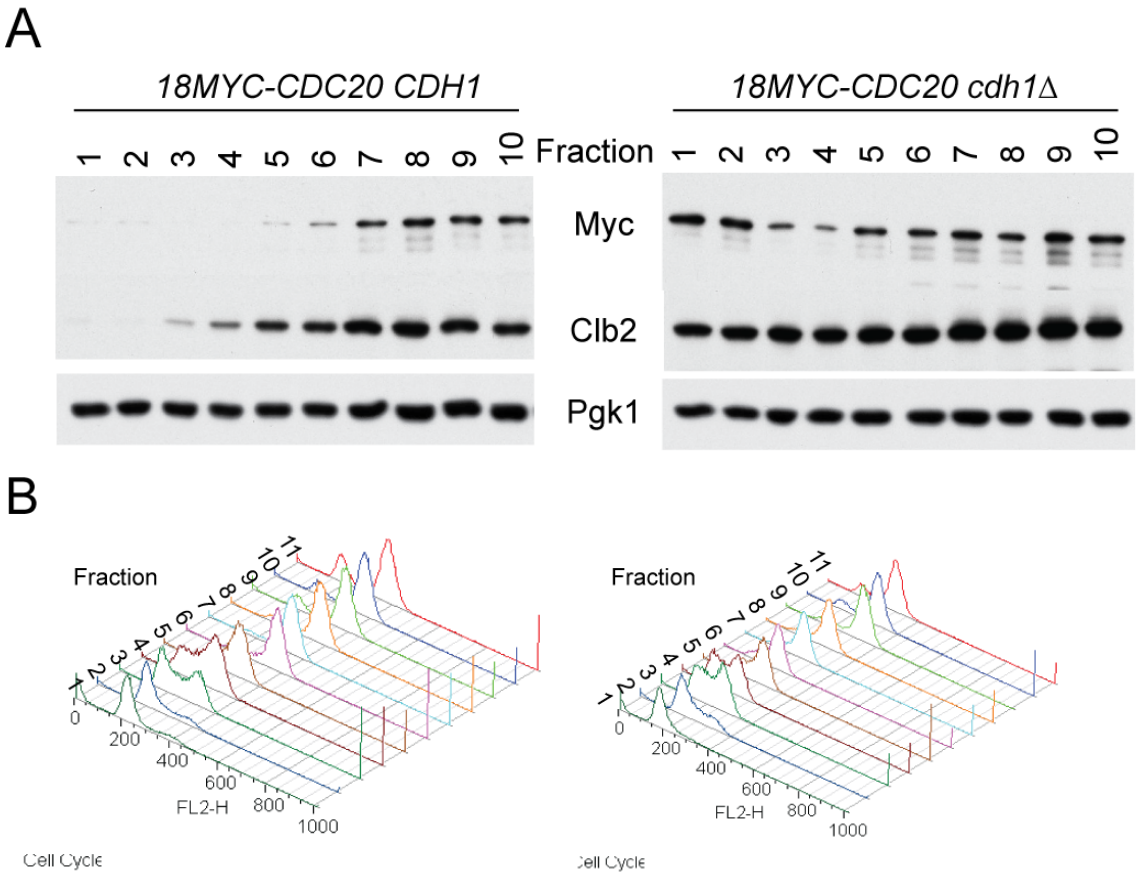

Figure 4.5 Deletion of *CDH1* partially stabilizes Cdc20. **A** *CDH1 18MYC-CDC20* and *cdh1 18MYC-CDC20* strains were elutriated, and the resultant fractions were immunoblotted for Myc and Clb2. Pgk1 serves as a loading control. **B** FACS to assess DNA content for the fractions collected in (A)

involved in the degradation of Cdc20. This finding correlates with the characterization above of destruction box-dependent and independent mechanisms of Cdc20 proteolysis.

Inducible Cdc20 is degraded by both Cdh1- dependent and independent mechanisms

Depletion of Cdc20 results in a reversible metaphase arrest. An allele of *MET3-HA-CDC20* replacing the endogenous copy of *CDC20* allows for methionine-repressible *CDC20* transcription; in the absence of methionine *CDC20* is constitutively expressed. *MET3-HA-CDC20 CDH1* and *MET3-HA-CDC20 cdh1* strains were constructed and grown to log phase in media lacking methionine. Methionine was then added, and 30 minutes after addition strains did not have any detectable Cdc20 in either *CDH1* or *cdh1* backgrounds (Figure 4.6). *cdh1* strains readily arrest in the first cycle after shutoff of *CDC20* transcription, similar to *CDH1* control cells. Upon induction of *CDC20* to release the cells, Cdc20 levels increase much more in a *cdh1* than in a *CDH1* background, suggesting that APC-Cdh1 can effectively dampen Cdc20 levels during mitotic exit. However, this effect is short lived, and Cdc20 rapidly stabilizes at a lower level (though still higher than *CDH1* cells) (Figure 4.6).

These results are consistent with the effects of *CDH1* deletion on Cdc20 levels from the endogenous promoter, and on the effects of Cdc20 destruction box mutation, in demonstrating Cdh1- and db-dependent Cdc20 degradation, and independent degradation independent of Cdh1 and destruction boxes.

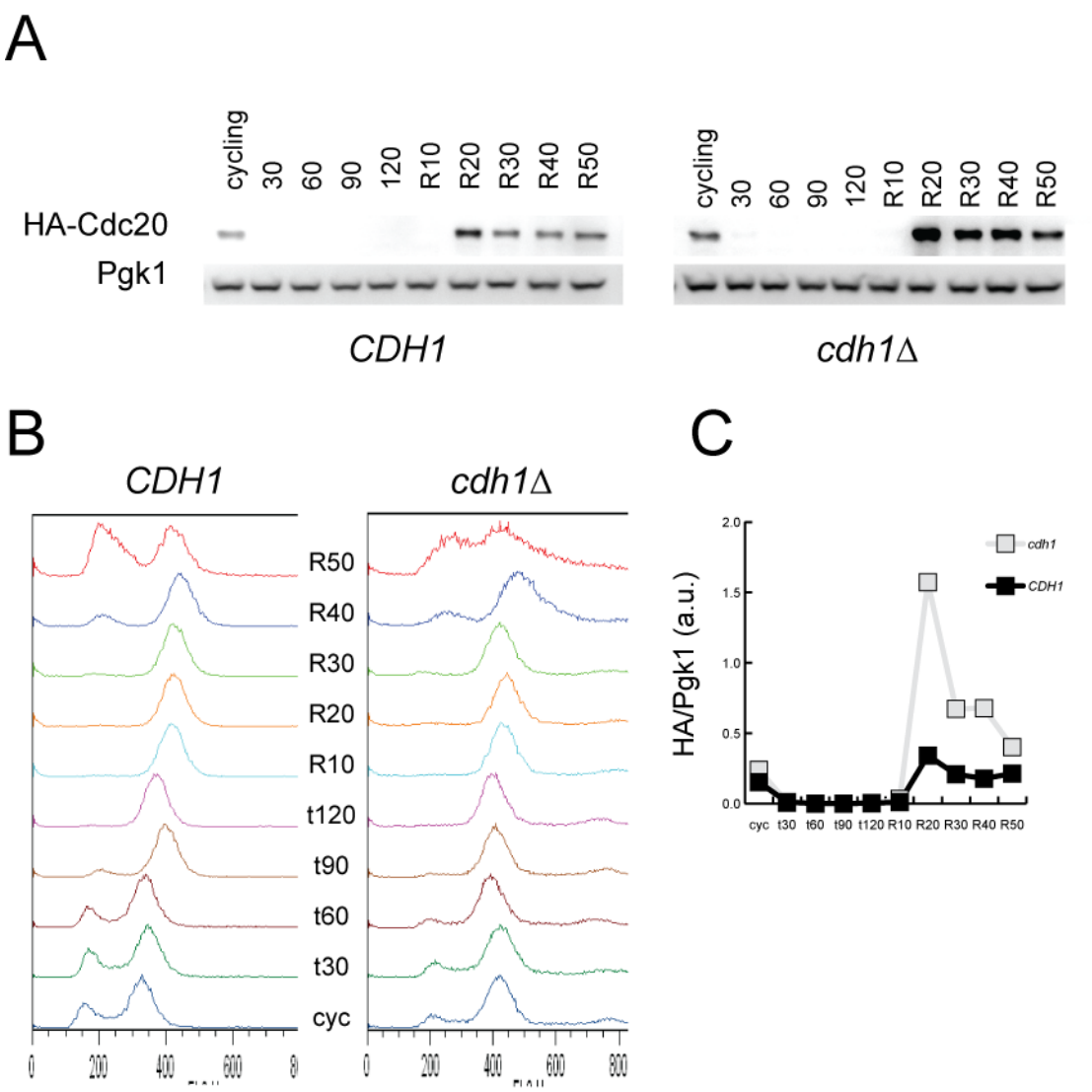

Figure 4.6 Inducible Cdc20 is degraded by both Cdh1 dependent and independent mechanisms. **A** Methionine was added at time 0 to cycling *CDH1* and *cdh1* strains, with *MET3pr-HA-CDC20* (methionine repressible) replacing endogenous *CDC20*, to shutoff *CDC20* transcription. After two hours, these cells were released into methionine-free media, inducing *CDC20* transcription. Samples were taken every ten minutes thereafter (R10, R20, etc). HA-Cdc20 was immunoblotted against, with Pgk1 serving as a loading control. **B** DNA content of the strains in (A) was assessed by FACS. **C** Quantification of immunoblots in (A).

Discussion

The regulatory control of Cdc20 has implications for the proper ordering of cell cycle events. Multiple mechanisms are involved in its regulation including transcriptional control, Cdc20 protein destruction, and CDK phosphorylation of the APC. Both the transcriptional control and at least part of the CDK phosphorylation of the APC (specifically of Cdc16, Cdc23, and Cdc27) are dispensable for essentially normal cell cycle progression (Rudner and Murray, 2000; Yeong et al., 2001). This work addresses the mechanisms by which Cdc20 protein stability is regulated, clarifying the agents, timing and motifs involved in Cdc20 destruction.

Conflicting reports exist in the literature as to what mediates the destruction of Cdc20. Studies have variously implicated the APC but presumably not Cdh1 (Prinz et al., 1998; Shirayama et al., 1998), APC-Cdh1 specifically (Huang et al., 2001), and an APC-independent mechanism (Goh et al., 2000). Here we find evidence for both APC-Cdh1 dependent and independent mechanisms.

APC-Cdh1 effectively restrains Cdc20 levels from mitotic exit through the subsequent G1 (Figure 4.5). This provides a simple mechanism for temporal separation of APC-Cdc20 and APC-Cdh1 activity, by Cdh1-dependent removal of Cdc20. Other mechanisms, such as dephosphorylating core APC components, may also contribute. Beginning in late G1/early S, a Cdh1-independent mechanism is responsible for Cdc20 degradation. We speculate that this may play role in limiting Cdc20 accumulation prior to anaphase so as to prevent premature cohesin cleavage, or may contribute to efficient engagement of the spindle checkpoint during aberrant mitoses (since Cdc20 is the

ultimate target of this checkpoint). The molecular basis for APC-Cdh1 independent degradation of Cdc20 is unknown.

APC dependent but destruction box independent degradation of Cdc20 was reported in S phase and mitosis (Prinz et al., 1998); it is possible that this is the Cdh1- and destruction box-independent Cdc20 degradation we observe. We have not evaluated the role of APC-dependent but coactivator-independent ubiquitination of Cdc20.

Work based upon overexpression studies of *CDC20* alleles with destruction box deletions, has arrived at conflicting conclusions for the relative contributions of the two destruction boxes (Goh et al., 2000; Prinz et al., 1998; Shirayama et al., 1998). We find both destruction boxes to contribute to Cdc20 instability, particularly during G1. However, the stabilization conferred by destruction box ablation appears only partial; peak mitotic levels of Cdc20-db3 are higher than α-factor blocked levels, while small G1 elutriated *cdh1* cells have similar Cdc20 levels to their large 2C DNA content counterparts. This suggests that APC-Cdh1 mediates the destruction of Cdc20 through both destruction box dependent and independent mechanisms. One possible targeting motif is a potential KEN box in the C-terminal portion of Cdc20; the contribution of this motif to Cdc20 instability has not been evaluated.

This work, taken as a whole, argues for a Cdh1 and destruction box dependent mechanism targeting Cdc20 for destruction from late mitosis through the subsequent G1, and a separate Cdh1 and destruction box independent mechanism degrading Cdc20 from S-phase into mitosis. The Cdh1 dependent degradation likely contributes to the strict alternation of APC-Cdc20 and APC-Cdh1 activity, thus promoting separate degradative

regimes during anaphase onset and spindle disassembly. These findings go some way to reconciling the conflicts in the literature, clarifying regulation of Cdc20 protein levels.

CHAPTER FIVE

Conclusions, Questions and Future Directions

CDK phosphorylation and Acm1 regulate Cdh1 activity

Through a careful exact gene replacement study, we have found CDK phosphorylation of Cdh1 to be essential for inactivating APC-Cdh1, and this inactivation essential for viability. Acm1, which is not required for normal cell cycle progression or APC-Cdh1 inhibition, can block Cdh1 sufficiently to allow a fraction of cells to construct bipolar spindles, but not undergo anaphase or complete the cell cycle. This establishes CDK phosphorylation as the major and essential regulator of APC-Cdh1 activity, and places Acm1 in a minor supporting role. We fail to find any evidence that Cdc5 phosphorylation is able to inhibit Cdh1 activity.

A failure of CDK phosphorylation of Cdh1 results in a predominantly monopolar spindle arrest. SPB separation can be promoted by expression of an undegradable mitotic cyclin, but not the kinesin Cin8 as had been previously reported (Crasta et al., 2006). A fraction of *CDH1-m11* cells construct bipolar spindles, which nevertheless fail to progress to anaphase owing to a failure to accumulate Cdc20 and consequently to cleave cohesin.

This approach has thus allowed for the determination of the physiologically significant regulators of Cdh1 activity, as well as mechanisms by which failure to inactivate Cdh1 interferes with cell cycle progression.

Does Acm1, in the absence of inhibitory CDK phosphorylation of Cdh1, permit bipolar spindle construction through mitotic cyclin accumulation?

How Acm1 allows for bipolar spindle assembly in a fraction of these cells is not clear. We find that increasing the gene dosage of *ACM1* results in a corresponding increase in mitotic cyclin levels, and independently that expression of undegradable cyclins promotes SPB separation. It is possible that a single copy of *ACM1* allows for a fraction of cells to construct bipolar spindles by inhibiting the APC sufficiently to allow for at least transient accumulation of mitotic cyclins, which could drive bipolar spindle assembly. If this is the case, then altering the copy number of *CLB2*, or replacing the endogenous gene with an allele coding for a partially stabilized cyclin such as with the KEN box ablated, would be predicted to increase the proportion of bipolar spindles seen at the CDH1-m11 arrest. An alternate, but not mutually exclusive possibility is that the accumulation of other APC substrates contributes significantly to bipolar spindle assembly.

Is there a physiological role for Cdh1 nuclear export?

The physiological role of nuclear export in Cdh1 regulation, if any, remains unclear and not easily addressed. As Msn5, which exports Cdh1 from the nucleus, is not essential, it is unlikely that nuclear export is a critical inhibitor of Cdh1. It is not known whether preventing nuclear export alters the *CDH1-m11* terminal phenotype; it is conceivable that a shift towards monopolar spindle arrest would result from deletion of *MSN5*. However, given the numerous other proteins shuttled by Msn5, such a result could also plausibly explained by pleiotropic effects.

Cdh1 export is phosphorylation dependent (Jaquenoud et al, 2002), and experiments are planned to test whether specific partially CDK-unphosphorylatable Cdh1 alleles are constitutively nuclear. This will be performed with partially unphosphorylatable GFP-tagged Cdh1 alleles under the GAL1 promoter, which will be integrated into cells with HTB2-mCherry marking the nucleus. By arresting the cells with α-factor, inducing GFP-Cdh1 alleles, and then releasing them, the Cdh1 nuclear export dynamics will be measured as they progress through the cell cycle. If a specific site or cluster of sites is responsible for nuclear export, then alleles lacking such site(s) will be expected to be constitutively nuclear. If specific sites are responsible, it will be interesting to see whether these same sites are also involved in blocking APC interaction. Alternatively, if nuclear export is based upon generic binding of CDK phosphorylation sites, all partially unphosphorylatable Cdh1 alleles will result in slowed nuclear export.

Does Cdh1 drive its own inactivation through transcription?

As mitotic cyclins are responsible for turning off the G1 regulon (Amon et al., 1993) and Cdh1 promotes mitotic cyclin degradation, a failure to inactivate Cdh1 likely results in sustained G1 regulon expression. This is suggested by the sustained polarized growth found in *CDH1-m11* cells. In a normal cell cycle, Cdh1 inactivation likely involves the progressive phosphorylation of Cdh1 until it is inactivated. If, for some reason, Cdh1 inactivation fails (such as by a stochastic failure to sufficiently phosphorylate it), persistent Cdh1 activity might prevent the shutoff of the G1 regulon. The result of this could be sustained transcription of proteins responsible for Cdh1 inactivation, including the G1 cyclins, *ACM1*, and *CLB5* (Spellman et al., 1998). This is

testable through the use of reporters, such as fluorescent proteins placed under the control of these respective promoters, as well as by microarray analysis. If this is the case, then *ACM1* transcription alone is not sufficient to inactivate Cdh1; however the combination of Acm1 and the perhaps more important cyclins would likely be sufficient in the more physiological context of phosphorylatable Cdh1.

Of note, this mechanism could plausibly also drive *PDS1* transcription (Spellman et al., 1998) if Cdh1 inactivation fails. This would have the effect of preventing premature anaphase, especially if Cdh1 has some ability to ubiquitinate Pds1.

Acm1 as a Cdh1 buffer

In the absence of Cdh1 phosphorylation, a single copy of *ACM1* is insufficient to permit cell cycle progression. However, it does allow a fraction of cells to separate their SPBs. The induction of Acm1 in late G1, in the context of a normal cell cycle, may serve to buffer APC-Cdh1 which has not been inactivated. If inactivation of Cdh1 by phosphorylation is delayed, it is plausible that the expression of Acm1 will allow for timely bipolar spindle construction and cell cycle progression.

How does inhibitory multisite Cdh1 phosphorylation work?

Multisite phosphorylation is a common but poorly understood regulatory mechanism; Cdh1, with its 11 putative CDK sites, is an excellent example of such multisite phosphorylation. The principles by which such regulatory mechanisms function, and whether they can be generalized or simply categorized, remain largely unclear. Numerous possibilities exist. Distinct sites may mediate different regulatory

mechanisms. Partially overlapping subsets of sites may mediate different regulatory mechanisms (Komeili and O'Shea, 1999). Clusters of sites may determine regional electrostatics important for protein protein interactions (Holt et al., 2009). Apparently strict counting mechanisms have been reported (Nash et al., 2001). Only through the characterization of numerous proteins regulated by multisite phosphorylation can principles and predominant circuitry be inferred. We have attempted to explore the multisite phosphorylation of Cdh1, and have made some progress. We have found that no individual, nor two adjacent, phosphorylation sites are required. Genetically separable alleles collectively covering all phosphorylation sites were found, with specific synthetic interactions found with N-terminal site ablation and the single deletions of *ACM1* and *CLB5*. N-terminal sites were found to contribute more significantly to Cdh1 inactivation than C-terminal sites. These results preclude the interpretation of any strict counting mechanism. Sites are genetically separable, which may in part reflect the specificity of inhibitory phosphorylation; we were not able to infer any strict separation of regulatory mechanisms. Further characterization of nuclear localization determinants by the experiments outlined has the potential to shed further light on the underlying architecture of Cdh1 multisite phosphorylation. This will undoubtedly need to be supplemented with precise biochemical studies.

Temporally separating Cdc20 and Cdh1 activity

APC-Cdc20 and APC-Cdh1 act sequentially, helping to order anaphase and mitotic exit. We have examined the regulatory mechanisms restraining Cdh1 activation in detail, as well as addressing open questions pertaining to the regulation of Cdc20. Our

work on the regulation of Cdc20 argues for a Cdh1 and destruction box dependent mechanism targeting Cdc20 for destruction from late mitosis through the subsequent G1, and a separate Cdh1 and destruction box independent mechanism degrading Cdc20 from S-phase into mitosis. The Cdh1-independent degradation may lower Cdc20 levels so as to prevent premature Cdc20 activation. The Cdh1 dependent degradation of Cdc20 can directly contribute to the strict alternation of destructive phases, and may allow for Cdc20 specific substrates to accumulate before Cdh1 is inactivated in late G1/S.

CHAPTER SIX

Materials and Methods

Yeast strains and plasmids.

Standard methods were used throughout. All strains are W303. See Table 5.1 for strains used. See Table 5.2 for plasmids used.

Time Courses

CDH1-m11 GALL-HA-ACM1 time courses were performed by arrest in YPG + 10nM α-factor for 135 minutes at 30°, followed either by glucose addition or resuspension in YPD + 10nM α-factor for 30 minutes. (Both procedures were found to result in complete clearance of exogenous Acm1 by western blot, and had identical SPB phenotypes.) For time lapse microscopy, strains were washed 3X in SC media, placed onto SC + Glucose agar pads, and imaged as in (Bean et al., 2006), discussed below. For bulk culture time courses, cells were removed from α-factor by 3 washes in cold YEP, and released into YPD at 30°C. For fluorescent microscopy in these timecourses, cells were fixed at room temperature for 15 minutes using a 4% paraformaldehyde buffer, washed twice with Sorbitol-Phosphate buffer ((1.2M sorbitol, 200 μM MgCl2, 100 mM KPO4, pH 7.5)), and otherwise handled as in (Drapkin et al, *Molecular Systems Biology*, *in press*).

MET3pr-CLB2-kd time courses were carried out similarly except that pregrowth, arrest and 60 min of release were carried out in 0.2g/L methionine (10X standard concentration). Transfer to methionine-free medium by three washes then induced *MET3-CLB2-kd*.

Temperature sensitive *scc1-73* and corresponding controls were blocked in α-factor for 165 minutes at 23°, and glucose added for 30 minutes to inactivate *GAL-ACM1*. After 3 washes in ice-cold YEP, cells were released at 30° and shifted to 37° 30 minutes post-release to inactivate *scc1-73*.

All other α-factor time courses were performed by blocking for between two and three hours in α-factor, washing 3X in α-factor-free media, and releasing into the indicated culture conditions. Washing of α-factor arrested cells requires centrifugation; filtration leads to clumping of these cells.

MET3-HA-CDC20 time courses were performed by adding 0.2g/L methionine to methionine-free synthetic media, arresting for between two and three hours, filtered onto nitrocellulose membranes, washed and release into methionine-free medium. GALL-CDC20 time courses were performed by centrifugation of log phase cells in YPG, washing, resuspension into YPD, arrest for two to three hours, 3X washing, and release into YPG. *GALL-CDC20* blocks requires resuspension into galactose-free media for the arrest; simple addition of glucose is inadequate for a clean arrest.

Centrifugal elutriations were performed using 1L of log phase culture with a Beckman JE5.0 elutriator rotor, running at 3000RPM with sequential fractions elutriated off by stepwise increase in pump speed.

Fixed cell fluorescence microscopy

Fluorescence and DIC images were acquired using an Axioplan 2 microscope (Carl Zeiss MicroImaging Corp.) with a 63X 1.4 numerical aperture Plan- Apochromat objective, coupled to a Hamamatsu C4742-95 CCD camera (Sciscope Instrument). Camera and microscope were interfaced with the OpenLab software (Improvision). Filters and dichroics used were made by Chroma. YFP was detected with a YFP filter, mCherry with a Cy3 filter, CFP with a CFP filter, and GFP with a narrow band pass FITC filter. For spindle analysis seven optical sections were taken at 0.3 micron spacing; for illustrative purposes these were merged into two-dimensional maximum projections. Acquisition was automated using an OpenLab script written by B. Drapkin.

Time-lapse Microscopy

Time-lapse microscopy was performed as described (Bean et al., 2006). Briefly, fields of single cells were imaged with fluorescence time-lapse microscopy at 30 °C using a Leica DMIRE2 inverted microscope with a Ludl motorized stage (Bean et al., 2006). Images were acquired with a Hamamatsu Orca-ER camera. Custom Visual Basic software integrated with ImagePro Plus was used for automated image acquisition and microscope control.

Immunoblots

Western Blots were performed using standard methods. Antibody concentrations used were: anti-Pgk1 1:10,000 (Invitrogen), anti-HA 12CA5 1:1,000 (Roche), rabbit polyclonal anti-Clb2 1:10,000, Myc 9E10 1:1,000 (Santa Cruz Biotechnology), Clb5 yN-

17 (Santa Cruz), Cdc5 yC-19 (Santa Cruz), and HRP-conjugated secondary antibodies at 1:4,000. ECL signal was measured in a Fujifilm DarkBox with CCD camera, and quantified using MultiGauge software (Fujifilm).

Flow Cytometry

DNA content was assessed through propidium iodide staining of ribonuclease treated cells on a FACSCalibur machine (BD Biosciences), as described (Epstein and Cross, 1992).

Quantitative PCR

Quantitative PCR was performed using SYBR green (Qiagen) according to the manufacturer's instructions, and data analyzed by SDS 2.2 (Applied Biosystems).

Cloning:

CDC20, *CDH1-pkm*, and first four N-terminal *CDH1* CDK site mutagenesis was performed by Quickchange Multi-Site Directed Mutagenesis (Stratagene) using the following primers:

Cdc20-db1: AATGCAGCAATTAGCGGTAACgcTTCTGTAgcTTCTATTGCGTCCCCAACAAAGC

Cdc20-db2: CTGAACATTAGAAACTCCAAAgcTCCCAGTgcACAAGCCTCTGCCAATTCTATT

S125A: CTCAGAGAGCgcTATAGATCGC

S259A: GTTTTAGATGCCCCggCATTAGC

CDH1T12A: CCATTCATGAATAATGCGCCTTCCTCCTCCCC

CDH1S16A: GAATAATACGCCTTCCAGTGCACCACTCAAGGGTTCTG

T12AS16A: CATTCATGAATAATGCGCCTTCCAGTGCACCACTCAAGGGTTC

CDH1T42A: CGCCTCACTATTATCAGCTCCCTCCAGGCG

CDH1-pbm was constructed by PCR, by creating separate overlapping fragments followed by PCR using the most 5' and 3' primers. The following primers were employed:

CDHS15/41Af:GCCTTCCgCCTCCCCACTCAAGGGTTCTGAAAGTAAGAGGGTA

TCGAAAAGGCCAATATCTAGTTCTTCGTCCGCCTCACTATTAgCATCTCC

CDH156/172AR:GCGTGGcATGTGGCGAAAATTCCTCTAAACCAGCAGCTTCAG

GAGGTGGAGTTGcTACTCGTTCCAG

CDHS15Rev: CTTGAGTGGGGAGGcGGAAGGC

CDHS172AFor: GAATTTTCGCCACATgCCACGC

For JRP91 (pRS406 *ACM1*), *ACM1* was cloned as a ClaI fragment and placed into pRS406 at the ClaI site. 406-HLP112 is HLP112 BglI swapped into pRS406. For 405-GALL-HLP109, *HA3-ACM1* was cloned as an XbaI/XhoI fragment into a 405-GALL plasmid backbone.

For construction of Myc-tagged Cin8 alleles, an N-terminal 6MYC tag was subcloned out of pTK138 (6MYC-CIN8) via AgeI/PacI and into the corresponding region of pEH113, 250 and 394 (CIN8, CIN8-alaKEN, and CIN8-KED respectively) that had been BglI-swapped into a pRS406 backbone. Resultant plasmids were transformed into the endogenous locus after PacI linearization, and clones screened to ensure presence of the 6MYC tag (which in principle can be lost in transformation due to resection past the tag prior to integration).

Table 5.1 (pages 104-108)

Strain Name	Genotype
3023-2-1	*MATa cdh1-m11::LEU2::URA3::cdh1-m11::TRP1*
3023-2-2	*MATa cdh1-m11::TRP1::URA3::cdh1-m11::LEU2*
JRC35B-8d	*MATa cdh1-m11::LEU2::URA3::cdh1-m11::TRP1 cdc23-1*
JRC36B-5d	*MATa cdh1-m11::TRP1::URA3::cdh1-m11::LEU2 cdc23-1*
JRC374A-5b	*MATa GAL1-3FLAG-ACM1-URA3::ura3 ADE2*
JRC374C-3a	*MATa GAL1-3FLAG-ACM1-URA3::ura3 acm1::KanMX ADE2*
MNX29-3b	*MATa CDH1-m11 GAL1-3FLAG-ACM1-URA3::ura3*
MNX29-8b	*MATa CDH1-m11 acm1::KanMX GAL1-3FLAG-ACM1-URA3::ura3*
JRC258B-9c	*MATa CDH1-pkm GAL1-3FLAG-ACM1-URA3::ura3 ADE2?*
JRC275B-11d	*MATa CDH1-pkm GAL1-3FLAG-ACM1-URA3::ura3 acm1::KanMX*
JRC362C-7c	*MATalpha CDH1-pbm GAL1-3FLAG-ACM1-URA3::ura3*
JRC373D-6c	*MATa bar1 CDH1-pbm GAL1-3FLAG-ACM1-URA3::ura3 acm1::KanMX*
JRC307C-2c	*MATa bar1 CDH1-m11 GALL-HA-ACM1-LEU2::leu2 MYO1-mCherry::HIS3 TRP1::CFP-TUB1*
JRC307A-2a	*MATa bar1 CDH1 GALL-HA-ACM1-LEU2::leu2 MYO1-mCherry::HIS3 TRP1::CFP-TUB1*
JRC318A-9c	*MATa bar1 CDH1 GALL-HA-ACM1-LEU2::leu2 HIS3::GFP-TUB1 SPC42-CFP-TRP1 MYO1-mCherry::HIS3 ADE2*
JRC318A-11d	*MATa bar1 CDH1-m11 GALL-HA-ACM1-LEU2::leu2 HIS3::GFP-TUB1 SPC42-CFP-TRP1 MYO1-mCherry::HIS3 ade2*
JR313	*MATa bar1 CDH1-m11 GALL-HA-ACM1-LEU2::leu2 HIS3::GFP-TUB1 SPC42-CFP-TRP1 MYO1-mCherry::HIS3 ACM1::URA3 ade2*
JR314	*MATa bar1 CDH1-m11 GALL-HA-ACM1-LEU2::leu2 HIS3::GFP-TUB1 SPC42-CFP-TRP1 MYO1-mCherry::HIS3 4XACM1::URA3 ade2*
JR315	*MATa bar1 CDH1-m11 GALL-HA-ACM1-LEU2::leu2 HIS3::GFP-TUB1 SPC42-CFP-TRP1 MYO1-mCherry::HIS3 2XACM1::URA3 ade2*
330I-7b	*MATa bar1 GALL-HA3-ACM1::LEU2 SPC42-CFP::TRP1 HIS3::GFP-TUB1 MYO1-mCherry::HIS3 acm1::KanMX*
395B-1b	*MATa bar1 CDH1-m11 GALL-HA-ACM1-LEU2::leu2 SPC42-CFP-TRP1 HIS3::GFP-TUB1 MYO1-mCherry::HIS3 acm1::KanMX*
JRC430A-9a	*MATa bar1 CDH1 GALL-HA-ACM1-LEU2::leu2 18MYC-CDC20-TRP1*
JRC430A-5a	*MATa bar1 CDH1-m11 GALL-HA-ACM1-LEU2::leu2 18MYC-CDC20-TRP1*
JRC431B-4a	*MATa bar1 CDH1 GALL-HA-ACM1-LEU2::leu2 PDS1-18MYC-LEU2*
JRC431D-4b	*MATa bar1 CDH1-m11 GALL-HA-ACM1-LEU2::leu2 PDS1-18MYC-LEU2*
JRC389A-6d	*MATa bar1 CDH1-m11 GALL-HA-ACM1-LEU2::leu2HTB2-mCherry-HIS5 SPC29-YFP-HIS3 CFP-TUB1-TRP1 MYO1-mCherry-HIS3*
JRC390A-5a	*MATa bar1 CDH1-m11 GALL-HA-ACM1-LEU2::leu2HTB2-mCherry-HIS5 SPC29-YFP-HIS3 scc1-73 TRP+ ade2*
JRC304	*MATa bar1 CDH1 GALL-HA-ACM1-LEU2::leu2 HIS3::GFP-TUB1 SPC42-CFP-TRP1 MYO1-mCherry::HIS3 6MYC-CIN8::ura3::CIN8 ADE2*
JRC306	*MATa bar1 CDH1 GALL-HA-ACM1-LEU2::leu2 HIS3::GFP-TUB1 SPC42-CFP-TRP1 MYO1-mCherry::HIS3 6MYC-CIN8-alaKEN::ura3::CIN8 ADE2*
JRC301	*MATa bar1 CDH1-m11 GALL-HA-ACM1-LEU2::leu2 HIS3::GFP-TUB1 SPC42-CFP-TRP1 MYO1-mCherry::HIS3 6MYC-CIN8::ura3::CIN8 ade2*
JRC303	*MATa bar1 CDH1-m11 GALL-HA-ACM1-LEU2::leu2 HIS3::GFP-TUB1 SPC42-CFP-TRP1 MYO1-mCherry::HIS3 6MYC-CIN8-db::ura3::CIN8-alaKEN ade2*
JR325	*MATa bar1 CDH1-m11 GALL-HA-ACM1-LEU2::leu2 HIS3::GFP-TUB1 SPC42-CFP-TRP1 MYO1-mCherry::HIS3 ade2 MET3pr-CLB2-kd::URA3*
JR326	*MATa bar1 CDH1 GALL-HA-ACM1-LEU2::leu2 HIS3::GFP-TUB1 SPC42-CFP-TRP1 MYO1-mCherry::HIS3 ade2 MET3pr-CLB2-kd::URA3*

JRC370A-6d	*MATa bar1 Clb2,kd trp1::TRP1::GAL1-SIC1(2X) HIS3:GFP-TUB1 SPC42-CFP::TRP1*
JR393A-2d	*MATa bar1 CDH1-m11 GALL-HA-ACM1-LEU2::leu2 trp1::TRP1::GAL1-SIC1(2X) CLB2-ken,db SPC42-CFP::TRP1 HIS3::GFP-TUB1 MYO1-mCherry::HIS3*
JRC344F-12d	*MATa bar1 CIN8-GFP::URA3 SPC42-CFP::TRP1 acm1::KanMX*
JRC312A-5b	*MATa bar1 CDH1-pkm CIN8-GFP::URA3 SPC42-CFP::TRP1 acm1::KanMX*
JRC406B-4b	*MATa bar1 CDH1 GALL-HA-ACM1-LEU2::leu2 HIS3::GFP-TUB1 SPC42-CFP-TRP1 MYO1-mCherry::HIS3 mad2::KanMX ade2*
JRC406C-4b	*MATa bar1 CDH1-m11 GALL-HA-ACM1-LEU2::leu2 HIS3::GFP-TUB1 SPC42-CFP-TRP1 MYO1-mCherry::HIS3 mad2::KanMX ade2*
JRC379A-4d	*MATa bar1 CDH1-m11 GALL-HA-ACM1-LEU2::leu2 HT2B-mCherry-HIS5 MYO1-GFP-KanMX*
JRC379A-1a	*MATa bar1 CDH1 GALL-HA-ACM1-LEU2::leu2 HT2B-mCherry-HIS5 MYO1-GFP-KanMX*
JRC388A-5c	*MATa CDH1-11m HT2B-mCherry-HIS5 405-GALL-109 MYO1-mCherry::HIS3 SPC29-YFP-HIS3 CFP-TUB1-TRP1*
JR90	*MATa TRP1-18MYC-CDC20-WT ADE2 URA3::ura3 pRS313:GAL4-MR-HIS3*
JR91	*MATa TRP1-18MYC-CDC20-WT ADE2 GALL-HA-CDH1-WT-URA3::ura3 pRS313:GAL4-MR-HIS3*
JRC142-8c	*MATa CDH1-3N*
JRC143-2b	*MATa CDH1-4N*
JRC144-9c	*MATa CDH1-7C*
JRC145-2a	*MATa CDH1-4C*
JRC146-4d	*MATa CDH1-WT*
JRC147-1c	*MATa CDH1-8C*
JRC148-5d	*MATa CDH1-1C*
JRC149B-8d	*MATa CDH1-2C*
2151-1C	*MATa cdh1::HIS3*
JRC397A-4a	*MATa GAL1-3FLAG-ACM1-URA3::ura3*
JRC177A-3d	*MAT? CDH1-3N GAL1-3FLAG-ACM1-URA3::ura3*
JRC113-4b	*MATa CDH1-4N GAL1-3FLAG-ACM1-URA3::ura3*
MNX32-6a	*MATa CDH1-7N GAL1-3FLAG-ACM1-URA3::ura3*
JRC115-3a	*MATa CDH1-9N GAL1-3FLAG-ACM1-URA3::ura3*
JRC116-6a	*MATa CDH1-10N GAL1-3FLAG-ACM1-URA3::ura3*
JRC117-1b	*MATa CDH1-11N GAL1-3FLAG-ACM1-URA3::ura3*
JRC180d-6d	*MAT? CDH1-1C GAL1-3FLAG-ACM1-URA3::ura3*
JRC182D-7b	*MAT? CDH1-2C GAL1-3FLAG-ACM1-URA3::ura3*
JRC179C-4b	*MAT? CDH1-4C GAL1-3FLAG-ACM1-URA3::ura3*
JRC181B-7c	*MATalpha CDH1-7C GAL1-3FLAG-ACM1-URA3::ura3*
JRC135-10b	*MATa CDH1-8C GAL1-3FLAG-ACM1-URA3::ura3*
JRC437A-6c	*MATa CDH1-4N GAL-3FLAG-ACM1-URA3::ura3*
JRC3437A-4d	*MATa CDH1-4N clb5::HIS3 GAL-3FLAG-ACM1-URA3::ura3*
JRC437A-9c	*MATa CDH1-4N clb6::KanMX GAL-3FLAG-ACM1-URA3::ura3*
JRC437A-6a	*MATA CDH1-4N clb5::HIS3 clb6::KanMX GAL-3FLAG-ACM1-URA3::ura3*
JRC439A-11d	*MATa CDH1-7C GAL-3FLAG-ACM1-URA3::ura3*
JRC439A-5d	*MATa CDH1-7C clb5::HIS3 GAL-3FLAG-ACM1-URA3::ura3*
JRC439A-5b	*MATa CDH1-7C clb6::KanMX GAL-3FLAG-ACM1-URA3::ura3*
JRC439A-3d	*MATa CDH1-7C clb5::HIS3 clb6::KanMX GAL-3FLAG-ACM1-URA3::ura3*
JRC436A-10a	*MATa CDH1 GAL-3FLAG-ACM1-URA3::ura3*

JRC436A-6c	*MATa CDH1 clb5::HIS3 GAL-3FLAG-ACM1-URA3::ura3*
JRC436A-1c	*MATa CDH1 clb6::KanMX GAL-3FLAG-ACM1-URA3::ura3*
JRC436A-1d	*MATa CDH1 clb5::HIS3 clb6::KanMX GAL-3FLAG-ACM1-URA3::ura3*
JRC438A-4c	*MATa CDH1-8C GAL-3FLAG-ACM1-URA3::ura3*
JRC438A-1b	*MATa CDH1-8C clb5::HIS3 GAL-3FLAG-ACM1-URA3::ura3*
JRC438A-6c	*MATa CDH1-8C clb6::KanMX GAL-3FLAG-ACM1-URA3::ura3*
JRC438A-4a	*MATa CDH1-8C clb5::HIS3 clb6::KanMX GAL-3FLAG-ACM1-URA3::ura3*
JRC177A-3d	*MAT CDH1-3N GAL1-3FLAG-ACM1-URA3::ura3*
JRC177A-5c	*MAT CDH1-3N GAL1-3FLAG-ACM1-URA3::ura3 acm1::KanMX msn5::HIS3*
JRC177A-7a	*MATalpha CDH1-3N GAL1-3FLAG-ACM1-URA3::ura3 msn5::HIS3*
JRC177D-12b	*MATalpha CDH1-3N GAL1-3FLAG-ACM1-URA3::ura3 acm1::KanMX*
JRC262A-2a	*MATa CDH1-T12A GAL1-3FLAG-ACM1-URA3::ura3*
JRC262A-1c	*MATa CDH1-T12A GAL1-3FLAG-ACM1-URA3::ura3 acm1::KanMX*
JRC262A-9d	*MATa CDH1-T12A GAL1-3FLAG-ACM1-URA3::ura3 msn5::HIS3*
JRC262A-9c	*MATa CDH1-T12A GAL1-3FLAG-ACM1-URA3::ura3 acm1::KanMX msn5::HIS3*
JRC263A-9d	*MATa CDH1-S16A GAL1-3FLAG-ACM1-URA3::ura3*
JRC263A-2b	*MATa CDH1-S16A GAL1-3FLAG-ACM1-URA3::ura3 acm1::KanMX*
JRC263A-5b	*MATa CDH1-S16A GAL1-3FLAG-ACM1-URA3::ura3 msn5::HIS3*
JRC263A-3b	*MATa CDH1-S16A GAL1-3FLAG-ACM1-URA3::ura3 acm1::KanMX msn5::HIS3*
JRC264A-3b	*MATa CDH1-S42A GAL1-3FLAG-ACM1-URA3::ura3*
JRC264A-2b	*MATa CDH1-S42A GAL1-3FLAG-ACM1-URA3::ura3 acm1::KanMX*
JRC264A-2a	*MATa CDH1-S42A GAL1-3FLAG-ACM1-URA3::ura3 msn5::HIS3*
JRC264A-1b	*MATa CDH1-S42A GAL1-3FLAG-ACM1-URA3::ura3 acm1::KanMX msn5::HIS3*
JRC265A-8c	*MATa CDH1-T157A GAL1-3FLAG-ACM1-URA3::ura3*
JRC265A-2b	*MATa CDH1-T157A GAL1-3FLAG-ACM1-URA3::ura3 acm1::KanMX*
JRC265A-7d	*MATa CDH1-T157A GAL1-3FLAG-ACM1-URA3::ura3 msn5::HIS3*
JRC265A-1c	*MATa CDH1-T157A GAL1-3FLAG-ACM1-URA3::ura3 acm1::KanMX msn5::HIS3*
JRC276A-3d	*MATa CDH1-T12A-S16A GAL1-3FLAG-ACM1-URA3::ura3*
JRC276A-12b	*MATa CDH1-T12A-S16A GAL1-3FLAG-ACM1-URA3::ura3 acm1::KanMX*
JRC276A-8a	*MATa CDH1-T12A-S16A GAL1-3FLAG-ACM1-URA3::ura3 msn5::HIS3*
JRC276A-9c	*MATa CDH1-T12A-S16A GAL1-3FLAG-ACM1-URA3::ura3 acm1::KanMX msn5::HIS3*
JRC310A-10a	*MATa CDH1-T12A-S42A GAL1-3FLAG-ACM1-URA3::ura3*
JRC310B-3a	*MATa CDH1-T12A-S42A GAL1-3FLAG-ACM1-URA3::ura3 acm1::KanMX*
JRC310A-3a	*MATa CDH1-T12A-S42A GAL1-3FLAG-ACM1-URA3::ura3 msn5::HIS3 acm1::KanMX*
JRC310A-3b	*MATa CDH1-T12A-S42A GAL1-3FLAG-ACM1-URA3::ura3 msn5::HIS3*
JRC398B-8c	*MATa CDH1-T12A-T157A GAL1-3FLAG-ACM1-URA3::ura3 msn5::HIS3*
JRC398B-9b	*MATa CDH1-T12A-T157A GAL1-3FLAG-ACM1-URA3::ura3 acm1::KanMX msn5::HIS3*
JRC398A-12d	*MATa CDH1-T12A-T157A GAL1-3FLAG-ACM1-URA3::ura3*
JRC398C-1b	*MATa CDH1-T12A-T157A GAL1-3FLAG-ACM1-URA3::ura3 acm1::KanMX*
JRC311A-9d	*MATa CDH1-S16A-S42A GAL1-3FLAG-ACM1-URA3::ura3*
JRC311A-11d	*MATa CDH1-S16A-S42A acm1::KanMX GAL1-3FLAG-ACM1-URA3::ura3*
JRC311A-7c	*MATa CDH1-S16A-S42A msn5::HIS3 acm1::KanMX GAL1-3FLAG-ACM1-URA3::ura3*
JRC311A-7d	*MATa CDH1-S16A-S42A msn5::HIS3 GAL1-3FLAG-ACM1-URA3::ura3*
JRC320A-6b	*MATalpha CDH1-S16A-T157A GAL1-3FLAG-ACM1-URA3::ura3*
JRC320A-7a	*MATalpha CDH1-S16A-T157A acm1::KanMX msn5::HIS3 GAL1-3FLAG-ACM1-URA3::ura3*

JRC320A-1a	*MATalpha CDH1-S16A-T157A msn5::HIS3 GAL1-3FLAG-ACM1-URA3::ura3*
JRC320A-4d	*MATalpha CDH1-S16A-T157A acm1::KanMX GAL1-3FLAG-ACM1-URA3::ura3*
JRC267A-3d	*MATa CDH1-S42A-T157A GAL1-3FLAG-ACM1-URA3::ura3*
JRC267A-7b	*MATa CDH1-S42A-T157A GAL1-3FLAG-ACM1-URA3::ura3 acm1::KanMX*
JRC267A-10a	*MATa CDH1-S42A-T157A GAL1-3FLAG-ACM1-URA3::ura3 msn5::HIS3*
JRC267A-4c	*MATa CDH1-S42A-T157A GAL1-3FLAG-ACM1-URA3::ura3 acm1::KanMX msn5::HIS3*
JRC280A-1b	*MATa CDH1-T12A-S16A-T157A GAL1-3FLAG-ACM1-URA3::ura3*
JRC280A-6a	*MATa CDH1-T12A-S16A-T157A GAL1-3FLAG-ACM1-URA3::ura3 msn5::HIS3*
JRC280B-7c	*MATa CDH1-T12A-S16A-T157A GAL1-3FLAG-ACM1-URA3::ura3 acm1::KanMX*
JRC280B-5b	*MATa CDH1-T12A-S16A-T157A GAL1-3FLAG-ACM1-URA3::ura3 acm1::KanMX msn5::HIS3*
JRC269B-2b	*MATa CDH1-S16A-S42A-T157A GAL1-3FLAG-ACM1-URA3::ura3*
JRC269B-1b	*MATa CDH1-S16A-S42A-T157A GAL1-3FLAG-ACM1-URA3::ura3 acm1::KanMX*
JRC269A-6c	*MATa CDH1-S16A-S42A-T157A GAL1-3FLAG-ACM1-URA3::ura3 msn5::HIS3*
JRC269A-1a	*MATa CDH1-S16A-S42A-T157A GAL1-3FLAG-ACM1-URA3::ura3 acm1::KanMX msn5::HIS3*
MNX33-3c	*MATa CDH1-4N msn5null::HIS3 GAL1-3FLAG-ACM1-URA3::ura3*
MNX33-7d	*MATa CDH1-4N acm1::KanMX GAL1-3FLAG-ACM1-URA3::ura3*
MNX33-1d	*MATa CDH1-4N msn5null::HIS3 acm1::KanMX GAL1-3FLAG-ACM1-URA3::ura3*
JRC181D-5c	*MATa CDH1-7C GAL1-3FLAG-ACM1-URA3::ura3 msn5::HIS3*
JRC181C-1b	*MATalpha CDH1-7C GAL1-3FLAG-ACM1-URA3::ura3 acm1::KanMX*
JRC181D-3a	*MATalpha CDH1-7C GAL1-3FLAG-ACM1-URA3::ura3 acm1::KanMX msn5::HIS3*
JRC397A-9b	*MATa GAL1-3FLAG-ACM1-URA3::ura3 acm1::KanMX*
JRC397A-9a	*MATa GAL1-3FLAG-ACM1-URA3::ura3 msn5::HIS3*
JRC397A-1c	*MATa GAL1-3FLAG-ACM1-URA3::ura3 acm1::KanMX msn5::HIS3*
JRC177A-7a	*MATalpha CDH1-3N GAL1-3FLAG-ACM1-URA3::ura3 msn5::HIS3*
JRC177D-12b	*MATalpha CDH1-3N GAL1-3FLAG-ACM1-URA3::ura3 acm1::KanMX*
JRC177A-5c	*MAT CDH1-3N GAL1-3FLAG-ACM1-URA3::ura3 acm1::KanMX msn5::HIS3*
MNX31-6c	*MATa CDH1-8c msn5::HIS3 GAL1-3FLAG-ACM1-URA3::ura3*
MNX31-6d	*MATa CDH1-8c msn5::HIS3 acm1::KanMX GAL1-3FLAG-ACM1-URA3::ura3*
MNX34-11c	*MATa CDH1-8c acm1::KanMX GAL1-3FLAG-ACM1-URA3::ura3*
JRC135-10b	*MATa CDH1-8C GAL1-3FLAG-ACM1-URA3::ura3*
JRC267A-3d	*MATa CDH1-S42A-T157A GAL1-3FLAG-ACM1-URA3::ura3*
JRC267A-7b	*MATa CDH1-S42A-T157A GAL1-3FLAG-ACM1-URA3::ura3 acm1::KanMX*
JRC267A-10a	*MATa CDH1-S42A-T157A GAL1-3FLAG-ACM1-URA3::ura3 msn5::HIS3*
JRC267A-4c	*MATa CDH1-S42A-T157A GAL1-3FLAG-ACM1-URA3::ura3 acm1::KanMX msn5::HIS3*
JRC280A-1b	*MATa CDH1-T12A-S16A-T157A GAL1-3FLAG-ACM1-URA3::ura3*
JRC280A-6a	*MATa CDH1-T12A-S16A-T157A GAL1-3FLAG-ACM1-URA3::ura3 msn5::HIS3*
JRC280B-7c	*MATa CDH1-T12A-S16A-T157A GAL1-3FLAG-ACM1-URA3::ura3 acm1::KanMX*
JRC280B-5b	*MATa CDH1-T12A-S16A-T157A GAL1-3FLAG-ACM1-URA3::ura3 acm1::KanMX msn5::HIS3*
JRC268B-3c	*MATa CDH1-T12A-S42A-T157A GAL1-3FLAG-ACM1-URA3::ura3*
JRC255A-3c	*CDH1-T12A-S42A-T157A acm1::KanMX GAL1-3FLAG-ACM1-URA3::ura3 ade2*
JRC268A-10d	*MATa CDH1-T12A-S42A-T157A GAL1-3FLAG-ACM1-URA3::ura3 msn5::HIS3*
JRC268A-10b	*MATa CDH1-T12A-S42A-T157A GAL1-3FLAG-ACM1-URA3::ura3 acm1::KanMX msn5::HIS3*
JRC269B-2b	*MATa CDH1-S16A-S42A-T157A GAL1-3FLAG-ACM1-URA3::ura3*
JRC269B-1b	*MATa CDH1-S16A-S42A-T157A GAL1-3FLAG-ACM1-URA3::ura3 acm1::KanMX*

JRC269A-6c	*MATa CDH1-S16A-S42A-T157A GAL1-3FLAG-ACM1-URA3::ura3 msn5::HIS3*
JRC269A-1a	*MATa CDH1-S16A-S42A-T157A GAL1-3FLAG-ACM1-URA3::ura3 acm1::KanMX msn5::HIS3*
JR13	*MATa HIS3::GFP-TUB1 MYO1-GFP-KANMX bar1 MYC-CDC20-TRP1 ADE2*
JR52	*MATa HIS3::GFP-TUB1 MYO1-GFP-KAN bar1 TRP1-18MYC-CDC20-db1 ADE2*
JR55	*MATa HIS3::GFP-TUB1 MYO1-GFP-KANMX bar1 MYC-CDC20-db2-TRP1 ADE2*
JR53	*MATa HIS3::GFP-TUB1 MYO1-GFP-KAN bar1 TRP1-18MYC-CDC20-db3 ADE2*

Table 5.2

Plasmid Name	Description	Plasmid Notes
FC695	pRS406 *cdh1-m11::TRP1*	cut with BglII to integrate at CDH1
FC697	pRS406 *cdh1-m11::LEU2*	cut with BglII to integrate at CDH1
JRP67	pRS406 *CDH1-pkm (S125A-S259A)*	cut with BglII to integrate at CDH1
JRP90	pRS406 *CDH1-pbm (S15A-S41A-S156A-S172A)*	cut with BglII to integrate at CDH1
406-HLP112	pRS406 *GAL1-3FLAG-ACM1*	cut with StuI to integrate at ura3
405-GALL-HLP109	pRS405 *GALL-HA-ACM1*	cut with XcmI to integrate at leu2
DJC235	*18MYC-CDC20-TRP1*	cut with MluI integrate at CDC20
JRP87	pRS406 *6MYC-CIN8*	cut with PacI to integrate at CIN8
JRP88	pRS406 *6MYC-CIN8 alaKEN*	cut with PacI to integrate at CIN8
JRP89	pRS406 *6MYC-CIN8-KED*	cut with PacI to integrate at CIN8
JRP91	pRS406 *ACM1*	cut with StuI to integrate at ura3
JRP95	pRS406 *MET3-CLB2-ken,db*	cut with StuI to integrate at ura3
DJC235	pRS404 *18MYC-CDC20*	MluI to integrate at CDC20
JRP1	*18MYC-CDC20-db1-TRP1*	MluI to integrate at CDC20
JRP2	*18MYC-CDC20-db2-TRP1*	MluI to integrate at CDC20
JRP3	*18MYC-CDC20-db3-TRP1*	MluI to integrate at CDC20
FC681	pRS406 *CDH1*	cut with BglII to integrate at CDH1
FC687	pRS406 *CDH1-m11*	cut with BglII to integrate at CDH1
FC801	pRS406 *cdh1::TRP1*	cut with BglII to integrate at CDH1
JRP4	pRS406 *cdh1::LEU2*	cut with BglII to integrate at CDH1
JRP5	pRS406 *GALL-HA-CDH1*	cut with BglII to integrate at CDH1
JRP6	pRS406 *GALL-HA-CDH1-m11*	cut with BglII to integrate at CDH1
JRP55	pRS406 *CDH1-T12A*	cut with BglII to integrate at CDH1
JRP56	pRS406 *CDH1-S16A*	cut with BglII to integrate at CDH1
JRP57	pRS406 *CDH1-T42A*	cut with BglII to integrate at CDH1
JRP58	pRS406 *CDH1-T12A T42A*	cut with BglII to integrate at CDH1
JRP59	pRS406 *CDH1-S16A T42A*	cut with BglII to integrate at CDH1
JRP60	pRS406 *CDH1-T12A-T157A*	cut with BglII to integrate at CDH1
JRP62	pRS406 *CDH1-T42A-T157A*	cut with BglII to integrate at CDH1
JRP63	pRS406 *CDH1-T12A-T42A-T157A*	cut with BglII to integrate at CDH1
JRP64	pRS406 *CDH1-S16A-T42A-T157A*	cut with BglII to integrate at CDH1
JRP78	pRS406 *CDH1-S16A-T157A*	cut with BglII to integrate at CDH1

References

Akada, R., Kallal, L., Johnson, D.I. and Kurjan, J. (1996) Genetic relationships between the G protein beta gamma complex, Ste5p, Ste20p and Cdc42p: investigation of effector roles in the yeast pheromone response pathway. *Genetics*, **143**, 103-117.

Amon, A., Irniger, S. and Nasmyth, K. (1994) Closing the cell cycle circle in yeast: G2 cyclin proteolysis initiated at mitosis persists until the activation of G1 cyclins in the next cycle. *Cell*, **77**, 1037-1050.

Amon, A., Tyers, M., Futcher, B. and Nasmyth, K. (1993) Mechanisms that help the yeast cell cycle clock tick: G2 cyclins transcriptionally activate G2 cyclins and repress G1 cyclins. *Cell*, **74**, 993-1007.

Archambault, V., Li, C.X., Tackett, A.J., Wasch, R., Chait, B.T., Rout, M.P. and Cross, F.R. (2003) Genetic and biochemical evaluation of the importance of Cdc6 in regulating mitotic exit. *Mol Biol Cell*, **14**, 4592-4604.

Bai, C., Sen, P., Hofmann, K., Ma, L., Goebl, M., Harper, J.W. and Elledge, S.J. (1996) SKP1 connects cell cycle regulators to the ubiquitin proteolysis machinery through a novel motif, the F-box. *Cell*, **86**, 263-274.

Bean, J.M., Siggia, E.D. and Cross, F.R. (2006) Coherence and timing of cell cycle start examined at single-cell resolution. *Mol Cell*, **21**, 3-14.

Benanti, J.A., Matyskiela, M.E., Morgan, D.O. and Toczyski, D.P. (2009) Functionally distinct isoforms of Cik1 are differentially regulated by APC/C-mediated proteolysis. *Mol Cell*, **33**, 581-590.

Benmaamar, R. and Pagano, M. (2005) Involvement of the SCF complex in the control of Cdh1 degradation in S-phase. *Cell Cycle*, **4**, 1230-1232.

Burton, J.L., Tsakraklides, V. and Solomon, M.J. (2005) Assembly of an APC-Cdh1-substrate complex is stimulated by engagement of a destruction box. *Mol Cell*, **18**, 533-542.

Charles, J.F., Jaspersen, S.L., Tinker-Kulberg, R.L., Hwang, L., Szidon, A. and Morgan, D.O. (1998) The Polo-related kinase Cdc5 activates and is destroyed by the mitotic cyclin destruction machinery in S. cerevisiae. *Curr Biol*, **8**, 497-507.

Cohen-Fix, O., Peters, J.M., Kirschner, M.W. and Koshland, D. (1996) Anaphase initiation in Saccharomyces cerevisiae is controlled by the APC-dependent degradation of the anaphase inhibitor Pds1p. *Genes Dev*, **10**, 3081-3093.

Crasta, K., Huang, P., Morgan, G., Winey, M. and Surana, U. (2006) Cdk1 regulates centrosome separation by restraining proteolysis of microtubule-associated proteins. *Embo J*, **25**, 2551-2563.

Crasta, K., Lim, H.H., Giddings, T.H., Jr., Winey, M. and Surana, U. (2008) Inactivation of Cdh1 by synergistic action of Cdk1 and polo kinase is necessary for proper assembly of the mitotic spindle. *Nat Cell Biol*, **10**, 665-675.

Cross, F.R. (2003) Two redundant oscillatory mechanisms in the yeast cell cycle. *Dev Cell*, **4**, 741-752.

Cross, F.R., Archambault, V., Miller, M. and Klovstad, M. (2002) Testing a mathematical model of the yeast cell cycle. *Mol Biol Cell*, **13**, 52-70.

Cross, F.R. and Tinkelenberg, A.H. (1991) A potential positive feedback loop controlling CLN1 and CLN2 gene expression at the start of the yeast cell cycle. *Cell*, **65**, 875-883.

Deshaies, R.J. and Ferrell, J.E., Jr. (2001) Multisite phosphorylation and the countdown to S phase. *Cell*, **107**, 819-822.

Di Fiore, B. and Pines, J. (2007) Emi1 is needed to couple DNA replication with mitosis but does not regulate activation of the mitotic APC/C. *J Cell Biol*, **177**, 425-437.

Dirick, L. and Nasmyth, K. (1991) Positive feedback in the activation of G1 cyclins in yeast. *Nature*, **351**, 754-757.

Draetta, G., Luca, F., Westendorf, J., Brizuela, L., Ruderman, J. and Beach, D. (1989) Cdc2 protein kinase is complexed with both cyclin A and B: evidence for proteolytic inactivation of MPF. *Cell*, **56**, 829-838.

Elia, A.E., Cantley, L.C. and Yaffe, M.B. (2003) Proteomic screen finds pSer/pThr-binding domain localizing Plk1 to mitotic substrates. *Science*, **299**, 1228-1231.

Enquist-Newman, M., Sullivan, M. and Morgan, D.O. (2008) Modulation of the mitotic regulatory network by APC-dependent destruction of the Cdh1 inhibitor Acm1. *Mol Cell*, **30**, 437-446.

Epstein, C.B. and Cross, F.R. (1992) CLB5: a novel B cyclin from budding yeast with a role in S phase. *Genes Dev*, **6**, 1695-1706.

Evans, T., Rosenthal, E.T., Youngblom, J., Distel, D. and Hunt, T. (1983) Cyclin: a protein specified by maternal mRNA in sea urchin eggs that is destroyed at each cleavage division. *Cell*, **33**, 389-396.

Fitch, I., Dahmann, C., Surana, U., Amon, A., Nasmyth, K., Goetsch, L., Byers, B. and Futcher, B. (1992) Characterization of four B-type cyclin genes of the budding yeast Saccharomyces cerevisiae. *Mol Biol Cell*, **3**, 805-818.

Fridman, V., Gerson-Gurwitz, A., Movshovich, N., Kupiec, M. and Gheber, L. (2009) Midzone organization restricts interpolar microtubule plus-end dynamics during spindle elongation. *EMBO Rep*, **10**, 387-393.

Gmachl, M., Gieffers, C., Podtelejnikov, A.V., Mann, M. and Peters, J.M. (2000) The RING-H2 finger protein APC11 and the E2 enzyme UBC4 are sufficient to ubiquitinate substrates of the anaphase-promoting complex. *Proc Natl Acad Sci U S A*, **97**, 8973-8978.

Goh, P.Y., Lim, H.H. and Surana, U. (2000) Cdc20 protein contains a destruction-box but, unlike Clb2, its proteolysisis not acutely dependent on the activity of anaphase-promoting complex. *Eur J Biochem*, **267**, 434-449.

Gordon, D.M. and Roof, D.M. (2001) Degradation of the kinesin Kip1p at anaphase onset is mediated by the anaphase-promoting complex and Cdc20p. *Proc Natl Acad Sci U S A*, **98**, 12515-12520.

Grosskortenhaus, R. and Sprenger, F. (2002) Rca1 inhibits APC-Cdh1(Fzr) and is required to prevent cyclin degradation in G2. *Dev Cell*, **2**, 29-40.

Hall, M.C., Jeong, D.E., Henderson, J.T., Choi, E., Bremmer, S.C., Iliuk, A.B. and Charbonneau, H. (2008) Cdc28 and Cdc14 control stability of the anaphase-promoting complex inhibitor Acm1. *J Biol Chem*, **283**, 10396-10407.

Hall, M.C., Warren, E.N. and Borchers, C.H. (2004) Multi-kinase phosphorylation of the APC/C activator Cdh1 revealed by mass spectrometry. *Cell Cycle*, **3**, 1278-1284.

Hartwell, L.H., Mortimer, R.K., Culotti, J. and Culotti, M. (1973) Genetic Control of the Cell Division Cycle in Yeast: V. Genetic Analysis of cdc Mutants. *Genetics*, **74**, 267-286.

Higuchi, T. and Uhlmann, F. (2005) Stabilization of microtubule dynamics at anaphase onset promotes chromosome segregation. *Nature*, **433**, 171-176.

Hildebrandt, E.R. and Hoyt, M.A. (2001) Cell cycle-dependent degradation of the Saccharomyces cerevisiae spindle motor Cin8p requires APC(Cdh1) and a bipartite destruction sequence. *Mol Biol Cell*, **12**, 3402-3416.

Holt, L.J., Hutti, J.E., Cantley, L.C. and Morgan, D.O. (2007) Evolution of Ime2 phosphorylation sites on Cdk1 substrates provides a mechanism to limit the effects of the phosphatase Cdc14 in meiosis. *Mol Cell*, **25**, 689-702.

Holt, L.J., Tuch, B.B., Villen, J., Johnson, A.D., Gygi, S.P. and Morgan, D.O. (2009) Global analysis of Cdk1 substrate phosphorylation sites provides insights into evolution. *Science*, **325**, 1682-1686.

Hoyt, M.A., He, L., Loo, K.K. and Saunders, W.S. (1992) Two Saccharomyces cerevisiae kinesin-related gene products required for mitotic spindle assembly. *J Cell Biol*, **118**, 109-120.

Huang, J.N., Park, I., Ellingson, E., Littlepage, L.E. and Pellman, D. (2001) Activity of the APC(Cdh1) form of the anaphase-promoting complex persists until S phase and prevents the premature expression of Cdc20p. *J Cell Biol*, **154**, 85-94.

Huh, W.K., Falvo, J.V., Gerke, L.C., Carroll, A.S., Howson, R.W., Weissman, J.S. and O'Shea, E.K. (2003) Global analysis of protein localization in budding yeast. *Nature*, **425**, 686-691.

Irniger, S. and Nasmyth, K. (1997) The anaphase-promoting complex is required in G1 arrested yeast cells to inhibit B-type cyclin accumulation and to prevent uncontrolled entry into S-phase. *J Cell Sci*, **110 (Pt 13)**, 1523-1531.

Jackson, L.P., Reed, S.I. and Haase, S.B. (2006) Distinct mechanisms control the stability of the related S-phase cyclins Clb5 and Clb6. *Mol Cell Biol*, **26**, 2456-2466.

Jaquenoud, M., van Drogen, F. and Peter, M. (2002) Cell cycle-dependent nuclear export of Cdh1p may contribute to the inactivation of APC/C(Cdh1). *Embo J*, **21**, 6515-6526.

Jaspersen, S.L., Charles, J.F. and Morgan, D.O. (1999) Inhibitory phosphorylation of the APC regulator Hct1 is controlled by the kinase Cdc28 and the phosphatase Cdc14. *Curr Biol*, **9**, 227-236.

Juang, Y.L., Huang, J., Peters, J.M., McLaughlin, M.E., Tai, C.Y. and Pellman, D. (1997) APC-mediated proteolysis of Ase1 and the morphogenesis of the mitotic spindle. *Science*, **275**, 1311-1314.

Kaffman, A., Rank, N.M., O'Neill, E.M., Huang, L.S. and O'Shea, E.K. (1998) The receptor Msn5 exports the phosphorylated transcription factor Pho4 out of the nucleus. *Nature*, **396**, 482-486.

Khmelinskii, A., Roostalu, J., Roque, H., Antony, C. and Schiebel, E. (2009) Phosphorylation-dependent protein interactions at the spindle midzone mediate cell cycle regulation of spindle elongation. *Dev Cell*, **17**, 244-256.

King, R.W., Glotzer, M. and Kirschner, M.W. (1996) Mutagenic analysis of the destruction signal of mitotic cyclins and structural characterization of ubiquitinated intermediates. *Mol Biol Cell*, **7**, 1343-1357.

King, R.W., Peters, J.M., Tugendreich, S., Rolfe, M., Hieter, P. and Kirschner, M.W. (1995) A 20S complex containing CDC27 and CDC16 catalyzes the mitosis-specific conjugation of ubiquitin to cyclin B. *Cell*, **81**, 279-288.

Komeili, A. and O'Shea, E.K. (1999) Roles of phosphorylation sites in regulating activity of the transcription factor Pho4. *Science*, **284**, 977-980.

Kraft, C., Vodermaier, H.C., Maurer-Stroh, S., Eisenhaber, F. and Peters, J.M. (2005) The WD40 propeller domain of Cdh1 functions as a destruction box receptor for APC/C substrates. *Mol Cell*, **18**, 543-553.

Kramer, E.R., Scheuringer, N., Podtelejnikov, A.V., Mann, M. and Peters, J.M. (2000) Mitotic regulation of the APC activator proteins CDC20 and CDH1. *Mol Biol Cell*, **11**, 1555-1569.

Lasorella, A., Stegmuller, J., Guardavaccaro, D., Liu, G., Carro, M.S., Rothschild, G., de la Torre-Ubieta, L., Pagano, M., Bonni, A. and Iavarone, A. (2006) Degradation of Id2 by the anaphase-promoting complex couples cell cycle exit and axonal growth. *Nature*, **442**, 471-474.

Leverson, J.D., Joazeiro, C.A., Page, A.M., Huang, H., Hieter, P. and Hunter, T. (2000) The APC11 RING-H2 finger mediates E2-dependent ubiquitination. *Mol Biol Cell*, **11**, 2315-2325.

Lew, D.J. and Reed, S.I. (1993) Morphogenesis in the yeast cell cycle: regulation by Cdc28 and cyclins. *J Cell Biol*, **120**, 1305-1320.

Li, W., Wu, G. and Wan, Y. (2007) The dual effects of Cdh1/APC in myogenesis. *Faseb J*, **21**, 3606-3617.

Listovsky, T., Oren, Y.S., Yudkovsky, Y., Mahbubani, H.M., Weiss, A.M., Lebendiker, M. and Brandeis, M. (2004) Mammalian Cdh1/Fzr mediates its own degradation. *Embo J*, **23**, 1619-1626.

Martinez, J.S., Jeong, D.E., Choi, E., Billings, B.M. and Hall, M.C. (2006) Acm1 is a negative regulator of the CDH1-dependent anaphase-promoting complex/cyclosome in budding yeast. *Mol Cell Biol*, **26**, 9162-9176.

Mumberg, D., Muller, R. and Funk, M. (1994) Regulatable promoters of Saccharomyces cerevisiae: comparison of transcriptional activity and their use for heterologous expression. *Nucleic Acids Res*, **22**, 5767-5768.

Nash, P., Tang, X., Orlicky, S., Chen, Q., Gertler, F.B., Mendenhall, M.D., Sicheri, F., Pawson, T. and Tyers, M. (2001) Multisite phosphorylation of a CDK inhibitor sets a threshold for the onset of DNA replication. *Nature*, **414**, 514-521.

Ostapenko, D., Burton, J.L., Wang, R. and Solomon, M.J. (2008) Pseudosubstrate inhibition of the anaphase-promoting complex by Acm1: regulation by proteolysis and Cdc28 phosphorylation. *Mol Cell Biol*, **28**, 4653-4664.

Passmore, L.A. and Barford, D. (2005) Coactivator functions in a stoichiometric complex with anaphase-promoting complex/cyclosome to mediate substrate recognition. *EMBO Rep*, **6**, 873-878.

Petroski, M.D. and Deshaies, R.J. (2003) Context of multiubiquitin chain attachment influences the rate of Sic1 degradation. *Mol Cell*, **11**, 1435-1444.

Pfleger, C.M., Lee, E. and Kirschner, M.W. (2001) Substrate recognition by the Cdc20 and Cdh1 components of the anaphase-promoting complex. *Genes Dev*, **15**, 2396-2407.

Prinz, S., Hwang, E.S., Visintin, R. and Amon, A. (1998) The regulation of Cdc20 proteolysis reveals a role for APC components Cdc23 and Cdc27 during S phase and early mitosis. *Curr Biol*, **8**, 750-760.

Reimann, J.D., Freed, E., Hsu, J.Y., Kramer, E.R., Peters, J.M. and Jackson, P.K. (2001) Emi1 is a mitotic regulator that interacts with Cdc20 and inhibits the anaphase promoting complex. *Cell*, **105**, 645-655.

Reis, A., Levasseur, M., Chang, H.Y., Elliott, D.J. and Jones, K.T. (2006) The CRY box: a second APCcdh1-dependent degron in mammalian cdc20. *EMBO Rep*, **7**, 1040-1045.

Richardson, H.E., Wittenberg, C., Cross, F. and Reed, S.I. (1989) An essential G1 function for cyclin-like proteins in yeast. *Cell*, **59**, 1127-1133.

Rodrigo-Brenni, M.C. and Morgan, D.O. (2007) Sequential E2s drive polyubiquitin chain assembly on APC targets. *Cell*, **130**, 127-139.

Ross, K.E. and Cohen-Fix, O. (2003) The role of Cdh1p in maintaining genomic stability in budding yeast. *Genetics*, **165**, 489-503.

Rudner, A.D. and Murray, A.W. (2000) Phosphorylation by Cdc28 activates the Cdc20-dependent activity of the anaphase-promoting complex. *J Cell Biol*, **149**, 1377-1390.

Saunders, W.S. and Hoyt, M.A. (1992) Kinesin-related proteins required for structural integrity of the mitotic spindle. *Cell*, **70**, 451-458.

Schneider, B.L., Patton, E.E., Lanker, S., Mendenhall, M.D., Wittenberg, C., Futcher, B. and Tyers, M. (1998) Yeast G1 cyclins are unstable in G1 phase. *Nature*, **395**, 86-89.

Schuyler, S.C., Liu, J.Y. and Pellman, D. (2003) The molecular function of Ase1p: evidence for a MAP-dependent midzone-specific spindle matrix. Microtubule-associated proteins. *J Cell Biol*, **160**, 517-528.

Schwab, M., Lutum, A.S. and Seufert, W. (1997) Yeast Hct1 is a regulator of Clb2 cyclin proteolysis. *Cell*, **90**, 683-693.

Schwab, M., Neutzner, M., Mocker, D. and Seufert, W. (2001) Yeast Hct1 recognizes the mitotic cyclin Clb2 and other substrates of the ubiquitin ligase APC. *Embo J*, **20**, 5165-5175.

Schwob, E. and Nasmyth, K. (1993) CLB5 and CLB6, a new pair of B cyclins involved in DNA replication in Saccharomyces cerevisiae. *Genes Dev*, **7**, 1160-1175.

Sethi, N., Monteagudo, M.C., Koshland, D., Hogan, E. and Burke, D.J. (1991) The CDC20 gene product of Saccharomyces cerevisiae, a beta-transducin homolog, is required for a subset of microtubule-dependent cellular processes. *Mol Cell Biol*, **11**, 5592-5602.

Shirayama, M., Toth, A., Galova, M. and Nasmyth, K. (1999) APC(Cdc20) promotes exit from mitosis by destroying the anaphase inhibitor Pds1 and cyclin Clb5. *Nature*, **402**, 203-207.

Shirayama, M., Zachariae, W., Ciosk, R. and Nasmyth, K. (1998) The Polo-like kinase Cdc5p and the WD-repeat protein Cdc20p/fizzy are regulators and substrates of the anaphase promoting complex in Saccharomyces cerevisiae. *Embo J*, **17**, 1336-1349.

Sigrist, S.J. and Lehner, C.F. (1997) Drosophila fizzy-related down-regulates mitotic cyclins and is required for cell proliferation arrest and entry into endocycles. *Cell*, **90**, 671-681.

Sikorski, R.S., Michaud, W.A. and Hieter, P. (1993) p62cdc23 of Saccharomyces cerevisiae: a nuclear tetratricopeptide repeat protein with two mutable domains. *Mol Cell Biol*, **13**, 1212-1221.

Skotheim, J.M., Di Talia, S., Siggia, E.D. and Cross, F.R. (2008) Positive feedback of G1 cyclins ensures coherent cell cycle entry. *Nature*, **454**, 291-296.

Snead, J.L., Sullivan, M., Lowery, D.M., Cohen, M.S., Zhang, C., Randle, D.H., Taunton, J., Yaffe, M.B., Morgan, D.O. and Shokat, K.M. (2007) A coupled

chemical-genetic and bioinformatic approach to Polo-like kinase pathway exploration. *Chem Biol*, **14**, 1261-1272.

Song, S., Grenfell, T.Z., Garfield, S., Erikson, R.L. and Lee, K.S. (2000) Essential function of the polo box of Cdc5 in subcellular localization and induction of cytokinetic structures. *Mol Cell Biol*, **20**, 286-298.

Song, S. and Lee, K.S. (2001) A novel function of Saccharomyces cerevisiae CDC5 in cytokinesis. *J Cell Biol*, **152**, 451-469.

Spellman, P.T., Sherlock, G., Zhang, M.Q., Iyer, V.R., Anders, K., Eisen, M.B., Brown, P.O., Botstein, D. and Futcher, B. (1998) Comprehensive identification of cell cycle-regulated genes of the yeast Saccharomyces cerevisiae by microarray hybridization. *Mol Biol Cell*, **9**, 3273-3297.

Stern, B. and Nurse, P. (1996) A quantitative model for the cdc2 control of S phase and mitosis in fission yeast. *Trends Genet*, **12**, 345-350.

Strickfaden, S.C., Winters, M.J., Ben-Ari, G., Lamson, R.E., Tyers, M. and Pryciak, P.M. (2007) A mechanism for cell-cycle regulation of MAP kinase signaling in a yeast differentiation pathway. *Cell*, **128**, 519-531.

Sudakin, V., Ganoth, D., Dahan, A., Heller, H., Hershko, J., Luca, F.C., Ruderman, J.V. and Hershko, A. (1995) The cyclosome, a large complex containing cyclin-selective ubiquitin ligase activity, targets cyclins for destruction at the end of mitosis. *Mol Biol Cell*, **6**, 185-197.

Thornton, B.R., Ng, T.M., Matyskiela, M.E., Carroll, C.W., Morgan, D.O. and Toczyski, D.P. (2006) An architectural map of the anaphase-promoting complex. *Genes Dev*, **20**, 449-460.

Thornton, B.R. and Toczyski, D.P. (2003) Securin and B-cyclin/CDK are the only essential targets of the APC. *Nat Cell Biol*, **5**, 1090-1094.

van Hemert, M.J., Deelder, A.M., Molenaar, C., Steensma, H.Y. and van Heusden, G.P. (2003) Self-association of the spindle pole body-related intermediate filament protein Fin1p and its phosphorylation-dependent interaction with 14-3-3 proteins in yeast. *J Biol Chem*, **278**, 15049-15055.

Verma, R., Annan, R.S., Huddleston, M.J., Carr, S.A., Reynard, G. and Deshaies, R.J. (1997) Phosphorylation of Sic1p by G1 Cdk required for its degradation and entry into S phase. *Science*, **278**, 455-460.

Visintin, R., Craig, K., Hwang, E.S., Prinz, S., Tyers, M. and Amon, A. (1998) The phosphatase Cdc14 triggers mitotic exit by reversal of Cdk-dependent phosphorylation. *Mol Cell*, **2**, 709-718.

Visintin, R., Prinz, S. and Amon, A. (1997) CDC20 and CDH1: a family of substrate-specific activators of APC-dependent proteolysis. *Science*, **278**, 460-463.

Wang, Y., Spatz, M.K., Kannan, K., Hayk, H., Avivi, A., Gorivodsky, M., Pines, M., Yayon, A., Lonai, P. and Givol, D. (1999) A mouse model for achondroplasia produced by targeting fibroblast growth factor receptor 3. *Proc Natl Acad Sci U S A*, **96**, 4455-4460.

Wäsch, R. and Cross, F.R. (2002) APC-dependent proteolysis of the mitotic cyclin Clb2 is essential for mitotic exit. *Nature*, **418**, 556-562.

Weinstein, J. (1997) Cell cycle-regulated expression, phosphorylation, and degradation of p55Cdc. A mammalian homolog of CDC20/Fizzy/slp1. *J Biol Chem*, **272**, 28501-28511.

Woodbury, E.L. and Morgan, D.O. (2007) Cdk and APC activities limit the spindle-stabilizing function of Fin1 to anaphase. *Nat Cell Biol*, **9**, 106-112.

Yamano, H., Gannon, J., Mahbubani, H. and Hunt, T. (2004) Cell cycle-regulated recognition of the destruction box of cyclin B by the APC/C in Xenopus egg extracts. *Mol Cell*, **13**, 137-147.

Yeong, F.M., Lim, H.H., Padmashree, C.G. and Surana, U. (2000) Exit from mitosis in budding yeast: biphasic inactivation of the Cdc28-Clb2 mitotic kinase and the role of Cdc20. *Mol Cell*, **5**, 501-511.

Yeong, F.M., Lim, H.H., Wang, Y. and Surana, U. (2001) Early expressed Clb proteins allow accumulation of mitotic cyclin by inactivating proteolytic machinery during S phase. *Mol Cell Biol*, **21**, 5071-5081.

Yoon, H.J., Feoktistova, A., Wolfe, B.A., Jennings, J.L., Link, A.J. and Gould, K.L. (2002) Proteomics analysis identifies new components of the fission and budding yeast anaphase-promoting complexes. *Curr Biol*, **12**, 2048-2054.

Zachariae, W., Schwab, M., Nasmyth, K. and Seufert, W. (1998a) Control of cyclin ubiquitination by CDK-regulated binding of Hct1 to the anaphase promoting complex. *Science*, **282**, 1721-1724.

Zachariae, W., Shevchenko, A., Andrews, P.D., Ciosk, R., Galova, M., Stark, M.J., Mann, M. and Nasmyth, K. (1998b) Mass spectrometric analysis of the anaphase-promoting complex from yeast: identification of a subunit related to cullins. *Science*, **279**, 1216-1219.

Zhu, G., Spellman, P.T., Volpe, T., Brown, P.O., Botstein, D., Davis, T.N. and Futcher, B. (2000) Two yeast forkhead genes regulate the cell cycle and pseudohyphal growth. *Nature*, **406**, 90-94.